

Improving Deep Ensembles by Estimating Confusion Matrices

Danil Kuzin
Lancaster University

Olga Isupova
University of Oxford

Steven Reece
University of Oxford

Brooke D Simmons
Lancaster University

17 Oct 2024

Abstract

Ensembling in deep learning improves accuracy and calibration over single networks. The traditional aggregation approach, ensemble averaging, treats all individual networks equally by averaging their outputs. Inspired by crowdsourcing we propose an aggregation method called soft Dawid Skene for deep ensembles that estimates confusion matrices of ensemble members and weighs them according to their inferred performance. Soft Dawid Skene aggregates soft labels in contrast to hard labels often used in crowdsourcing. We empirically show the superiority of soft Dawid Skene in accuracy, calibration and out of distribution detection in comparison to ensemble averaging in extensive experiments.

1 Introduction

Ensembling is a popular approach to improve accuracy and calibration of deep neural networks (Lakshminarayanan et al., 2017). Predictions of individual neural networks are aggregated by averaging predicted probabilities, this is called ensemble averaging (EA). Despite its simplicity, EA shows strong results in accuracy, calibration and uncertainty estimation outperforming other Bayesian and non-Bayesian specialised methods (Ashukha et al., 2020; Ovadia et al., 2019; Wortsman et al., 2022; Pei et al., 2022; Kim et al., 2023; Gustafsson et al., 2020; Franchi et al., 2022).

However, this simplest approach does not take into account the structural differences of the ensemble members. Consider an ensemble of three neural networks. Model A specializes in recognizing animals but frequently misclassifies vehicles. Model B is the opposite — highly accurate at vehicles but poorer at animals. Model C has the average performance on both. EA gives same weights for all three models when making predictions, but model A should be trusted more for animals, while model B should be preferred for vehicles, and model C

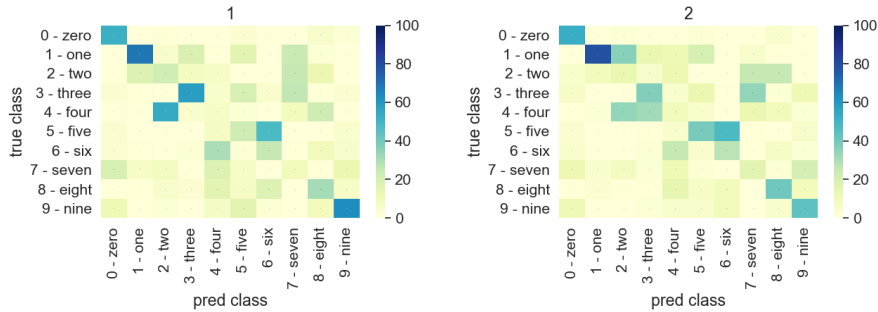


Figure 1: True confusion matrices for two ensemble members on the MNIST distributional shift experiment with rotation of 60° .

should complement their predictions. Ideally, we want an aggregation method to infer individual strengths and weaknesses and then weigh models accordingly, rather than treating all models equally.

One way to estimate the expertise of ensemble members is through confusion matrices, which show how often a model predicts each class versus the true class. In the example above, model C has a diagonal confusion matrix, the confusion matrix for model A has higher diagonal weights for animal rows, but more uniform weights for vehicle rows. Confusion matrices quantify the expertise across ensemble members. However, we do not have access to ground truth classes while making predictions, thus the aggregation method should estimate confusion matrices.

Aggregation of different classifier predictions and estimation of their confusion matrices is explored in crowdsourcing literature (Sheng and Zhang, 2019). Majority voting (MV) is a baseline in which the mode of class predictions is chosen. MV weighs each classifier equally and does not estimate confusion matrices (similar to EA). The popular approach that estimates confusion matrices and hence weighs the classifiers differently is Dawid Skene (DS) (Dawid and Skene, 1979), which uses the expectation-maximization (EM) algorithm (Dempster et al., 1977). The Bayesian version of this model is Bayesian classifier combination (BCC) (Ghahramani and Kim, 2003; Simpson et al., 2013).

Crowdsourcing is usually used to aggregate labels from humans, who normally provide only a class label for each data point without confidence of this label, i.e. a *hard label*. When aggregating the outputs of neural networks the output probabilities are usually available, i.e. *soft labels*. These outputs can be biased or miscalibrated (Guo et al., 2017). Despite this miscalibration, it has been demonstrated, soft labels improve the generalisation of neural networks (Hinton et al., 2015; Peterson et al., 2019; Uma et al., 2020; Grossmann et al., 2022). Therefore, we propose to use soft labels for aggregating predictions of an ensemble.

In the context of crowdsourcing, EA corresponds to MV, where outputs of

each crowd member have an equal weight in the consensus answer. MV has been a strong baseline in crowdsourcing literature (as EA in ensembling) and is often used in practice due to its simplicity. However, for hard labeling, crowdsourcing models that weigh crowd members differently according to their skills outperform MV (Dawid and Skene, 1979; Ghahramani and Kim, 2003; Zhou et al., 2012; Simpson et al., 2013; Li et al., 2019). Using this insight, we explore whether using aggregation with different weights would be beneficial for soft labels as well.

We propose an extension of DS model to soft labels, which we call Soft Dawid Skene (SDS). DS assumes the crowd labels have the multinomial distribution which we replace with the Dirichlet distribution. We still use the EM-algorithm, but M step is no longer analytically tractable, so we use the automatic differentiation approach (Paszke et al., 2019). We also add Polyak averaging to the E step to stabilize the convergence (Polyak, 1990). We then conduct extensive experiments on MNIST, CIFAR10/100, and ImageNet distributional shift data, showing that estimation of the confusion matrices improves the accuracy and calibration of the ensemble. We also conduct the out-of-distribution detection experiments to demonstrate usefulness of inferred uncertainties. Our main contributions are:

- We propose a soft label voting model and algorithm for aggregation of classifiers.
- We apply this algorithm to aggregate predictions of an ensemble of neural networks.
- Experiments on distributional shift data and out-of-distribution detection show superiority of the proposed algorithm to baselines.

2 Motivation

Even for simple identical architectures and small datasets, ensemble members can have different expertise, therefore weighing them equally for the aggregated prediction, as it is done in EA, may be suboptimal.

To demonstrate it, Figure 1 presents the confusion matrices for two different ensemble members that show the proportion of predicted and true labels for each class. These are results for the MNIST dataset (LeCun et al., 1998) with additionally applied rotation transformation for validation data (a detailed explanation of the experimental setup is given in section 6). Although these confusion matrices are generated for the ensemble members trained in the same way, there are multiple substantial differences in them. For example, when model 2 predicts “3” the probabilities that the true class for this data point are “3” or “4” are almost equal. In contrast, model 1 predicts “3” with the high probability of being correct. Therefore, when we combine predictions of these models, we should weigh model 1 more than model 2 when they predict “3”. This example shows that the confusion matrices contain valuable information about reliability of the ensemble members, which can be used for inferring joint predictions.

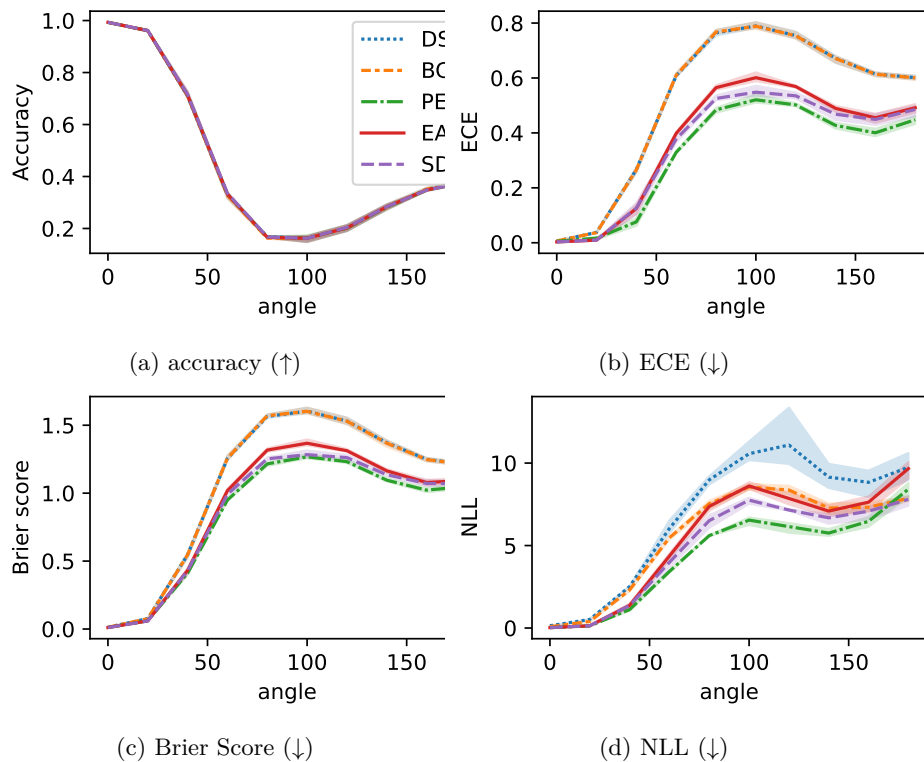


Figure 2: Results on MNIST with rotations of increasing angle: (a) accuracy, (b) ECE, (c) Brier score, (d) NLL. Here, several methods demonstrate similar performance, and some lines are not visible. Thus, all methods have similar accuracy and DS and BCC methods have similar ECE and Brier score.

The confusion matrices in Figure 1 are computed using the ground truth labels, which are not available in practice. There are methods from crowdsourcing literature that estimate these confusion matrices on the fly without access to the ground truth, such as (Dawid and Skene, 1979; Simpson et al., 2013). However, most of them use only hard labels, that are class assignments from crowd members. Therefore, they ignore all the information about individual model uncertainty encoded in soft labels, i.e., predicted probabilities of each class, when they are applied in ensembling.

As it turns out this information encoded in soft labels is important for inferring ensemble predictions, because EA, that does not use confusion matrices but uses soft labels, outperforms crowdsourcing models, that estimate confusion matrices but use hard labels. This is despite the fact that probability estimates of modern neural networks can be miscalibrated. Figure 2 shows this on the rotated MNIST example (more details about the experiment and metrics used can be found in section 6). Unsurprisingly, here crowdsourcing models DS (Dawid and

Skene, 1979) and BCC (Simpson et al., 2013), that use hard labels and thus ignore ensemble members’ uncertainty, show worse results in calibration metrics (expected calibration error (ECE) (Naeini et al., 2015) and Brier score (Brier, 1950)) than EA (Lakshminarayanan et al., 2017), that utilises soft labels.

In these two examples in Figure 1 and 2 we have shown that both model reliability, that can be estimated with a confusion matrix, and model uncertainty encoded in soft labels, are useful for inferring accurate and calibrated predictions of an ensemble. Therefore, we propose the *Soft Dawid Skene model* that uses both these sources of information.

3 Soft Dawid Skene (SDS) model

We assume that there is a dataset of N data points and there are K classifiers. Data points belong to one of the J true labels $t_i \in \{1, \dots, J\}, i \in \{1, \dots, N\}$. However, we only observe probabilities of each of J labels predicted by classifiers. Let $\mathbf{c}_i^{(k)} = \{c_{il}^{(k)}\}_{l=1}^J \in [0, 1]^J$ denote the vector of probabilities of classifier k for data item $i, k \in \{1, \dots, K\}, i \in \{1, \dots, N\}$. We assume that classifiers are conditionally independent given the true labels and each has its own confusion matrix $\mathbf{\Pi}^{(k)} = \{\pi_{jl}^{(k)}\}_{j,l=1}^J \in [0, \infty)^{J \times J}$, which is a prior matrix of probabilities of misclassification, $\pi_{jl}^{(k)}$ is the indicator of the probability that classifier k predicts label l when the true label is j . By an ‘indicator’ here we mean the parameter of the corresponding Dirichlet distribution as it is shown below. Hereafter, we will refer to $\mathbf{\Pi}^{(k)}$ as confusion matrices for simplicity.

The assumption of classifier conditional independence is strong as predictions of neural networks may be correlated. However, we show empirically that even with this assumption predictions made by our model are better than EA. Some work on correlated confusion matrices in crowdsourcing is undertaken in, e.g., (Ghahramani and Kim, 2003), but it is out of scope of this paper.

We model the distribution for t_i as multinomial with parameters $\boldsymbol{\nu} = \{\nu_j\}_{j=1}^J \in [0, 1]^J: p(t_i = j | \boldsymbol{\nu}) = \nu_j$.

The prior of classifiers’ predicted probabilities \mathbf{c}_i^k is set as the Dirichlet distribution: $\mathbf{c}_i^{(k)} \sim \text{Dir}(\boldsymbol{\pi}_{t_i}^{(k)})$, where $\boldsymbol{\pi}_{t_i}^{(k)} = \{\pi_{t_i l}^{(k)}\}_{l=1}^J$. That is

$$p(\mathbf{c}_i^{(k)} | \boldsymbol{\pi}_{t_i}^{(k)}) = \frac{1}{B(\boldsymbol{\pi}_{t_i}^{(k)})} \prod_{l=1}^J c_{il}^{(k) \pi_{t_i l}^{(k)} - 1},$$

where $B(\cdot)$ is the Beta function. And with the assumption of conditional independence of classifiers, the distribution of predictions of all classifiers $\mathbf{c}_i = \{\mathbf{c}_i^{(k)}\}_{k=1}^K$ is $p(\mathbf{c}_i | t_i, \mathbf{\Pi}) = \prod_k p(\mathbf{c}_i^{(k)} | \boldsymbol{\pi}_{t_i}^{(k)})$, where $\mathbf{\Pi} = \{\mathbf{\Pi}^{(k)}\}_{k=1}^K$.

To summarise, in SDS the observed data is classifiers’ labels $\mathbf{C} = \{\mathbf{c}_i\}_{i=1}^N$, latent data is true labels $\mathbf{t} = \{t_i\}_{i=1}^N$, and parameters are priors of class probabilities $\boldsymbol{\nu}$ and confusion matrices $\mathbf{\Pi}$.

4 EM algorithm

An EM algorithm (Dempster et al., 1977) is an iterative algorithm that fits the model by finding the maximum likelihood estimate of the marginal likelihood $p(\mathbf{C} | \boldsymbol{\nu}, \mathbf{\Pi}) = \int p(\mathbf{C}, \mathbf{t} | \boldsymbol{\nu}, \mathbf{\Pi}) d\mathbf{t}$ using the Q function:

$$Q(\boldsymbol{\nu}, \mathbf{\Pi} | \boldsymbol{\nu}^{\text{old}}, \mathbf{\Pi}^{\text{old}}) = \mathbb{E}_{\mathbf{t} | \mathbf{C}, \boldsymbol{\nu}^{\text{old}}, \mathbf{\Pi}^{\text{old}}} [\log p(\mathbf{C}, \mathbf{t} | \boldsymbol{\nu}, \mathbf{\Pi})],$$

where $\boldsymbol{\nu}^{\text{old}}, \mathbf{\Pi}^{\text{old}}$ are the values of parameters at the previous iteration. In our model the Q function is

$$\begin{aligned} Q &= \sum_i \sum_j p(t_i = j | \mathbf{C}, \boldsymbol{\nu}^{\text{old}}, \mathbf{\Pi}^{\text{old}}) \\ &\times \left[\log \nu_j + \sum_k \sum_l (\pi_{jl}^{(k)} - 1) \log c_{il}^{(k)} \right. \\ &\left. - \sum_k \left(\sum_l \log \Gamma(\pi_{jl}^{(k)}) - \log \Gamma\left(\sum_l \pi_{jl}^{(k)}\right) \right) \right], \end{aligned} \quad (1)$$

where $\Gamma(\cdot)$ is the Gamma function. And we want to find the parameters that maximize it by iterating E and M steps: $Q \rightarrow \max_{\boldsymbol{\nu}, \mathbf{\Pi}} Q$.

M Step. In the maximization (M) step, we find the new estimates of the parameters that maximize Q : $\boldsymbol{\nu}^{\text{new}}, \mathbf{\Pi}^{\text{new}} = \arg \max_{\boldsymbol{\nu}, \mathbf{\Pi}} Q(\boldsymbol{\nu}, \mathbf{\Pi} | \boldsymbol{\nu}^{\text{old}}, \mathbf{\Pi}^{\text{old}})$. Hereafter, we omit the superscripts “new” and “old” for readability.

Maximise $\boldsymbol{\nu}$. Maximization of $\boldsymbol{\nu}$ subject to $\sum_j \nu_j = 1$, as this is a probability distribution, is a convex constrained optimization problem, which can be solved with Lagrange multipliers: $\mathcal{L}_{\boldsymbol{\nu}} = \sum_i \sum_j p(t_i = j | \mathbf{C}, \boldsymbol{\nu}, \mathbf{\Pi}) \log \nu_j - \lambda(\sum_j \nu_j - 1) \rightarrow \max_{\boldsymbol{\nu}}$, where λ is a Lagrange multiplier. The optimal class priors is just a mean probability of class being j given the current estimates of confusion matrices and observed classifier labels:

$$\nu_j = \frac{\sum_i p(t_i = j | \mathbf{C}, \boldsymbol{\nu}, \mathbf{\Pi})}{\sum_i \sum_{j'} p(t_i = j' | \mathbf{C}, \boldsymbol{\nu}, \mathbf{\Pi})}. \quad (2)$$

Maximise $\mathbf{\Pi}$. In this step we want to find the new estimates of confusion matrices $\mathbf{\Pi}$ that maximize Q . In our model confusion matrices are not required to be normalized, as they are only used as priors for the Dirichlet distributions. However, the gradient of Q with respect to $\mathbf{\Pi}$ involves the digamma functions, and the updated values of $\mathbf{\Pi}$ are analytically intractable.

Instead, we use automatic differentiation from PyTorch (Paszke et al., 2019) to perform the M step for $\mathbf{\Pi}$. That is, we set Q function (eq. (1)) as a loss function and $\mathbf{\Pi}$ as parameters for optimisation. Additionally, optimiser’s weight decay limits the large values, that would otherwise cause instability at the E step. We use AdamW optimiser (Loshchilov and Hutter, 2017). The exact values of weight decay play a small role, just some weight decay needs to be present. We do not need to run the optimiser until convergence, as we have an outer loop of the EM algorithm. We found that 5 optimiser steps are sufficient.

E Step. At the expectation (E) step we compute the expectations of the Q function to update estimates of latent \mathbf{t} with the current estimates of $\boldsymbol{\nu}$ and $\mathbf{\Pi}$:

$$\begin{aligned} \log p(t_i = j | \mathbf{C}, \boldsymbol{\nu}, \mathbf{\Pi}) &\propto \log \nu_j + \sum_{k,l} (\pi_{jl}^{(k)} - 1) \log c_{il}^{(k)} \\ &- \sum_k \left(\sum_l \log \Gamma(\pi_{jl}^{(k)}) - \log \Gamma(\sum_l \pi_{jl}^{(k)}) \right). \end{aligned} \quad (3)$$

Let $p_{\text{new}}(t_i)$ be the new estimates of \mathbf{t} from eq. (3), $p_{\text{old}}(t_i)$ be the current estimates of \mathbf{t} , and $\alpha \in [0, 1]$ be the weight of the new estimate. We use Polyak averaging (Polyak, 1990):

$$p(t_i = j | \mathbf{C}, \boldsymbol{\nu}, \mathbf{\Pi}) = (1 - \alpha)p_{\text{old}}(t_i) + \alpha p_{\text{new}}(t_i), \quad (4)$$

to improve the stability of the algorithm due to the approximate M step.

4.1 Full Algorithm

The EM algorithm requires initial values of the parameters and latent variables and stopping criteria. For initialization of $\mathbf{\Pi}$ and $\boldsymbol{\nu}$, we use one iteration of the DS algorithm (Dawid and Skene, 1979) on hard versions of \mathbf{C} , i.e., class values that have the maximum value in the corresponding probability vector. For the initial values of probabilities of \mathbf{t} we use the EA algorithm (Lakshminarayanan et al., 2017). The EM algorithm iterates until convergence of the Q function. However, in practice we found that the fixed number of iterations is sufficient. The full algorithm is shown in Algorithm 1. The values of all hyperparameters of the algorithm used in the experiments can be found in Appendix D. We provide an illustrative example how SDS works in Appendix C.

Algorithm 1 EM algorithm for SDS

```

Initialise  $\mathbf{\Pi}$  and  $\boldsymbol{\nu}$  with the DS algorithm
Initialise  $\mathbf{t}$  with the EA algorithm
while true do
  E step:
    Compute  $\log p(t_i = j | \mathbf{C}, \mathbf{\Pi}^{\text{old}})$  for all  $i, j$  (3)
    Update  $\mathbf{t}$  with Polyak averaging (4)
  M step:
    Update  $\boldsymbol{\nu}$  using (2)
    Update  $\mathbf{\Pi}$  with the automatic differentiation optimiser on (1)
  Check convergence of  $Q$  function
end while

```

5 Related works

Ensemble learning and crowdsourcing are two relevant areas for weighted aggregation of models.

Ensembling. Despite the popularity of ensembling only EA or hard label MV are used for aggregation. Many works on ensembling focus on diversifying ensemble members: e.g., bagging (Breiman, 1996; Huang et al., 2015; Rew et al., 2021; Wei et al., 2024), particle-based inference, (D’Angelo and Fortuin, 2021), or others (Jain et al., 2020; Zhang et al., 2020a). These approaches are complimentary to ours as they still use averaging for aggregation of ensemble member predictions.

We consider the case where pre-trained neural networks are used in an ensemble to predict on new data, without access to the training data during prediction and ensembling. This is in contrast to boosting-type and stacked ensembling methods, when a top-level classifier is trained using responses from ensemble members, e.g. (Mao, 1998; Zhang et al., 2020b; Moghimi et al., 2016; Young et al., 2018; Das et al., 2022; Li and Pan, 2022; Walach and Wolf, 2016; Li et al., 2022). This is also different to probabilistic ensembling (Wang and Ji, 2023), which builds a mixture of Gaussians (MoG) using Laplace approximation (Daxberger et al., 2021) and requires training labels. Ensemble members are trained sequentially in a boosting manner.

To the best of our knowledge, from the ensembling literature (Ganaie et al., 2022; Dong et al., 2020) EA or hard label MV are the only methods for prediction aggregation that exist for our setting. Averaging method from (Huang et al., 2015) can satisfy our setting but it is only applicable for the autoencoder neural networks.

Crowdsourcing. While the majority of the crowdsourcing literature use hard labels, there are a few works that deal with soft labels from crowd members (Nazábal et al., 2015; Méndez Méndez et al., 2022; Augustin et al., 2017; Chung et al., 2019). However, to the best of our knowledge none are applicable to our setting of ensembling deep learning models. They either use the mode (or median) of soft crowd labels (Méndez Méndez et al., 2022; Chung et al., 2019; Collins et al., 2022), i.e., the equivalent of EA, or they are used for the problems where the ground truth labels are expected to be soft (Augustin et al., 2017), e.g., in text categorization where a label for each document is the set of proportions of each category in the text. In contrast to the latter setting we expect soft labels from ensemble (crowd) members but the ground truth label to be a single class label, i.e., a hard label.

Nazábal et al. (2015) similarly to us propose a soft label extension of the existing crowdsourcing method, BCC in their case. Steyvers et al. (2022) at the intersection of crowdsourcing and ensembling combine soft predictions from human and machine classifiers. However, in contrast to our method, inference of test ground truth classes in both these works requires at least part of the training ground truth classes to be known. Thus, they are unapplicable in our setting.

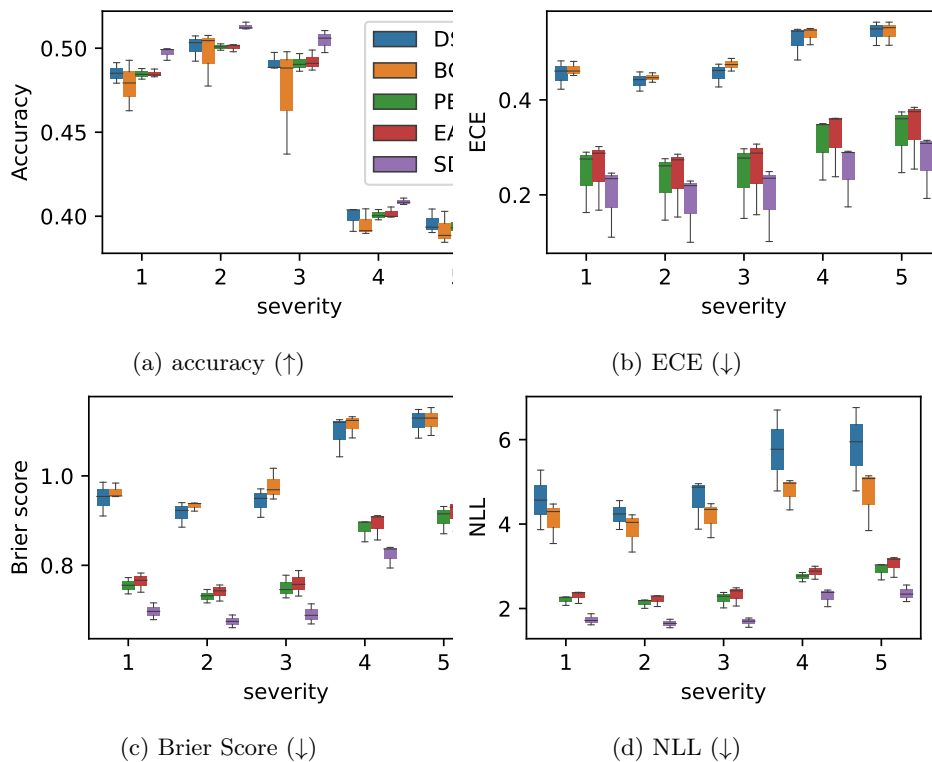


Figure 3: Results on CIFAR10 with Frosted Glass Blur corruption of increasing severity: (a) accuracy, (b) ECE, (c) Brier score, (d) NLL.

6 Experiments

Ensembling is used to improve accuracy and calibration. Calibrated predictions provide an invaluable tool for safe deployment, when a data distribution may deviate from the training distribution. Therefore, we evaluate the proposed SDS on the distributional shift and out-of-distribution detection datasets (Ovadia et al., 2019). Full implementation details are given in Appendix E.

We use MNIST (LeCun et al., 1998), CIFAR10/100 (Krizhevsky et al., 2009), and ImageNet-1K (Russakovsky et al., 2015) datasets with a distributional shift by providing the corrupted versions of validation data. For MNIST we use the rotated validation data with the angle of rotation varying from 0° to 180° . For CIFAR10/100 and ImageNet we use corruptions from Hendrycks and Dietterich (2019). Results on validation data without corruption can be found in Appendix G. Additionally, we evaluate SDS on out-of-distribution (OOD) detection. We consider the pairs of in/out-distributions as: CIFAR10/100, CIFAR10/SVHN (Netzer et al., 2011), CIFAR100/10, CIFAR100/SVHN, where we vary the ratio of OOD examples.

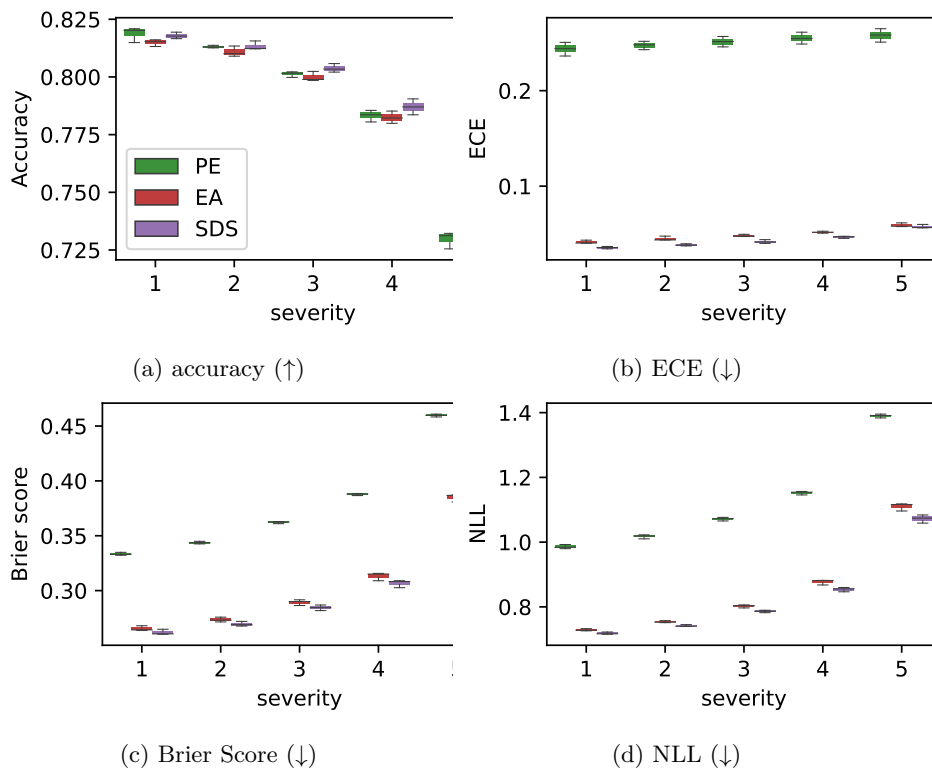


Figure 4: Results on CIFAR100 with Brightness corruption of increasing severity: (a) accuracy, (b) ECE, (c) Brier score, (d) NLL.

For all datasets we use an ensemble of 3 members and we repeat experiments 3 times, i.e., taking $3 * 3 = 9$ independently trained networks and combining them into ensembles. Different ensemble sizes are considered in Appendix H.

We compare 5 methods: DS (Dawid and Skene, 1979), BCC (Simpson et al., 2013), EA (Lakshminarayanan et al., 2017), probabilistic ensembling (PE) (Wang and Ji, 2023) and SDS. DS and BCC use the hard labels from ensemble members, whereas EA and SDS use the soft labels. The full approach from Wang and Ji (2023) would be unfair as it includes training different ensemble members. We employ the plug-and-play version of PE, where only MoG is built on Laplace approximations of the existing ensemble members. It is worth noting that PE still has unfair advantage as Laplace approximation requires access to training labels, while all the rest of methods do not use any labels and training data in general. Also, PE is much more computationally expensive in comparison to other methods. Full computational costs are provided in Appendix I. Moreover, we cannot apply PE to ImageNet data as it requires 977 GiB of GPU memory.

We also consider an online version of SDS where we fix confusion matrices after estimating them (without supervision) on a batch of data and then we

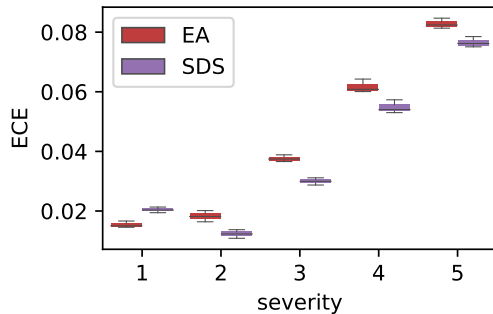


Figure 5: ECE (\downarrow) results on ImageNet with Zoom Blur corruption of increasing severity. The other 3 metrics have similar results for both methods.

infer only true labels via E step for the rest of the data which can be done in a streaming way (Appendix F).

We evaluate accuracy, expected calibration error (ECE) (Naeini et al., 2015), Brier score (Brier, 1950), and negative log-likelihood (NLL). The 3 latter metrics are used for measuring calibration. For the OOD experiment we measure the area under receiver operating characteristic curve (AUROC).

6.1 Rotated MNIST

The results for rotated MNIST are present in Figure 2. In terms of accuracy all methods show similar performance. Hard label DS and BCC have also similar ECE and Brier score, that are worse than the results of both soft label EA and SDS. BCC, however, outperforms EA in terms of NLL for large angles of rotations. SDS outperforms DS, BCC, and EA in all 3 calibration metrics. This confirms that using both soft labels and confusion matrix estimation is beneficial for calibrated prediction ensembling. PE shows the best results in calibration metrics, but it does that with much higher computational cost and use of training labels.

6.2 CIFAR10

The results for “Frosted Glass Blur” corruption on CIFAR10 are in Figure 3. Full results for all corruption types can be found in Appendix J.1. SDS has better results in terms of all 4 metrics. For all the other corruption types SDS has either similar or better results than EA and PE in all 4 metrics. DS and BCC demonstrate poorer performance than the other methods in the majority of cases.

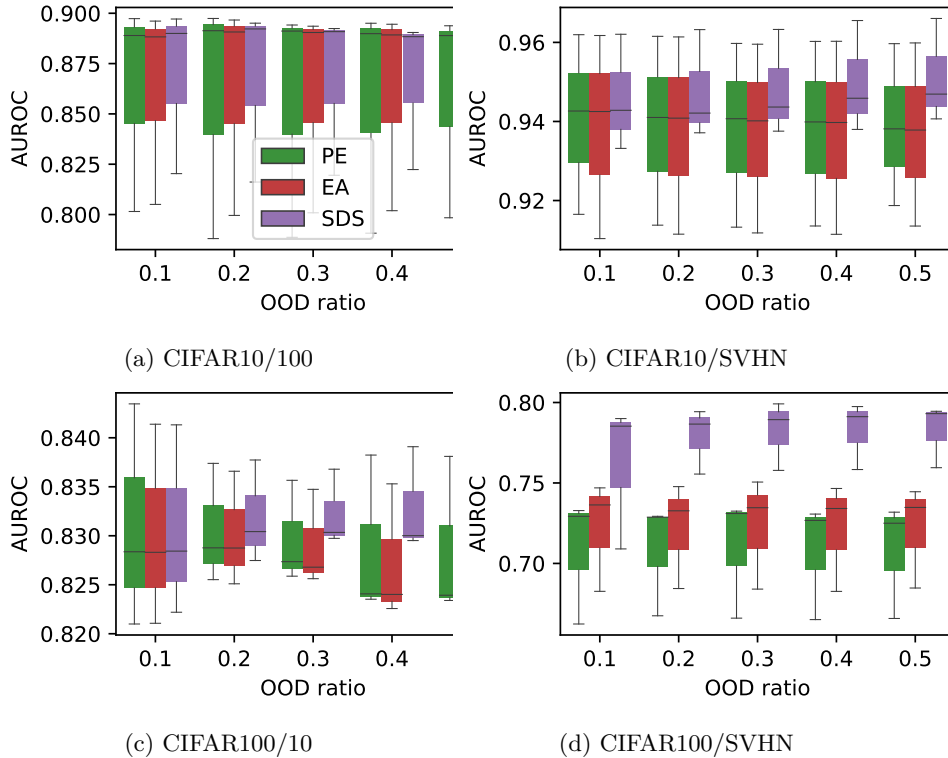


Figure 6: AUROC (\uparrow) results for OOD of increasing ratio of OOD examples in the validation dataset.

6.3 CIFAR100

Figure 4 shows the results for “Brightness” corruption on CIFAR100. All corruption type results can be found in Appendix J.2 (for visibility we exclude poor calibration DS and BCC results from the figure but they can be found in Appendix). SDS provides the best results in all calibration metrics and for most of severity levels in accuracy. For the other corruption types in comparison to EA, SDS shows similar results in accuracy and NLL, while SDS has better performance in Brier score and ECE than EA. In 19% cases EA outperforms in Brier and ECE for some severity levels. However, the absolute values for both methods in these cases are very small, therefore, SDS still provides good results. PE outperforms SDS in only 35% cases in calibration metrics and it achieves this at a much higher computational cost and requires the use of training labels.

6.4 ImageNet

Figure 5 presents the ECE results on ImageNet with “Zoom Blur” corruption. We present results of EA and SDS for ECE only as for the other metrics performances of both methods are very similar (we excluded DS and BCC for better visibility due to poor performance of these methods). Full results including DS and BCC for all corruption types are in Appendix J.3. For the majority of corruption types SDS outperforms EA in ECE. All other metrics have similar results for both methods.

6.5 Out-of-distribution Detection

The OOD results are in Figure 6 (due to previous poor results we exclude DS and BCC). PE and EA show similar results in 3 dataset pairs while EA shows better performance on CIFAR100/SVHN pair. SDS shows similar AUROC on CIFAR10/100 pair and outperforms both PE and EA on other dataset pairs especially as the ratio of OOD examples increases. This shows that uncertainties estimation provided by SDS is more useful for this downstream task of OOD detection.

7 Conclusions

We present the Soft Dawid Skene method for ensembling (and crowdsourcing). Compared to EA, it additionally estimates the confusion matrices thus improving aggregated predictions by weighing ensemble members according to their inferred performance. Compared to DS, it operates with soft labels, which improves calibration of predictions by incorporating uncertainty of individual ensemble members. Inclusion of soft labels in Dawid Skene model requires different priors and different inference methods.

We perform extensive evaluation of SDS on classification datasets with a distributional shift and OOD detection and show that SDS demonstrates similar or better performance than the state-of-the-art EA both in terms of accuracy and calibration of the predictions. As we discussed above, EA is the only existing alternative for aggregation of ensemble members’ predictions that does not use training data. Therefore, for the first time we provide another competitive option for ensemble aggregation.

We only provide the empirical results for ensembles where each ensemble member is a neural network of the same architecture but trained independently on the same data. This is one of the most challenging settings for the model as it violates the assumption of conditional independence of ensemble members. We expect SDS to demonstrate even larger difference with EA for the settings where ensemble members are less correlated (for example, when coupled with bagging or knowledge distillation). We will explore these cases in the future.

A Introduction

This appendix provides technical details about the experiments and additional results for the main paper.

B Notation

Here we recall the main notation from the paper:

- N — the number of data points in a dataset;
- K — the number of classifiers, i.e., ensemble members;
- J — the number of classes;
- $\mathbf{t} = \{t_i\}_{i=1}^N, t_i \in \{1, \dots, J\}$ — true labels of the data points (hidden);
- $\mathbf{C} = \{\mathbf{c}_i\}_{i=1}^N, \mathbf{c}_i = \{\mathbf{c}_i^{(k)}\}_{k=1}^K, \mathbf{c}_i^{(k)} = \{c_{il}^{(k)}\}_{l=1}^J \in [0, 1]^J$ — predicted probabilities of class labels given by the ensemble members;
- $\mathbf{\Pi} = \{\mathbf{\Pi}^{(k)}\}_{k=1}^K, \mathbf{\Pi}^{(k)} = \{\pi_{jl}^{(k)}\}_{j,l=1}^J \in [0, \infty)^{J \times J}$ — confusion matrices (more precisely, these are parameters of the prior Dirichlet distribution of the actual confusion matrices, but we refer to $\mathbf{\Pi}^{(k)}$ as a confusion matrix for simplicity);
- $\boldsymbol{\nu} = \{\nu_j\}_{j=1}^J \in [0, 1]^J$ — prior multinomial distribution of the true labels.

C Illustrative example of how SDS works in practice

In this section we provide an example how SDS works in practice and how the use of confusion matrices and soft labels allows it to outperform baselines.

Let us consider a sample (one data point) from CIFAR100 with Brightness corruption at severity level 3 (section 6.3 of the main paper). For this sample SDS predicts the correct class label and EA does not. Hereafter, we refer to the softmax output as the model’s confidence.

This data sample (number 35 in the validation dataset) belongs to class 73. The three ensemble members predict classes 57, 95, and 38, respectively. EA predicts class 57 because ensemble member 1 is overconfident in its prediction (with a confidence of 0.22), which dominates the votes from the other two members (whose maximum confidences are 0.12 and 0.13, respectively).

SDS, however, predicts the correct class, 73. Its decision is more nuanced than that of EA. The prediction of a class label is the maximum of probabilities given in eq. (3) in the main paper:

$$\log p(t_i = j | \mathbf{C}, \boldsymbol{\nu}, \mathbf{\Pi}) \propto \log \nu_j + \sum_{k,l} (\pi_{jl}^{(k)} - 1) \log c_{il}^{(k)} - \sum_k \left(\sum_l \log \Gamma(\pi_{jl}^{(k)}) - \log \Gamma(\sum_l \pi_{jl}^{(k)}) \right).$$

Let us focus on the second term of this equation (which determines the class prediction in this case):

$$\sum_{k,l} (\pi_{jl}^{(k)} - 1) \log c_{il}^{(k)}. \quad (\text{A.1})$$

The other two terms of eq. (3) are similar for different j and thus do not define the class label.

First, we need to notice that all soft labels (class probabilities) from each ensemble member are used in the decision, not just the class with the maximum confidence, as it is usually the case for EA.

Now, let us interpret the confusion matrices learned by SDS. When class 73 is the correct class, ensemble member 1, according to confusion matrices learnt by SDS, would output classes [23, 30, **67**, 72, **73**, 87, 91, **95**] with higher probabilities (higher than average).

If we check the top-10 classes predicted by ensemble member 1 for our sample, they are [57, 69, 65, 38, **67**, 27, **95**, 79, 32, **73**]. The highlighted class labels appear in both lists, meaning they will significantly contribute in eq. (A.1) as votes for class 73.

Similarly, when class 73 is the correct class, ensemble member 2, according to SDS, would output classes [**30**, 67, **73**, 93, **95**] with higher probabilities.

For our data sample, ensemble member 2 outputs the top-10 classes as: [**95**, **73**, 74, 44, **30**, 27, 72, 38, 50, 19]. Thus, three elements in the sum from eq. (A.1) significantly contribute to the vote for class 73.

Finally, when class 73 is the correct class, SDS has learned that ensemble member 3 would output classes [10, 23, 30, 44, 62, 67, 70, **73**, 84, 91, 93, **95**].

The top-10 classes that ensemble member 3 predicts for the given data sample are: [38, 72, **95**, **73**, 69, 57, 34, 74]. Two elements would significantly contribute to the vote for class 73 in eq. (A.1).

In fact, these contributions are enough for SDS to predict the correct class, even though none of the ensemble members individually guesses the correct class.

From this example, we can see that SDS improves the performance by looking at all soft outputs from ensemble members combined with confusion matrices, i.e. learnt mistake patterns, for these ensemble members.

D Hyperparameters

Our proposed EM algorithm for Soft Dawid Skene (SDS) model has the following hyperparameters:

- α — the weight of the new estimate of \mathbf{t} in Polyak averaging in E-step of the algorithm (see eq.(11) in the main text);
- number of iterations of the full EM algorithm — though in theory it can be run until the convergence of the Q function, we find in practice it is enough to run it for the limited number of iterations;
- parameters of the optimiser used for M-step for optimising $\mathbf{\Pi}$:
 - type of optimiser. Any optimiser is suitable here, we use AdamW (Loshchilov and Hutter, 2017) in all our experiments;
 - learning rate of the optimiser. We found that 10^{-4} provided good results for all datasets;

- weight decay. Our initial experiments showed that the actual value of this parameter does not matter much as long as the weight decay is present, so we set it to 10^{-4} for all experiments;
- number of iterations of the optimiser — since this optimisation is internal inside the outer EM loop, we do not need to run the optimiser until convergence at every M-step. Our initial experiments showed that a small number of iterations (i.e. 5) already provided sufficient results. We use 5 for MNIST, CIFAR10/100. For ImageNet experiments even 1 iteration of the optimiser was sufficient.

For α we use the range $[10^0, 10^{-1}, 10^{-2}, 10^{-3}, 10^{-4}, 10^{-5}, 10^{-6}]$ for tuning. We also incorporated simple scheduling for α , where we changed its value once during the training. We optimise both when the change happens and to which value α changes.

It is worth noting that $\alpha = 1$ corresponds to the case when no Polyak averaging is used during the E step of the algorithm. By using it during tuning we simultaneously conducted an ablation study on whether Polyak averaging is required. For all datasets we have observed a very poor performance with $\alpha = 1$, therefore, we have confirmed that this step is essential for our algorithm.

For the number of iterations we set initially the number of iterations to be large (e.g., 500), and then choose the final number based on the historical performance over the number of iterations. Since we use 4 different metrics for comparison, which are not necessarily optimised with the same values of hyperparameters, we manually assess the result of different hyperparameter values and choose values that provide a good trade-off for all 4 metrics.

The final hyperparameter values we use in the experiments are given in Table 1. Here, the list of values for α means that we apply the change of values for α during the EM iterations and the second row of the table specifies at which iteration this change occurs.

Table 1: Hyperparameter values used in the experiments

Hyperparameter	MNIST	CIFAR-10	CIFAR-100	ImageNet
α	10^{-3}	10^{-3}	$[10^{-5}, 10^{-3}]$	$[10^{-3}, 10^{-5}]$
iteration number for α change	—	—	100	20
number of EM iterations	100	100	200	25

E Experimental Details

All experiments are conducted on 24GB NVIDIA Titan RTX GPU / Intel Core i9 10 Core CPU / 128 GB RAM machine with the Ubuntu operating system. We use PyTorch (Paszke et al., 2019) for implementation.

E.1 Datasets

We evaluate performance of SDS on different vision classification datasets.

- MNIST (LeCun et al., 1998): a dataset of handwritten digit recognition with greyscale images of size 28×28 pixels. Each image contains a digit that should be classified into one of 10 classes. For a corrupted version of validation data we rotate the images with angles of rotation ranging from 0° to 180° ;
- CIFAR10/100 (Krizhevsky et al., 2009): a dataset of 32×32 colour images with 10/100 classes respectively. For corrupted versions of validation data we use corruptions from Hendrycks and Dietterich (2019). These are 15 different corruptions ranging from Gaussian noise to fog weather, and each corruption type has 5 severity levels;
- ImageNet-1K (Russakovsky et al., 2015): a dataset of colour images with 1000 classes. For corrupted version of validation data we use corruptions from Hendrycks and Dietterich (2019).

Ensemble members are trained on the clean training data and then evaluated on the corrupted validation data.

In our experiments we first train an ensemble of neural networks on training data independently of each other with different random seeds, then we fit the aggregation algorithms on validation data and evaluate metrics on validation data. Aggregating algorithms do not use true labels to fit, therefore there is no overfitting in this procedure. PE as exception also includes the step of fitting Laplace approximation of each ensemble member on training data.

We further evaluate performance of SDS on OOD tasks. For this we use an ensemble with members trained on X and validation data from X as in-distribution examples and Y as out-of-distribution examples. For this experiment uncorrupted versions of datasets are employed. We take the validation data from X and at random replace a specified ratio of data points with random images from Y . We vary the ratio of these OOD examples as $[0.1, 0.2, 0.3, 0.4, 0.5]$. The pairs of X/Y are considered: CIFAR10/100, CIFAR10/SVHN (Netzer et al., 2011), CIFAR100/10, CIFAR100/SVHN. SVHN: a dataset of 32×32 colour images with 10 classes.

E.2 Neural Network Ensemble Members

E.2.1 MNIST

For MNIST we train 9 neural networks with the following architecture:

```
torch.nn.Sequential(  
    torch.nn.Conv2d(1, 32, 3),  
    torch.nn.ReLU(),  
    torch.nn.Conv2d(32, 64, 3),  
    torch.nn.ReLU(),
```

```

torch.nn.MaxPool2d(2),
torch.nn.Dropout(0.25),
torch.nn.Flatten(),
torch.nn.Linear(9216, 128),
torch.nn.ReLU(),
torch.nn.Dropout(0.25),
torch.nn.Linear(128, 10),
)

```

We train each network for 10 epochs, batch size 24, AdamW optimiser (Loshchilov and Hutter, 2017), learning rate 10^{-3} . No transformation is applied for the data except normalisation. We then combine these 9 neural networks into 3 ensembles of size 3.

E.2.2 CIFAR10

For CIFAR10 we train 9 Resnet18 (He et al., 2016) neural networks (torchvision implementation). We train each network for 40 epochs, batch size 128, stochastic gradient descent (SGD) optimiser, with 10^{-1} initial learning rate, momentum 0.9, weight decay 10^{-4} . Learning rate has a multistep PyTorch scheduler with decay at epochs 20 and 30 by $\gamma = 0.1$. During training random rotations (with degree 90°), random horizontal flip, and normalisation transformations are applied. Only normalisation is applied during inference. We then combine these 9 neural networks into 3 ensembles of size 3.

E.2.3 CIFAR100

For CIFAR100 we use 9 WideResNet28x10 (Zagoruyko and Komodakis, 2016) networks, which trained weights we take from Ashukha et al. (2020). Only normalisation transformation is applied during inference. We then combine these 9 neural networks into 3 ensembles of size 3.

E.2.4 ImageNet

For ImageNet we use 9 ResNet50 (He et al., 2016) networks with pretrained weights from Ashukha et al. (2020). Centre crop with size 224 and normalisation transforms are applied during inference. We then combine these 9 neural networks into 3 ensembles of size 3.

E.3 Ensembling method implementations

For DS we use the implementation from Ustalov et al. (2021)¹ (license Apache). PE implementation uses Laplace approximation from the *laplace* library (Daxberger et al., 2021)² (license MIT).

¹<https://github.com/Toloka/crowd-kit>

²<https://github.com/AlexImmer/Laplace/>

E.4 Metrics

We use the following metrics for comparison:

- Accuracy
- Expected calibrated error (ECE) (Naeini et al., 2015), which is a weighted difference of prediction accuracy and confidence of predictions. We use 300 bins for ECE computation in all experiments.
- Brier score (Brier, 1950), which is the mean difference between the predicted probabilities and the actual outcome
- Negative log likelihood (NLL)

For evaluation metrics we adapt the implementation from Ovadia et al. (2019)³ (license Apache).

F Additional results on online SDS

In this section, we explore an online version of SDS. In the vanilla SDS, as presented earlier, a batch of data is required for the model to learn confusion matrices and class probabilities. Here, we compare it with an online variant. First, we run the vanilla SDS on a subset of test data to learn prior class probabilities, ν and confusion matrices, $\mathbf{\Pi}$ (a learning step). We then fix these learned parameters. For the rest of test data, we only run one E-step of SDS to infer predictions (an inference step). This allows the inference step to be applied to streaming data, processing one data point at a time. Importantly, the entire online version, including both learning and inference, remains fully unsupervised.

Figure 7 presents comparison of the vanilla SDS (offline), online SDS and EA on ImageNet with “Fog” corruption in terms of ECE. We first randomly select 10,000 data points out of validation dataset and run the vanilla SDS on this subset of data. We then fix prior class probabilities ν and confusion matrices $\mathbf{\Pi}$ and apply only E-step on the remaining 40,000 validation data points. It makes the online version significantly faster. It takes around 22 seconds for the learning step (on 10,000 data points) and 1 second for the inference step (on 40,000 data points). By comparison, vanilla SDS takes 82 seconds for 40,000 data points and 114 seconds for the full 50,000 points. (A full computational cost analysis of SDS and baselines is provided in Appendix I.)

We also apply EA and another instance of vanilla SDS (offline SDS) to the 40,000 data points. The ECE results are given in Figure 7. We can see that the online SDS provides results in between of EA and offline SDS. It still gives the performance gain for higher levels of severities, but does it on a fraction of cost of offline SDS. Overall, the online version offers a trade-off between calibration performance and computational efficiency.

³https://github.com/google-research/google-research/blob/master/uq_benchmark_2019/metrics_lib.py

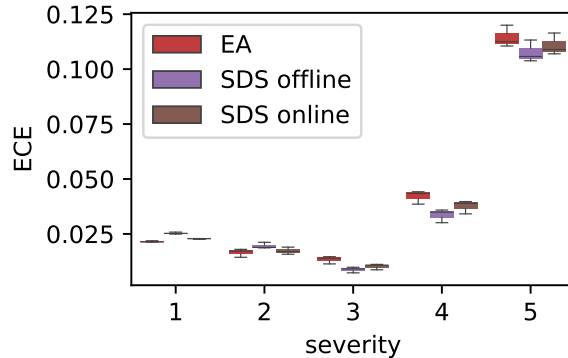


Figure 7: ECE (\downarrow) results for online SDS on ImageNet with Fog corruption of increasing severity.

G Additional results on within datasets

Here we provide the results for original validation data without corruptions. For MNIST it is included in Figure 2 of the main paper as the angle equal 0.

Figures 8–10 present these results for CIFAR10, CIFAR100 and ImageNet, respectively. On CIFAR10 all methods show similar performance with hard-label DS and BCC having less variance between independent runs and underperforming in terms of NLL. The results on CIFAR100 demonstrate advantages of EA and SDS in terms of all 3 calibration metrics, and ImageNet highlights superiority of EA and SDS in all 4 metrics measured.

H Additional results on varying ensemble sizes

Here, we provide the results for comparing different ensemble sizes. For illustrative purposes we show the results of EA (the main baseline) and SDS on CIFAR-100 data with Gaussian Noise corruption with severity 3 (Table 2) and Imagenet with Frost corruption with severity 3 (Table 3). The trend persists for other data. In general, performance slowly increases with the size of the ensembles. Relative performance between different methods stays mostly the same, some differences become significant with the increase of the ensemble size.

I Computational cost analysis

In this section we provide the wall-clock computational cost comparison. We would like to emphasise that we have not made it our goal to optimise implementation of any of the methods we are comparing, therefore, the computational cost provided should not be taken as a true optimal cost.

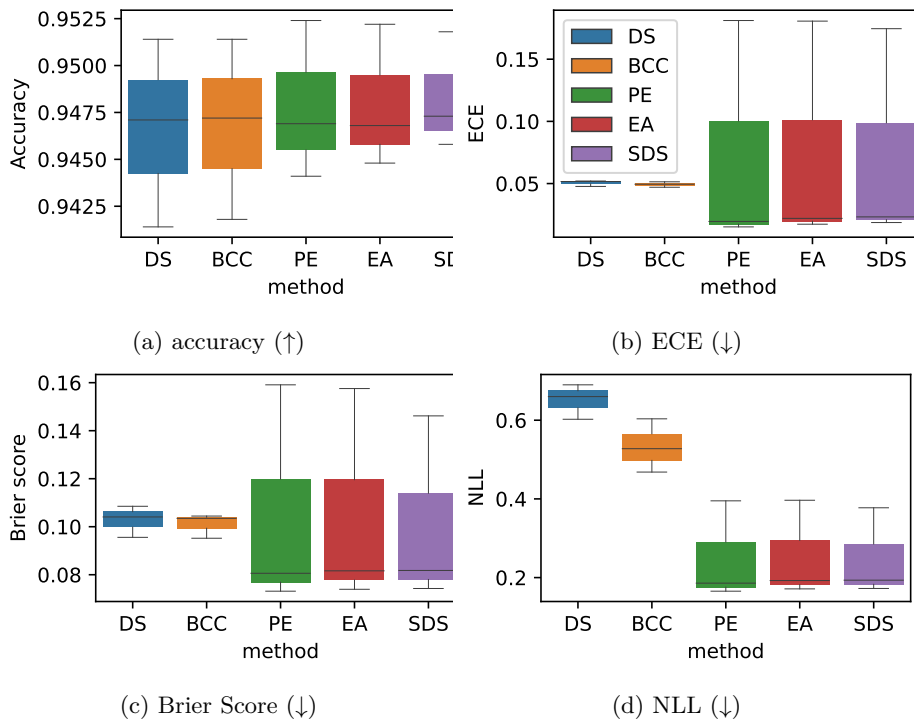


Figure 8: Results on CIFAR10 without corruptions.

Table 2: Results on CIFAR100 with varying ensemble size for Gaussian Noise corruption of severity 3. The mean and std are computed for 3 independent Monte Carlo runs.

Metric	Method	Ensemble size 3	Ensemble size 5	Ensemble size 7	Ensemble size 10
Accuracy	EA	0.116 ± 0.015	0.121 ± 0.010	0.123 ± 0.003	0.124 ± 0.004
	SDS	0.116 ± 0.015	0.121 ± 0.010	0.123 ± 0.003	0.124 ± 0.004
ECE	EA	0.476 ± 0.035	0.410 ± 0.013	0.386 ± 0.017	0.396 ± 0.017
	SDS	0.419 ± 0.033	0.359 ± 0.012	0.337 ± 0.016	0.346 ± 0.016
Brier score	EA	1.280 ± 0.039	1.209 ± 0.017	1.182 ± 0.020	1.193 ± 0.017
	SDS	1.213 ± 0.033	1.157 ± 0.013	1.135 ± 0.017	1.144 ± 0.014
NLL	EA	5.714 ± 0.265	5.374 ± 0.278	5.113 ± 0.254	5.137 ± 0.239
	SDS	5.611 ± 0.212	5.365 ± 0.240	5.115 ± 0.252	5.139 ± 0.246

DS, BCC, EA and SDS are all implemented in the same manner: ensemble members are run on validation data to make predictions (*pred*), then the aggregation method is run on saved predictions (*aggr*). The total run time (*total*) for these 4 methods is then: $pred + aggr$, where *pred* time would be exactly the

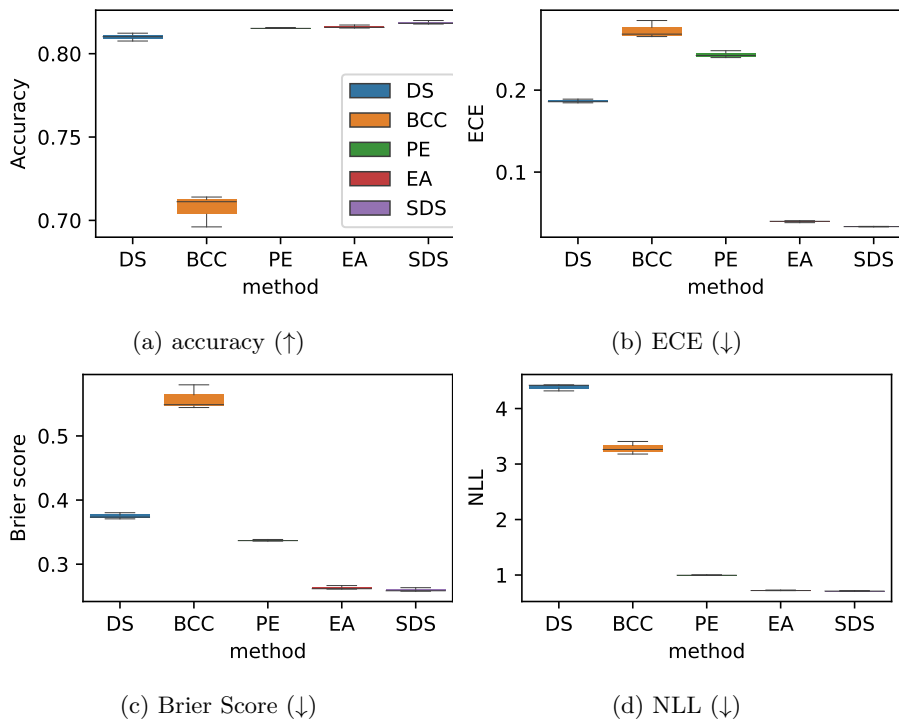


Figure 9: Results on CIFAR100 without corruptions.

Table 3: Results on ImageNet with varying ensemble size for Frost corruption of severity 3. The mean and std are computed for 3 independent Monte Carlo runs.

Metric	Method	Ensemble size 3	Ensemble size 5
Accuracy	EA	0.337 ± 0.001	0.345 ± 0.004
	SDS	0.337 ± 0.001	0.345 ± 0.004
ECE	EA	0.041 ± 0.003	0.022 ± 0.002
	SDS	0.034 ± 0.003	0.018 ± 0.002
Brier score	EA	0.794 ± 0.002	0.785 ± 0.003
	SDS	0.793 ± 0.002	0.785 ± 0.003
NLL	EA	3.478 ± 0.003	3.409 ± 0.025
	SDS	3.492 ± 0.003	3.423 ± 0.025

same for all 4 methods as they use the same predictions.

PE is conceptually different and it is also implemented via the laplace library (Daxberger et al., 2021), which makes it also different from the other methods. First, the Laplace approximation is run for each ensemble members on train data (*lap*). Then predictive samples from these approximations are

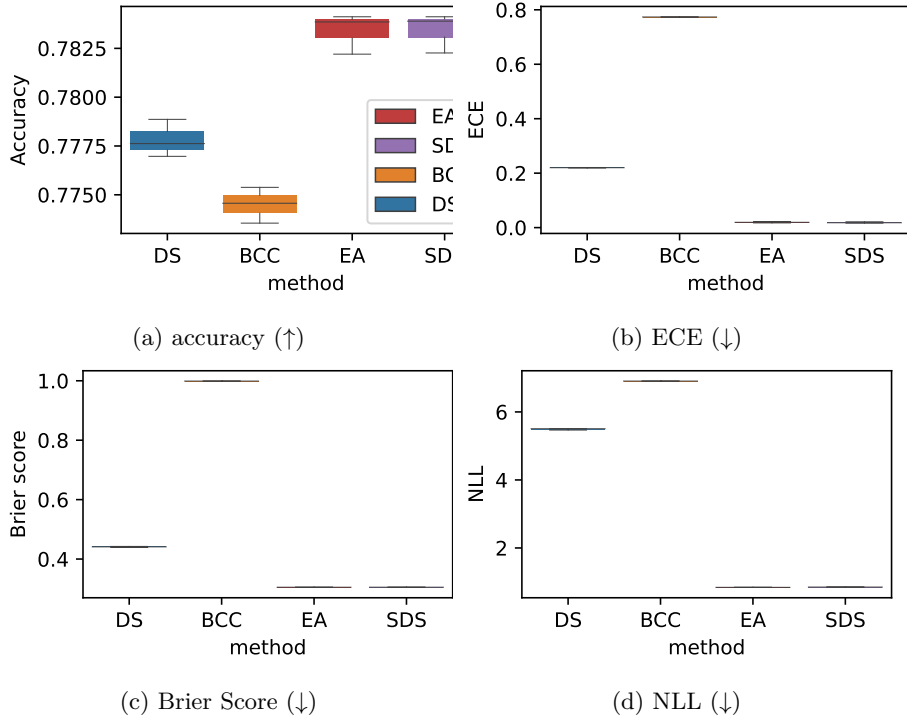


Figure 10: Results on ImageNet without corruptions.

generated on validation data ($pred$). The aggregation is done by taking the mean of predictions ($aggr$). Therefore, the total run time ($total$) for PE is: $lap + pred + aggr$.

Tables 4–5 present the wall-clock computational cost. The Laplace approximation step of PE makes it much slower than the other methods. Even on ImageNet data where we fail to run the prediction step due to the high memory demand because of the Laplace approximation PE would be the slowest method (only BCC has the higher $total$ time but any reasonable $pred$ time for PE would bring the $total$ cost higher).

EA being the simplest method is the fastest. SDS scales better for the large ImageNet dataset than both DS and BCC.

J Results for All Corruptions

All tables provide the mean and std results for 3 independent Monte Carlo runs of each experiment.

Table 4: Computational cost comparison in seconds of different methods for ensemble of size 3 on MNIST and CIFAR10.

Method	MNIST				CIFAR10			
	lap	pred	aggr	total	lap	pred	aggr	total
DS	—	5.5	0.77	6	—	27	0.69	28
BCC	—	5.5	1.04	7	—	27	1	28
PE	39	5	0.002	44	339	27	0.002	366
EA	—	5.5	0.001	6	—	27	0.002	27
SDS	—	5.5	0.88	6	—	27	0.89	28

Table 5: Computational cost comparison in seconds of different methods for ensemble of size 3 on CIFAR100 and ImageNet. X in PE results on ImageNet denote that we cannot run the prediction and aggregation steps.

Method	CIFAR100				ImageNet			
	lap	pred	aggr	total	lap	pred	aggr	total
DS	—	24	3	27	—	285	165	450
BCC	—	24	9	33	—	285	321	606
PE	339	70	0.01	409	597	X	X	>597
EA	—	24	0.05	24	—	285	0.3	285
SDS	—	24	11	35	—	285	114	399

J.1 CIFAR10

Results for all corruptions on CIFAR10 can be found in Tables 6–9.

Table 6: Results on CIFAR10 with noise corruptions of increasing severity.

Corruption Metric	Method	Severity 1	Severity 2	Severity 3	Severity 4	Severity 5
Accuracy	DS	0.676 ± 0.008	0.426 ± 0.014	0.260 ± 0.011	0.218 ± 0.020	0.191 ± 0.019
	BCC	0.678 ± 0.008	0.422 ± 0.009	0.249 ± 0.006	0.212 ± 0.023	0.187 ± 0.021
	PE	0.674 ± 0.012	0.422 ± 0.009	0.262 ± 0.012	0.219 ± 0.017	0.194 ± 0.022
	EA	0.674 ± 0.011	0.422 ± 0.009	0.261 ± 0.013	0.218 ± 0.017	0.193 ± 0.021
	SDS	0.689 ± 0.010	0.437 ± 0.010	0.268 ± 0.011	0.222 ± 0.016	0.195 ± 0.020
Gaussian Noise	DS	0.305 ± 0.012	0.545 ± 0.029	0.705 ± 0.028	0.739 ± 0.043	0.761 ± 0.046
	BCC	0.302 ± 0.016	0.519 ± 0.072	0.483 ± 0.082	0.404 ± 0.077	0.369 ± 0.064
	PE	0.140 ± 0.087	0.355 ± 0.095	0.493 ± 0.096	0.519 ± 0.097	0.527 ± 0.101
	EA	0.152 ± 0.082	0.363 ± 0.097	0.502 ± 0.097	0.530 ± 0.098	0.538 ± 0.100
	SDS	0.149 ± 0.036	0.302 ± 0.090	0.432 ± 0.090	0.460 ± 0.091	0.469 ± 0.093
Brier score	DS	0.619 ± 0.017	1.103 ± 0.039	1.416 ± 0.045	1.492 ± 0.064	1.535 ± 0.072
	BCC	0.614 ± 0.022	1.067 ± 0.098	1.145 ± 0.073	1.095 ± 0.074	1.079 ± 0.052
	PE	0.507 ± 0.014	0.903 ± 0.071	1.152 ± 0.104	1.209 ± 0.111	1.233 ± 0.113
	EA	0.511 ± 0.015	0.912 ± 0.076	1.163 ± 0.108	1.222 ± 0.113	1.246 ± 0.116
	SDS	0.460 ± 0.011	0.813 ± 0.056	1.061 ± 0.087	1.127 ± 0.089	1.155 ± 0.094
NLL	DS	3.016 ± 0.421	5.432 ± 1.093	8.605 ± 2.270	10.378 ± 3.304	13.834 ± 1.814
	BCC	2.821 ± 0.489	4.915 ± 1.034	5.606 ± 1.142	5.462 ± 0.771	5.372 ± 0.903
	PE	1.427 ± 0.100	2.891 ± 0.450	3.963 ± 0.625	4.232 ± 0.635	4.327 ± 0.612

Continued on next page

Table 6: Results on CIFAR10 with noise corruptions of increasing severity (continued).

Corruption Metric	Method	Severity 1	Severity 2	Severity 3	Severity 4	Severity 5
	EA	1.485 ± 0.133	3.021 ± 0.527	4.147 ± 0.721	4.427 ± 0.730	4.526 ± 0.705
	SDS	1.054 ± 0.003	1.989 ± 0.123	3.190 ± 0.472	3.672 ± 0.413	3.872 ± 0.521
Accuracy	DS	0.794 ± 0.009	0.659 ± 0.006	0.391 ± 0.011	0.329 ± 0.012	0.244 ± 0.019
	BCC	0.796 ± 0.007	0.663 ± 0.009	0.390 ± 0.009	0.310 ± 0.023	0.236 ± 0.005
	PE	0.797 ± 0.010	0.658 ± 0.009	0.392 ± 0.004	0.326 ± 0.007	0.243 ± 0.018
	EA	0.797 ± 0.009	0.658 ± 0.007	0.391 ± 0.005	0.326 ± 0.007	0.242 ± 0.017
	SDS	0.807 ± 0.007	0.673 ± 0.008	0.404 ± 0.006	0.336 ± 0.007	0.246 ± 0.015
Shot Noise	DS	0.192 ± 0.005	0.321 ± 0.014	0.577 ± 0.030	0.631 ± 0.035	0.698 ± 0.053
	BCC	0.188 ± 0.010	0.315 ± 0.022	0.555 ± 0.067	0.513 ± 0.137	0.465 ± 0.045
	PE	0.094 ± 0.013	0.153 ± 0.091	0.376 ± 0.085	0.422 ± 0.081	0.466 ± 0.080
	EA	0.101 ± 0.011	0.161 ± 0.091	0.384 ± 0.089	0.431 ± 0.082	0.476 ± 0.078
	SDS	0.102 ± 0.014	0.157 ± 0.041	0.321 ± 0.084	0.364 ± 0.078	0.410 ± 0.073
Brier score	DS	0.390 ± 0.009	0.650 ± 0.020	1.165 ± 0.041	1.278 ± 0.046	1.417 ± 0.078
	BCC	0.385 ± 0.011	0.643 ± 0.029	1.133 ± 0.094	1.144 ± 0.142	1.133 ± 0.042
	PE	0.318 ± 0.030	0.531 ± 0.013	0.944 ± 0.063	1.041 ± 0.069	1.139 ± 0.073
	EA	0.321 ± 0.027	0.536 ± 0.014	0.953 ± 0.066	1.052 ± 0.072	1.151 ± 0.075
	SDS	0.296 ± 0.021	0.481 ± 0.010	0.855 ± 0.049	0.954 ± 0.052	1.064 ± 0.056
NLL	DS	2.030 ± 0.274	3.267 ± 0.567	6.433 ± 1.717	6.984 ± 1.419	10.172 ± 3.358
	BCC	1.816 ± 0.256	2.919 ± 0.534	5.380 ± 1.146	5.358 ± 1.340	5.434 ± 0.700
	PE	0.818 ± 0.052	1.523 ± 0.123	3.103 ± 0.416	3.538 ± 0.447	3.921 ± 0.412
	EA	0.846 ± 0.037	1.586 ± 0.159	3.242 ± 0.490	3.699 ± 0.522	4.098 ± 0.482
	SDS	0.710 ± 0.033	1.104 ± 0.024	2.190 ± 0.080	2.664 ± 0.125	3.320 ± 0.191
Accuracy	DS	0.784 ± 0.004	0.612 ± 0.005	0.505 ± 0.012	0.356 ± 0.012	0.249 ± 0.013
	BCC	0.785 ± 0.005	0.614 ± 0.008	0.487 ± 0.039	0.346 ± 0.029	0.237 ± 0.034
	PE	0.786 ± 0.006	0.610 ± 0.007	0.507 ± 0.013	0.363 ± 0.013	0.257 ± 0.016
	EA	0.786 ± 0.006	0.610 ± 0.006	0.508 ± 0.012	0.364 ± 0.013	0.257 ± 0.019
	SDS	0.793 ± 0.004	0.624 ± 0.007	0.521 ± 0.010	0.370 ± 0.010	0.259 ± 0.019
Impulse Noise	DS	0.199 ± 0.009	0.337 ± 0.031	0.409 ± 0.041	0.489 ± 0.069	0.551 ± 0.098
	BCC	0.196 ± 0.011	0.344 ± 0.018	0.447 ± 0.022	0.507 ± 0.047	0.562 ± 0.137
	PE	0.088 ± 0.008	0.139 ± 0.066	0.173 ± 0.072	0.209 ± 0.054	0.256 ± 0.049
	EA	0.096 ± 0.005	0.161 ± 0.051	0.191 ± 0.065	0.222 ± 0.062	0.269 ± 0.058
	SDS	0.094 ± 0.021	0.138 ± 0.030	0.148 ± 0.042	0.167 ± 0.057	0.218 ± 0.054
Brier score	DS	0.409 ± 0.009	0.715 ± 0.036	0.889 ± 0.038	1.090 ± 0.070	1.240 ± 0.114
	BCC	0.405 ± 0.012	0.719 ± 0.027	0.940 ± 0.056	1.113 ± 0.040	1.255 ± 0.178
	PE	0.331 ± 0.027	0.563 ± 0.011	0.693 ± 0.018	0.847 ± 0.017	0.953 ± 0.032
	EA	0.333 ± 0.024	0.569 ± 0.015	0.701 ± 0.021	0.856 ± 0.022	0.965 ± 0.038
	SDS	0.316 ± 0.019	0.528 ± 0.010	0.650 ± 0.014	0.809 ± 0.013	0.918 ± 0.032
NLL	DS	2.019 ± 0.393	3.479 ± 0.765	4.278 ± 0.795	5.721 ± 1.000	8.498 ± 1.112
	BCC	1.785 ± 0.333	2.993 ± 0.607	3.739 ± 0.347	4.327 ± 0.757	4.436 ± 1.154
	PE	0.841 ± 0.010	1.557 ± 0.124	2.012 ± 0.154	2.518 ± 0.122	2.938 ± 0.183
	EA	0.870 ± 0.010	1.620 ± 0.161	2.088 ± 0.191	2.592 ± 0.151	3.024 ± 0.217
	SDS	0.803 ± 0.011	1.317 ± 0.078	1.653 ± 0.126	2.094 ± 0.093	2.524 ± 0.171

Table 7: Results on CIFAR10 with blur corruptions of increasing severity.

Corruption Metric	Method	Severity 1	Severity 2	Severity 3	Severity 4	Severity 5	
Defocus Blur	Accuracy	DS	0.943 ± 0.006	0.926 ± 0.003	0.870 ± 0.004	0.755 ± 0.013	0.436 ± 0.016
		BCC	0.944 ± 0.005	0.926 ± 0.003	0.870 ± 0.004	0.758 ± 0.015	0.398 ± 0.072
		PE	0.944 ± 0.004	0.930 ± 0.001	0.878 ± 0.002	0.766 ± 0.012	0.451 ± 0.015
		EA	0.945 ± 0.004	0.930 ± 0.001	0.877 ± 0.002	0.766 ± 0.014	0.450 ± 0.017
		SDS	0.946 ± 0.003	0.932 ± 0.001	0.882 ± 0.002	0.777 ± 0.012	0.465 ± 0.016
	ECE	DS	0.054 ± 0.003	0.069 ± 0.002	0.118 ± 0.007	0.216 ± 0.023	0.458 ± 0.069
		BCC	0.052 ± 0.002	0.067 ± 0.004	0.115 ± 0.011	0.211 ± 0.030	0.503 ± 0.016
		PE	0.074 ± 0.097	0.082 ± 0.101	0.087 ± 0.085	0.100 ± 0.025	0.200 ± 0.093
		EA	0.076 ± 0.095	0.083 ± 0.098	0.089 ± 0.078	0.105 ± 0.018	0.213 ± 0.094
		SDS	0.075 ± 0.093	0.083 ± 0.097	0.086 ± 0.081	0.096 ± 0.037	0.166 ± 0.078
	Brier score	DS	0.109 ± 0.008	0.141 ± 0.002	0.242 ± 0.008	0.447 ± 0.035	0.986 ± 0.068
		BCC	0.107 ± 0.006	0.138 ± 0.003	0.238 ± 0.012	0.441 ± 0.042	1.065 ± 0.081
		PE	0.109 ± 0.047	0.132 ± 0.043	0.206 ± 0.034	0.357 ± 0.012	0.763 ± 0.034
		EA	0.108 ± 0.045	0.132 ± 0.042	0.206 ± 0.031	0.358 ± 0.010	0.772 ± 0.039
		SDS	0.105 ± 0.039	0.128 ± 0.037	0.197 ± 0.028	0.335 ± 0.012	0.718 ± 0.022
	NLL	DS	0.695 ± 0.056	0.828 ± 0.022	1.410 ± 0.005	2.191 ± 0.444	4.823 ± 1.098
		BCC	0.560 ± 0.073	0.677 ± 0.105	1.078 ± 0.197	1.872 ± 0.369	4.198 ± 0.251
		PE	0.259 ± 0.126	0.313 ± 0.117	0.483 ± 0.087	0.862 ± 0.016	2.128 ± 0.140
		EA	0.263 ± 0.123	0.319 ± 0.113	0.494 ± 0.078	0.889 ± 0.015	2.215 ± 0.178
		SDS	0.258 ± 0.113	0.313 ± 0.106	0.466 ± 0.077	0.790 ± 0.033	1.883 ± 0.080
Frosted Glass Blur	Accuracy	DS	0.485 ± 0.006	0.501 ± 0.008	0.491 ± 0.005	0.400 ± 0.007	0.396 ± 0.007
		BCC	0.478 ± 0.015	0.497 ± 0.017	0.474 ± 0.033	0.395 ± 0.008	0.392 ± 0.010
		PE	0.485 ± 0.003	0.501 ± 0.002	0.491 ± 0.005	0.401 ± 0.003	0.394 ± 0.005
		EA	0.485 ± 0.002	0.501 ± 0.002	0.492 ± 0.006	0.402 ± 0.003	0.395 ± 0.003
		SDS	0.497 ± 0.004	0.513 ± 0.002	0.505 ± 0.007	0.409 ± 0.002	0.400 ± 0.003
	ECE	DS	0.455 ± 0.030	0.440 ± 0.020	0.455 ± 0.025	0.526 ± 0.036	0.543 ± 0.025
		BCC	0.464 ± 0.015	0.447 ± 0.010	0.474 ± 0.013	0.538 ± 0.019	0.544 ± 0.025
		PE	0.243 ± 0.070	0.228 ± 0.071	0.242 ± 0.080	0.310 ± 0.068	0.327 ± 0.070
		EA	0.252 ± 0.074	0.238 ± 0.073	0.251 ± 0.081	0.320 ± 0.071	0.338 ± 0.073
		SDS	0.197 ± 0.075	0.183 ± 0.072	0.195 ± 0.081	0.252 ± 0.067	0.272 ± 0.069
	Brier score	DS	0.950 ± 0.038	0.916 ± 0.028	0.943 ± 0.032	1.096 ± 0.046	1.121 ± 0.033
		BCC	0.964 ± 0.017	0.933 ± 0.010	0.978 ± 0.035	1.114 ± 0.025	1.124 ± 0.032
		PE	0.755 ± 0.018	0.731 ± 0.015	0.750 ± 0.026	0.882 ± 0.026	0.906 ± 0.032
		EA	0.763 ± 0.022	0.740 ± 0.018	0.759 ± 0.029	0.892 ± 0.031	0.916 ± 0.036
		SDS	0.697 ± 0.019	0.675 ± 0.014	0.690 ± 0.023	0.823 ± 0.026	0.844 ± 0.025
	NLL	DS	4.571 ± 0.704	4.222 ± 0.342	4.570 ± 0.599	5.753 ± 0.958	5.832 ± 0.992
		BCC	4.103 ± 0.497	3.865 ± 0.465	4.169 ± 0.431	4.778 ± 0.383	4.689 ± 0.731
		PE	2.204 ± 0.113	2.131 ± 0.111	2.228 ± 0.190	2.752 ± 0.111	2.917 ± 0.207
		EA	2.291 ± 0.149	2.215 ± 0.146	2.322 ± 0.230	2.860 ± 0.155	3.037 ± 0.259
		SDS	1.735 ± 0.132	1.646 ± 0.100	1.676 ± 0.112	2.287 ± 0.213	2.354 ± 0.196
Motion Blur	Accuracy	DS	0.902 ± 0.004	0.823 ± 0.003	0.713 ± 0.012	0.717 ± 0.009	0.607 ± 0.023
		BCC	0.902 ± 0.004	0.823 ± 0.003	0.671 ± 0.061	0.672 ± 0.069	0.569 ± 0.043
		PE	0.906 ± 0.002	0.831 ± 0.007	0.718 ± 0.014	0.719 ± 0.011	0.608 ± 0.020
		EA	0.907 ± 0.001	0.830 ± 0.007	0.718 ± 0.015	0.720 ± 0.011	0.609 ± 0.021
		SDS	0.909 ± 0.001	0.837 ± 0.007	0.730 ± 0.015	0.732 ± 0.011	0.625 ± 0.024
	ECE	DS	0.090 ± 0.004	0.161 ± 0.010	0.256 ± 0.030	0.252 ± 0.028	0.346 ± 0.052
		BCC	0.088 ± 0.006	0.157 ± 0.015	0.295 ± 0.040	0.293 ± 0.044	0.381 ± 0.013
		PE	0.084 ± 0.092	0.093 ± 0.058	0.115 ± 0.018	0.117 ± 0.017	0.148 ± 0.078
		EA	0.085 ± 0.089	0.096 ± 0.052	0.119 ± 0.023	0.120 ± 0.021	0.156 ± 0.081
		SDS	0.082 ± 0.089	0.092 ± 0.059	0.112 ± 0.011	0.111 ± 0.010	0.141 ± 0.048
	Brier score	DS	0.186 ± 0.003	0.330 ± 0.017	0.531 ± 0.045	0.527 ± 0.036	0.726 ± 0.071
		BCC	0.183 ± 0.005	0.325 ± 0.023	0.614 ± 0.102	0.611 ± 0.111	0.794 ± 0.051
		PE	0.166 ± 0.040	0.271 ± 0.026	0.423 ± 0.010	0.421 ± 0.010	0.571 ± 0.037
		EA	0.165 ± 0.038	0.272 ± 0.023	0.426 ± 0.012	0.423 ± 0.010	0.576 ± 0.041
		SDS	0.160 ± 0.033	0.257 ± 0.019	0.396 ± 0.007	0.394 ± 0.007	0.533 ± 0.032
	DS	1.066 ± 0.069	1.744 ± 0.074	2.551 ± 0.584	2.734 ± 0.102	3.350 ± 0.720	

NLL

Continued on next page

Table 7: Results on CIFAR10 with blur corruptions of increasing severity (continued).

Corruption Metric	Method	Severity 1	Severity 2	Severity 3	Severity 4	Severity 5
	BCC	0.869 ± 0.157	1.441 ± 0.264	2.668 ± 0.329	2.662 ± 0.350	3.296 ± 0.053
	PE	0.388 ± 0.109	0.647 ± 0.064	1.035 ± 0.042	1.038 ± 0.037	1.469 ± 0.124
	EA	0.395 ± 0.103	0.664 ± 0.054	1.071 ± 0.054	1.072 ± 0.049	1.524 ± 0.151
	SDS	0.381 ± 0.092	0.603 ± 0.048	0.927 ± 0.013	0.926 ± 0.016	1.265 ± 0.103

Continued on next page

Table 7: Results on CIFAR10 with blur corruptions of increasing severity (continued).

Corruption Metric	Method	Severity 1	Severity 2	Severity 3	Severity 4	Severity 5
Accuracy	DS	0.869 ± 0.008	0.831 ± 0.011	0.761 ± 0.013	0.680 ± 0.015	0.564 ± 0.022
	BCC	0.869 ± 0.007	0.832 ± 0.010	0.763 ± 0.013	0.689 ± 0.015	0.514 ± 0.103
	PE	0.877 ± 0.003	0.840 ± 0.005	0.769 ± 0.012	0.691 ± 0.012	0.580 ± 0.011
	EA	0.877 ± 0.005	0.840 ± 0.004	0.770 ± 0.011	0.693 ± 0.011	0.580 ± 0.012
	SDS	0.881 ± 0.004	0.848 ± 0.005	0.781 ± 0.012	0.708 ± 0.013	0.596 ± 0.011
Zoom Blur	DS	0.119 ± 0.006	0.150 ± 0.009	0.208 ± 0.022	0.272 ± 0.030	0.360 ± 0.045
	BCC	0.116 ± 0.008	0.146 ± 0.012	0.204 ± 0.025	0.266 ± 0.035	0.416 ± 0.056
	PE	0.084 ± 0.086	0.085 ± 0.069	0.095 ± 0.030	0.109 ± 0.015	0.139 ± 0.072
	EA	0.087 ± 0.081	0.089 ± 0.063	0.098 ± 0.023	0.115 ± 0.020	0.152 ± 0.068
	SDS	0.085 ± 0.084	0.086 ± 0.072	0.094 ± 0.042	0.101 ± 0.007	0.125 ± 0.039
Brier score	DS	0.244 ± 0.010	0.309 ± 0.015	0.435 ± 0.030	0.572 ± 0.034	0.768 ± 0.046
	BCC	0.241 ± 0.012	0.305 ± 0.017	0.427 ± 0.038	0.562 ± 0.046	0.878 ± 0.155
	PE	0.205 ± 0.035	0.255 ± 0.031	0.346 ± 0.021	0.449 ± 0.011	0.601 ± 0.010
	EA	0.206 ± 0.033	0.256 ± 0.028	0.348 ± 0.018	0.452 ± 0.008	0.606 ± 0.015
	SDS	0.198 ± 0.030	0.243 ± 0.026	0.326 ± 0.019	0.419 ± 0.012	0.559 ± 0.010
NLL	DS	1.321 ± 0.021	1.727 ± 0.128	2.115 ± 0.414	2.819 ± 0.515	3.643 ± 0.703
	BCC	1.079 ± 0.186	1.335 ± 0.216	1.808 ± 0.334	2.341 ± 0.410	3.683 ± 0.471
	PE	0.482 ± 0.090	0.605 ± 0.075	0.839 ± 0.043	1.125 ± 0.016	1.599 ± 0.069
	EA	0.492 ± 0.082	0.619 ± 0.064	0.863 ± 0.031	1.162 ± 0.023	1.661 ± 0.095
	SDS	0.471 ± 0.078	0.573 ± 0.068	0.777 ± 0.042	1.006 ± 0.036	1.367 ± 0.060

Table 8: Results on CIFAR10 with weather corruptions of increasing severity.

Corruption Metric	Method	Severity 1	Severity 2	Severity 3	Severity 4	Severity 5
Accuracy	DS	0.887 ± 0.013	0.767 ± 0.024	0.809 ± 0.019	0.782 ± 0.018	0.726 ± 0.018
	BCC	0.887 ± 0.012	0.769 ± 0.021	0.811 ± 0.015	0.784 ± 0.015	0.728 ± 0.014
	PE	0.889 ± 0.012	0.770 ± 0.023	0.810 ± 0.021	0.785 ± 0.018	0.728 ± 0.021
	EA	0.890 ± 0.012	0.771 ± 0.023	0.810 ± 0.021	0.787 ± 0.016	0.729 ± 0.020
	SDS	0.892 ± 0.010	0.780 ± 0.020	0.817 ± 0.016	0.794 ± 0.014	0.739 ± 0.018
Snow	DS	0.106 ± 0.008	0.213 ± 0.017	0.176 ± 0.011	0.200 ± 0.009	0.249 ± 0.009
	BCC	0.103 ± 0.005	0.208 ± 0.013	0.173 ± 0.009	0.197 ± 0.008	0.247 ± 0.010
	PE	0.074 ± 0.062	0.096 ± 0.015	0.087 ± 0.021	0.094 ± 0.009	0.110 ± 0.027
	EA	0.077 ± 0.060	0.105 ± 0.014	0.093 ± 0.021	0.101 ± 0.007	0.120 ± 0.023
	SDS	0.075 ± 0.057	0.096 ± 0.011	0.088 ± 0.019	0.095 ± 0.006	0.110 ± 0.018
Brier score	DS	0.217 ± 0.019	0.437 ± 0.034	0.362 ± 0.027	0.411 ± 0.022	0.514 ± 0.021
	BCC	0.213 ± 0.014	0.431 ± 0.028	0.357 ± 0.021	0.405 ± 0.017	0.507 ± 0.018
	PE	0.188 ± 0.055	0.358 ± 0.056	0.301 ± 0.055	0.337 ± 0.048	0.417 ± 0.045
	EA	0.189 ± 0.054	0.360 ± 0.054	0.303 ± 0.054	0.338 ± 0.045	0.420 ± 0.042
	SDS	0.182 ± 0.044	0.339 ± 0.042	0.289 ± 0.042	0.322 ± 0.036	0.397 ± 0.033
NLL	DS	1.237 ± 0.086	2.145 ± 0.111	1.842 ± 0.108	2.102 ± 0.109	2.633 ± 0.257
	BCC	1.042 ± 0.089	1.956 ± 0.184	1.661 ± 0.165	1.902 ± 0.203	2.353 ± 0.310
	PE	0.461 ± 0.130	0.928 ± 0.129	0.758 ± 0.123	0.860 ± 0.103	1.090 ± 0.097
	EA	0.472 ± 0.125	0.959 ± 0.120	0.781 ± 0.117	0.886 ± 0.093	1.129 ± 0.083
	SDS	0.455 ± 0.100	0.837 ± 0.084	0.719 ± 0.079	0.809 ± 0.069	0.984 ± 0.061
Frost	DS	0.880 ± 0.012	0.817 ± 0.011	0.700 ± 0.013	0.669 ± 0.012	0.546 ± 0.009
	BCC	0.881 ± 0.010	0.820 ± 0.008	0.705 ± 0.007	0.673 ± 0.008	0.518 ± 0.056
	PE	0.883 ± 0.009	0.820 ± 0.011	0.702 ± 0.017	0.670 ± 0.016	0.543 ± 0.019
	EA	0.883 ± 0.009	0.820 ± 0.010	0.702 ± 0.015	0.670 ± 0.016	0.544 ± 0.019
	SDS	0.887 ± 0.007	0.828 ± 0.009	0.714 ± 0.014	0.684 ± 0.015	0.557 ± 0.017
ECE	DS	0.112 ± 0.005	0.168 ± 0.005	0.275 ± 0.007	0.305 ± 0.007	0.422 ± 0.007
	BCC	0.109 ± 0.003	0.164 ± 0.007	0.270 ± 0.013	0.300 ± 0.012	0.447 ± 0.040
	PE	0.076 ± 0.060	0.089 ± 0.023	0.120 ± 0.044	0.133 ± 0.059	0.213 ± 0.083
	EA	0.080 ± 0.059	0.095 ± 0.021	0.131 ± 0.040	0.148 ± 0.051	0.222 ± 0.087

Continued on next page

Table 8: Results on CIFAR10 with weather corruptions of increasing severity (continued).

Corruption Metric	Method	Severity 1	Severity 2	Severity 3	Severity 4	Severity 5
Brier score	SDS	0.079 ± 0.059	0.090 ± 0.024	0.120 ± 0.023	0.136 ± 0.028	0.193 ± 0.061
	DS	0.228 ± 0.013	0.345 ± 0.013	0.565 ± 0.014	0.625 ± 0.013	0.864 ± 0.009
	BCC	0.224 ± 0.009	0.339 ± 0.011	0.557 ± 0.014	0.617 ± 0.014	0.911 ± 0.088
	PE	0.198 ± 0.048	0.286 ± 0.044	0.460 ± 0.035	0.503 ± 0.030	0.696 ± 0.010
	EA	0.198 ± 0.046	0.288 ± 0.041	0.463 ± 0.032	0.507 ± 0.027	0.703 ± 0.007
	SDS	0.190 ± 0.039	0.275 ± 0.034	0.429 ± 0.028	0.468 ± 0.023	0.637 ± 0.010
NLL	DS	1.318 ± 0.034	1.820 ± 0.113	2.890 ± 0.288	3.253 ± 0.370	4.567 ± 0.559
	BCC	1.105 ± 0.138	1.630 ± 0.221	2.587 ± 0.401	2.885 ± 0.430	4.184 ± 0.224
	PE	0.479 ± 0.121	0.735 ± 0.104	1.261 ± 0.076	1.418 ± 0.072	2.126 ± 0.036
	EA	0.491 ± 0.115	0.757 ± 0.093	1.308 ± 0.057	1.474 ± 0.052	2.218 ± 0.007
	SDS	0.468 ± 0.099	0.678 ± 0.084	1.035 ± 0.068	1.124 ± 0.056	1.537 ± 0.072

Continued on next page

Table 8: Results on CIFAR10 with weather corruptions of increasing severity (continued).

Corruption Metric	Method	Severity 1	Severity 2	Severity 3	Severity 4	Severity 5	
Fog	Accuracy	DS	0.931 ± 0.006	0.901 ± 0.007	0.864 ± 0.008	0.808 ± 0.011	0.612 ± 0.011
		BCC	0.931 ± 0.007	0.902 ± 0.007	0.866 ± 0.008	0.810 ± 0.013	0.589 ± 0.037
		PE	0.934 ± 0.003	0.905 ± 0.007	0.867 ± 0.009	0.810 ± 0.011	0.618 ± 0.011
		EA	0.934 ± 0.004	0.905 ± 0.007	0.868 ± 0.009	0.811 ± 0.012	0.619 ± 0.012
		SDS	0.935 ± 0.003	0.908 ± 0.006	0.873 ± 0.008	0.820 ± 0.011	0.632 ± 0.013
	ECE	DS	0.065 ± 0.003	0.092 ± 0.007	0.125 ± 0.009	0.175 ± 0.018	0.350 ± 0.028
		BCC	0.063 ± 0.002	0.088 ± 0.010	0.119 ± 0.015	0.169 ± 0.026	0.371 ± 0.016
		PE	0.080 ± 0.099	0.088 ± 0.095	0.092 ± 0.076	0.105 ± 0.048	0.141 ± 0.062
		EA	0.080 ± 0.097	0.090 ± 0.091	0.096 ± 0.075	0.109 ± 0.044	0.153 ± 0.063
		SDS	0.080 ± 0.094	0.089 ± 0.092	0.095 ± 0.078	0.104 ± 0.053	0.131 ± 0.037
	Brier score	DS	0.132 ± 0.008	0.188 ± 0.014	0.256 ± 0.016	0.362 ± 0.028	0.720 ± 0.043
		BCC	0.129 ± 0.006	0.183 ± 0.015	0.249 ± 0.021	0.355 ± 0.034	0.767 ± 0.052
		PE	0.129 ± 0.053	0.174 ± 0.056	0.224 ± 0.048	0.303 ± 0.042	0.562 ± 0.022
		EA	0.129 ± 0.052	0.174 ± 0.053	0.226 ± 0.048	0.304 ± 0.038	0.567 ± 0.022
		SDS	0.124 ± 0.044	0.168 ± 0.045	0.216 ± 0.041	0.288 ± 0.034	0.522 ± 0.016
	NLL	DS	0.874 ± 0.086	1.109 ± 0.130	1.390 ± 0.127	1.909 ± 0.319	4.165 ± 0.940
		BCC	0.669 ± 0.076	0.900 ± 0.164	1.164 ± 0.212	1.639 ± 0.323	3.460 ± 0.183
		PE	0.305 ± 0.139	0.413 ± 0.141	0.538 ± 0.122	0.741 ± 0.109	1.533 ± 0.095
		EA	0.311 ± 0.135	0.421 ± 0.134	0.553 ± 0.119	0.760 ± 0.101	1.588 ± 0.109
		SDS	0.304 ± 0.122	0.406 ± 0.120	0.518 ± 0.108	0.674 ± 0.086	1.253 ± 0.030
Brightness	Accuracy	DS	0.944 ± 0.006	0.941 ± 0.007	0.936 ± 0.006	0.930 ± 0.006	0.909 ± 0.011
		BCC	0.944 ± 0.006	0.941 ± 0.007	0.936 ± 0.006	0.930 ± 0.006	0.909 ± 0.012
		PE	0.946 ± 0.004	0.942 ± 0.005	0.938 ± 0.005	0.932 ± 0.005	0.911 ± 0.008
		EA	0.946 ± 0.004	0.943 ± 0.004	0.938 ± 0.005	0.931 ± 0.004	0.912 ± 0.007
		SDS	0.947 ± 0.003	0.943 ± 0.004	0.938 ± 0.005	0.933 ± 0.004	0.913 ± 0.007
	ECE	DS	0.053 ± 0.003	0.056 ± 0.003	0.060 ± 0.003	0.065 ± 0.003	0.085 ± 0.006
		BCC	0.052 ± 0.003	0.055 ± 0.003	0.059 ± 0.003	0.064 ± 0.003	0.083 ± 0.004
		PE	0.072 ± 0.094	0.074 ± 0.093	0.075 ± 0.091	0.076 ± 0.090	0.079 ± 0.084
		EA	0.074 ± 0.092	0.075 ± 0.091	0.076 ± 0.090	0.078 ± 0.088	0.081 ± 0.082
		SDS	0.073 ± 0.088	0.074 ± 0.088	0.075 ± 0.085	0.077 ± 0.086	0.081 ± 0.081
	Brier score	DS	0.108 ± 0.008	0.113 ± 0.009	0.122 ± 0.007	0.134 ± 0.007	0.173 ± 0.014
		BCC	0.106 ± 0.006	0.112 ± 0.007	0.120 ± 0.006	0.132 ± 0.006	0.171 ± 0.011
		PE	0.107 ± 0.048	0.112 ± 0.049	0.120 ± 0.049	0.129 ± 0.049	0.159 ± 0.052
		EA	0.107 ± 0.047	0.112 ± 0.047	0.120 ± 0.047	0.130 ± 0.048	0.159 ± 0.051
		SDS	0.104 ± 0.040	0.109 ± 0.041	0.116 ± 0.041	0.126 ± 0.042	0.155 ± 0.044
	NLL	DS	0.705 ± 0.068	0.727 ± 0.046	0.767 ± 0.062	0.839 ± 0.060	1.049 ± 0.047
		BCC	0.569 ± 0.078	0.584 ± 0.069	0.629 ± 0.094	0.690 ± 0.094	0.867 ± 0.095
		PE	0.256 ± 0.127	0.267 ± 0.129	0.284 ± 0.129	0.307 ± 0.128	0.378 ± 0.129
		EA	0.260 ± 0.124	0.272 ± 0.125	0.290 ± 0.125	0.314 ± 0.125	0.387 ± 0.125
		SDS	0.255 ± 0.113	0.267 ± 0.115	0.285 ± 0.115	0.309 ± 0.116	0.379 ± 0.112

Table 9: Results on CIFAR10 with digital corruptions of increasing severity.

Corruption Metric	Method	Severity 1	Severity 2	Severity 3	Severity 4	Severity 5
Accuracy	DS	0.920 ± 0.005	0.839 ± 0.008	0.749 ± 0.012	0.588 ± 0.033	0.200 ± 0.021
	BCC	0.921 ± 0.004	0.842 ± 0.011	0.754 ± 0.018	0.548 ± 0.046	0.181 ± 0.041
	PE	0.923 ± 0.004	0.840 ± 0.008	0.752 ± 0.012	0.583 ± 0.024	0.207 ± 0.029
	EA	0.924 ± 0.004	0.840 ± 0.008	0.753 ± 0.014	0.585 ± 0.024	0.206 ± 0.029
	SDS	0.926 ± 0.003	0.847 ± 0.008	0.764 ± 0.015	0.603 ± 0.027	0.208 ± 0.030
ECE	DS	0.075 ± 0.002	0.147 ± 0.015	0.226 ± 0.029	0.369 ± 0.064	0.636 ± 0.205
	BCC	0.072 ± 0.003	0.141 ± 0.023	0.220 ± 0.037	0.408 ± 0.023	0.463 ± 0.037
	PE	0.083 ± 0.095	0.099 ± 0.061	0.117 ± 0.017	0.169 ± 0.092	0.442 ± 0.209
	EA	0.084 ± 0.095	0.102 ± 0.056	0.123 ± 0.014	0.178 ± 0.096	0.456 ± 0.214
Contrast						

Continued on next page

Table 9: Results on CIFAR10 with digital corruptions of increasing severity (continued).

Corruption Metric	Method	Severity 1	Severity 2	Severity 3	Severity 4	Severity 5
	SDS	0.085 ± 0.094	0.101 ± 0.065	0.118 ± 0.031	0.158 ± 0.053	0.392 ± 0.197
Brier score	DS	0.151 ± 0.005	0.304 ± 0.022	0.466 ± 0.044	0.769 ± 0.090	1.390 ± 0.232
	BCC	0.148 ± 0.004	0.297 ± 0.029	0.459 ± 0.052	0.838 ± 0.058	1.164 ± 0.047
	PE	0.145 ± 0.053	0.264 ± 0.046	0.384 ± 0.031	0.606 ± 0.045	1.156 ± 0.193
	EA	0.145 ± 0.053	0.265 ± 0.044	0.386 ± 0.028	0.612 ± 0.047	1.173 ± 0.201
	SDS	0.140 ± 0.045	0.252 ± 0.038	0.361 ± 0.025	0.565 ± 0.033	1.088 ± 0.164
NLL	DS	0.942 ± 0.054	1.575 ± 0.226	2.285 ± 0.445	4.416 ± 1.635	11.990 ± 4.108
	BCC	0.750 ± 0.110	1.370 ± 0.275	2.023 ± 0.452	3.620 ± 0.361	4.389 ± 0.398
	PE	0.342 ± 0.137	0.636 ± 0.107	0.951 ± 0.078	1.602 ± 0.153	3.915 ± 0.637
	EA	0.350 ± 0.135	0.653 ± 0.101	0.983 ± 0.075	1.666 ± 0.172	4.103 ± 0.707
	SDS	0.341 ± 0.121	0.599 ± 0.085	0.834 ± 0.039	1.368 ± 0.117	3.185 ± 0.501

Continued on next page

Table 9: Results on CIFAR10 with digital corruptions of increasing severity (continued).

Corruption Metric	Method	Severity 1	Severity 2	Severity 3	Severity 4	Severity 5	
Elastic	Accuracy	DS	0.898 ± 0.005	0.894 ± 0.004	0.851 ± 0.004	0.776 ± 0.007	0.685 ± 0.012
		BCC	0.898 ± 0.005	0.894 ± 0.004	0.852 ± 0.004	0.776 ± 0.007	0.685 ± 0.011
		PE	0.902 ± 0.001	0.900 ± 0.002	0.857 ± 0.003	0.782 ± 0.007	0.688 ± 0.012
		EA	0.902 ± 0.001	0.900 ± 0.002	0.858 ± 0.003	0.782 ± 0.009	0.689 ± 0.011
		SDS	0.904 ± 0.001	0.902 ± 0.002	0.863 ± 0.003	0.792 ± 0.010	0.700 ± 0.011
	ECE	DS	0.094 ± 0.001	0.097 ± 0.002	0.134 ± 0.008	0.204 ± 0.014	0.280 ± 0.022
		BCC	0.092 ± 0.004	0.095 ± 0.005	0.131 ± 0.012	0.200 ± 0.018	0.278 ± 0.021
		PE	0.082 ± 0.090	0.084 ± 0.089	0.087 ± 0.071	0.098 ± 0.026	0.109 ± 0.046
		EA	0.083 ± 0.085	0.084 ± 0.086	0.091 ± 0.066	0.103 ± 0.019	0.118 ± 0.045
		SDS	0.083 ± 0.086	0.084 ± 0.086	0.089 ± 0.071	0.098 ± 0.036	0.107 ± 0.028
	Brier score	DS	0.192 ± 0.001	0.200 ± 0.002	0.277 ± 0.007	0.419 ± 0.022	0.585 ± 0.029
		BCC	0.189 ± 0.004	0.196 ± 0.004	0.273 ± 0.013	0.414 ± 0.027	0.581 ± 0.031
		PE	0.171 ± 0.042	0.177 ± 0.040	0.232 ± 0.031	0.335 ± 0.014	0.464 ± 0.021
		EA	0.170 ± 0.040	0.177 ± 0.038	0.233 ± 0.028	0.336 ± 0.011	0.468 ± 0.020
		SDS	0.166 ± 0.035	0.171 ± 0.034	0.223 ± 0.026	0.318 ± 0.012	0.440 ± 0.017
	NLL	DS	1.090 ± 0.055	1.186 ± 0.059	1.519 ± 0.052	2.151 ± 0.282	2.862 ± 0.365
		BCC	0.894 ± 0.139	0.931 ± 0.149	1.220 ± 0.222	1.811 ± 0.325	2.466 ± 0.395
		PE	0.397 ± 0.112	0.414 ± 0.104	0.549 ± 0.075	0.820 ± 0.017	1.184 ± 0.074
		EA	0.403 ± 0.105	0.423 ± 0.097	0.563 ± 0.067	0.845 ± 0.002	1.224 ± 0.081
		SDS	0.394 ± 0.099	0.409 ± 0.093	0.529 ± 0.068	0.758 ± 0.027	1.042 ± 0.037
Pixelate	Accuracy	DS	0.906 ± 0.009	0.831 ± 0.015	0.771 ± 0.014	0.591 ± 0.016	0.412 ± 0.008
		BCC	0.907 ± 0.008	0.834 ± 0.012	0.774 ± 0.012	0.568 ± 0.047	0.394 ± 0.028
		PE	0.908 ± 0.008	0.830 ± 0.016	0.769 ± 0.018	0.585 ± 0.020	0.404 ± 0.013
		EA	0.908 ± 0.008	0.832 ± 0.015	0.772 ± 0.016	0.587 ± 0.019	0.405 ± 0.013
		SDS	0.910 ± 0.005	0.839 ± 0.014	0.783 ± 0.013	0.601 ± 0.016	0.416 ± 0.011
	ECE	DS	0.088 ± 0.005	0.154 ± 0.010	0.210 ± 0.013	0.374 ± 0.026	0.541 ± 0.028
		BCC	0.086 ± 0.004	0.151 ± 0.010	0.208 ± 0.013	0.404 ± 0.031	0.526 ± 0.054
		PE	0.073 ± 0.074	0.082 ± 0.027	0.100 ± 0.015	0.197 ± 0.082	0.342 ± 0.081
		EA	0.074 ± 0.069	0.088 ± 0.026	0.110 ± 0.010	0.211 ± 0.076	0.354 ± 0.085
		SDS	0.074 ± 0.067	0.084 ± 0.032	0.106 ± 0.011	0.179 ± 0.055	0.287 ± 0.082
	Brier score	DS	0.179 ± 0.011	0.320 ± 0.022	0.432 ± 0.022	0.770 ± 0.031	1.107 ± 0.030
		BCC	0.176 ± 0.008	0.313 ± 0.019	0.426 ± 0.023	0.818 ± 0.072	1.088 ± 0.062
		PE	0.160 ± 0.050	0.267 ± 0.046	0.353 ± 0.039	0.625 ± 0.021	0.905 ± 0.050
		EA	0.160 ± 0.048	0.269 ± 0.044	0.355 ± 0.036	0.633 ± 0.021	0.917 ± 0.055
		SDS	0.155 ± 0.039	0.253 ± 0.034	0.330 ± 0.026	0.566 ± 0.017	0.824 ± 0.037
	NLL	DS	0.987 ± 0.091	1.604 ± 0.159	2.090 ± 0.227	3.582 ± 0.395	5.655 ± 0.881
		BCC	0.864 ± 0.120	1.445 ± 0.231	1.910 ± 0.358	3.436 ± 0.382	4.675 ± 1.212
		PE	0.380 ± 0.129	0.673 ± 0.106	0.919 ± 0.086	1.863 ± 0.137	3.052 ± 0.416
		EA	0.388 ± 0.123	0.693 ± 0.098	0.950 ± 0.075	1.951 ± 0.182	3.205 ± 0.502
		SDS	0.377 ± 0.107	0.641 ± 0.075	0.830 ± 0.038	1.377 ± 0.088	2.143 ± 0.155
JPEG	Accuracy	DS	0.810 ± 0.012	0.748 ± 0.011	0.727 ± 0.011	0.700 ± 0.011	0.664 ± 0.009
		BCC	0.811 ± 0.010	0.750 ± 0.010	0.728 ± 0.011	0.703 ± 0.010	0.665 ± 0.009
		PE	0.813 ± 0.009	0.751 ± 0.010	0.728 ± 0.011	0.705 ± 0.012	0.667 ± 0.010
		EA	0.813 ± 0.011	0.752 ± 0.010	0.728 ± 0.010	0.706 ± 0.011	0.669 ± 0.009
		SDS	0.821 ± 0.010	0.761 ± 0.010	0.739 ± 0.010	0.715 ± 0.010	0.680 ± 0.009
	ECE	DS	0.174 ± 0.010	0.229 ± 0.012	0.247 ± 0.017	0.269 ± 0.016	0.301 ± 0.021
		BCC	0.172 ± 0.010	0.227 ± 0.014	0.245 ± 0.019	0.265 ± 0.020	0.299 ± 0.023
		PE	0.083 ± 0.010	0.097 ± 0.022	0.103 ± 0.032	0.105 ± 0.045	0.117 ± 0.058
		EA	0.090 ± 0.011	0.105 ± 0.020	0.111 ± 0.030	0.114 ± 0.043	0.126 ± 0.057
		SDS	0.083 ± 0.012	0.095 ± 0.017	0.097 ± 0.025	0.101 ± 0.033	0.108 ± 0.045
	Brier score	DS	0.357 ± 0.018	0.472 ± 0.019	0.512 ± 0.025	0.554 ± 0.024	0.621 ± 0.031
		BCC	0.354 ± 0.018	0.469 ± 0.021	0.508 ± 0.029	0.549 ± 0.028	0.619 ± 0.032
		PE	0.292 ± 0.033	0.378 ± 0.023	0.407 ± 0.021	0.439 ± 0.018	0.488 ± 0.016
		EA	0.293 ± 0.031	0.380 ± 0.021	0.410 ± 0.020	0.442 ± 0.017	0.492 ± 0.017
		SDS	0.280 ± 0.026	0.360 ± 0.017	0.387 ± 0.017	0.417 ± 0.014	0.463 ± 0.013

Continued on next page

Table 9: Results on CIFAR10 with digital corruptions of increasing severity (continued).

Corruption Metric	Method	Severity 1	Severity 2	Severity 3	Severity 4	Severity 5
NLL	DS	1.818 ± 0.304	2.172 ± 0.291	2.376 ± 0.429	2.501 ± 0.361	2.782 ± 0.459
	BCC	1.623 ± 0.241	2.036 ± 0.297	2.175 ± 0.372	2.297 ± 0.387	2.530 ± 0.418
	PE	0.711 ± 0.072	0.925 ± 0.046	1.004 ± 0.054	1.092 ± 0.069	1.221 ± 0.100
	EA	0.732 ± 0.064	0.951 ± 0.045	1.033 ± 0.063	1.123 ± 0.084	1.257 ± 0.120
	SDS	0.680 ± 0.054	0.854 ± 0.029	0.915 ± 0.035	0.990 ± 0.040	1.094 ± 0.057

J.2 CIFAR100

Tables 10–13 present results for all corruptions on CIFAR100.

Table 10: Results on CIFAR100 with noise corruptions of increasing severity.

Corruption Metric	Method	Severity 1	Severity 2	Severity 3	Severity 4	Severity 5
Accuracy	DS	0.418 ± 0.010	0.217 ± 0.018	0.118 ± 0.015	0.088 ± 0.013	0.072 ± 0.011
	BCC	0.131 ± 0.019	0.035 ± 0.009	0.019 ± 0.007	0.012 ± 0.001	0.012 ± 0.003
	PE	0.427 ± 0.012	0.225 ± 0.023	0.124 ± 0.020	0.092 ± 0.018	0.073 ± 0.017
	EA	0.418 ± 0.012	0.215 ± 0.018	0.116 ± 0.015	0.086 ± 0.015	0.069 ± 0.014
	SDS	0.419 ± 0.013	0.213 ± 0.017	0.116 ± 0.015	0.086 ± 0.015	0.069 ± 0.014
ECE	DS	0.533 ± 0.008	0.708 ± 0.007	0.789 ± 0.010	0.822 ± 0.010	0.829 ± 0.013
	BCC	0.811 ± 0.021	0.904 ± 0.027	0.929 ± 0.033	0.943 ± 0.028	0.944 ± 0.035
	PE	0.103 ± 0.018	0.110 ± 0.044	0.218 ± 0.058	0.251 ± 0.063	0.265 ± 0.066
	EA	0.131 ± 0.014	0.338 ± 0.032	0.476 ± 0.035	0.520 ± 0.040	0.540 ± 0.044
	SDS	0.093 ± 0.009	0.286 ± 0.030	0.419 ± 0.033	0.461 ± 0.038	0.481 ± 0.041
Brier score	DS	1.090 ± 0.015	1.448 ± 0.017	1.620 ± 0.016	1.684 ± 0.015	1.704 ± 0.022
	BCC	1.652 ± 0.040	1.841 ± 0.044	1.884 ± 0.056	1.907 ± 0.044	1.910 ± 0.057
	PE	0.751 ± 0.011	0.942 ± 0.032	1.046 ± 0.042	1.075 ± 0.045	1.089 ± 0.047
	EA	0.773 ± 0.016	1.092 ± 0.033	1.280 ± 0.039	1.338 ± 0.043	1.367 ± 0.049
	SDS	0.757 ± 0.018	1.053 ± 0.027	1.213 ± 0.033	1.263 ± 0.037	1.289 ± 0.041
NLL	DS	12.256 ± 0.671	16.995 ± 0.243	20.008 ± 0.898	22.383 ± 0.378	22.891 ± 0.747
	BCC	11.115 ± 0.286	14.413 ± 0.464	16.562 ± 0.615	17.352 ± 0.618	17.833 ± 0.687
	PE	2.617 ± 0.044	3.707 ± 0.147	4.438 ± 0.208	4.701 ± 0.222	4.876 ± 0.243
	EA	2.698 ± 0.083	4.463 ± 0.204	5.714 ± 0.265	6.133 ± 0.293	6.369 ± 0.316
	SDS	2.712 ± 0.106	4.497 ± 0.180	5.611 ± 0.212	5.896 ± 0.242	6.063 ± 0.242
Accuracy	DS	0.571 ± 0.009	0.406 ± 0.011	0.180 ± 0.023	0.129 ± 0.019	0.084 ± 0.014
	BCC	0.259 ± 0.018	0.118 ± 0.024	0.029 ± 0.009	0.020 ± 0.006	0.014 ± 0.001
	PE	0.583 ± 0.008	0.416 ± 0.013	0.189 ± 0.026	0.136 ± 0.023	0.086 ± 0.019
	EA	0.577 ± 0.007	0.409 ± 0.011	0.179 ± 0.021	0.129 ± 0.020	0.081 ± 0.017
	SDS	0.586 ± 0.007	0.409 ± 0.011	0.179 ± 0.021	0.129 ± 0.020	0.081 ± 0.017
ECE	DS	0.405 ± 0.006	0.543 ± 0.009	0.742 ± 0.014	0.788 ± 0.014	0.823 ± 0.021
	BCC	0.701 ± 0.017	0.827 ± 0.028	0.914 ± 0.026	0.926 ± 0.028	0.939 ± 0.034
	PE	0.210 ± 0.011	0.098 ± 0.021	0.150 ± 0.056	0.207 ± 0.066	0.261 ± 0.080
	EA	0.040 ± 0.003	0.137 ± 0.019	0.383 ± 0.049	0.458 ± 0.058	0.531 ± 0.072
	SDS	0.030 ± 0.007	0.101 ± 0.013	0.329 ± 0.047	0.402 ± 0.055	0.472 ± 0.067
Brier score	DS	0.822 ± 0.014	1.110 ± 0.015	1.517 ± 0.028	1.611 ± 0.027	1.689 ± 0.035
	BCC	1.423 ± 0.035	1.680 ± 0.053	1.856 ± 0.045	1.878 ± 0.047	1.900 ± 0.053
	PE	0.612 ± 0.007	0.764 ± 0.015	0.978 ± 0.041	1.034 ± 0.047	1.085 ± 0.055
	EA	0.566 ± 0.011	0.789 ± 0.022	1.153 ± 0.054	1.255 ± 0.063	1.351 ± 0.079
	SDS	0.549 ± 0.009	0.772 ± 0.022	1.103 ± 0.045	1.191 ± 0.053	1.275 ± 0.066
NLL	DS	9.713 ± 0.102	12.492 ± 1.201	17.524 ± 0.346	19.078 ± 0.243	21.226 ± 1.179
	BCC	8.900 ± 0.218	11.329 ± 0.469	15.074 ± 0.639	16.114 ± 0.706	17.387 ± 0.844
	PE	1.985 ± 0.023	2.691 ± 0.060	3.914 ± 0.182	4.298 ± 0.221	4.722 ± 0.255
	EA	1.798 ± 0.035	2.777 ± 0.094	4.750 ± 0.268	5.404 ± 0.323	6.099 ± 0.402

Continued on next page

Table 10: Results on CIFAR100 with noise corruptions of increasing severity (continued).

Corruption Metric	Method	Severity 1	Severity 2	Severity 3	Severity 4	Severity 5
	SDS	1.753 \pm 0.029	2.771 \pm 0.114	4.715 \pm 0.208	5.285 \pm 0.296	5.896 \pm 0.356
Accuracy	DS	0.492 \pm 0.006	0.263 \pm 0.007	0.157 \pm 0.008	0.073 \pm 0.009	0.046 \pm 0.007
	BCC	0.158 \pm 0.014	0.045 \pm 0.012	0.022 \pm 0.007	0.016 \pm 0.001	0.017 \pm 0.000
	PE	0.500 \pm 0.006	0.261 \pm 0.007	0.152 \pm 0.007	0.068 \pm 0.008	0.043 \pm 0.007
	EA	0.500 \pm 0.006	0.267 \pm 0.009	0.156 \pm 0.007	0.073 \pm 0.010	0.046 \pm 0.008
	SDS	0.501 \pm 0.003	0.259 \pm 0.012	0.150 \pm 0.007	0.073 \pm 0.010	0.046 \pm 0.008
Impulse Noise	DS	0.454 \pm 0.010	0.587 \pm 0.022	0.616 \pm 0.014	0.650 \pm 0.018	0.697 \pm 0.039
	BCC	0.765 \pm 0.017	0.843 \pm 0.026	0.852 \pm 0.033	0.863 \pm 0.013	0.887 \pm 0.026
	PE	0.239 \pm 0.008	0.093 \pm 0.009	0.022 \pm 0.006	0.056 \pm 0.011	0.079 \pm 0.021
	EA	0.055 \pm 0.008	0.050 \pm 0.009	0.103 \pm 0.017	0.148 \pm 0.029	0.179 \pm 0.066
	SDS	0.086 \pm 0.007	0.042 \pm 0.006	0.089 \pm 0.013	0.127 \pm 0.028	0.157 \pm 0.060
Brier score	DS	0.940 \pm 0.015	1.267 \pm 0.027	1.379 \pm 0.018	1.486 \pm 0.024	1.560 \pm 0.050
	BCC	1.572 \pm 0.030	1.748 \pm 0.044	1.775 \pm 0.052	1.794 \pm 0.021	1.827 \pm 0.036
	PE	0.712 \pm 0.005	0.877 \pm 0.003	0.939 \pm 0.002	0.983 \pm 0.004	0.998 \pm 0.007
	EA	0.639 \pm 0.007	0.859 \pm 0.008	0.949 \pm 0.009	1.014 \pm 0.017	1.044 \pm 0.040
	SDS	0.641 \pm 0.004	0.863 \pm 0.009	0.949 \pm 0.007	1.003 \pm 0.014	1.030 \pm 0.033
NLL	DS	11.111 \pm 0.732	14.578 \pm 0.943	17.152 \pm 0.614	20.303 \pm 0.106	22.237 \pm 0.582
	BCC	9.885 \pm 0.222	12.168 \pm 0.414	13.498 \pm 0.587	14.759 \pm 0.863	15.699 \pm 1.284
	PE	2.454 \pm 0.035	3.430 \pm 0.045	3.933 \pm 0.042	4.398 \pm 0.025	4.618 \pm 0.067
	EA	2.162 \pm 0.047	3.295 \pm 0.068	3.898 \pm 0.062	4.457 \pm 0.082	4.749 \pm 0.185
	SDS	2.182 \pm 0.032	3.349 \pm 0.070	3.962 \pm 0.053	4.410 \pm 0.061	4.664 \pm 0.146

Table 11: Results on CIFAR100 with blur corruptions of increasing severity.

Corruption Metric	Method	Severity 1	Severity 2	Severity 3	Severity 4	Severity 5
Accuracy	DS	0.805 ± 0.002	0.766 ± 0.003	0.668 ± 0.006	0.524 ± 0.004	0.288 ± 0.004
	BCC	0.684 ± 0.004	0.573 ± 0.020	0.397 ± 0.002	0.219 ± 0.015	0.092 ± 0.006
	PE	0.813 ± 0.002	0.777 ± 0.004	0.682 ± 0.003	0.539 ± 0.005	0.300 ± 0.007
	EA	0.810 ± 0.002	0.771 ± 0.003	0.671 ± 0.003	0.524 ± 0.003	0.285 ± 0.002
	SDS	0.813 ± 0.001	0.778 ± 0.002	0.677 ± 0.000	0.523 ± 0.005	0.283 ± 0.001
Defocus Blur	DS	0.192 ± 0.002	0.228 ± 0.003	0.319 ± 0.007	0.454 ± 0.006	0.655 ± 0.022
	BCC	0.296 ± 0.004	0.405 ± 0.021	0.571 ± 0.004	0.735 ± 0.014	0.847 ± 0.002
	PE	0.243 ± 0.005	0.245 ± 0.005	0.232 ± 0.004	0.168 ± 0.007	0.076 ± 0.001
	EA	0.042 ± 0.001	0.046 ± 0.002	0.046 ± 0.001	0.079 ± 0.006	0.260 ± 0.017
	SDS	0.036 ± 0.001	0.041 ± 0.001	0.043 ± 0.001	0.052 ± 0.007	0.209 ± 0.015
Brier score	DS	0.385 ± 0.005	0.460 ± 0.006	0.645 ± 0.013	0.919 ± 0.009	1.339 ± 0.029
	BCC	0.606 ± 0.007	0.823 ± 0.040	1.159 ± 0.006	1.494 ± 0.028	1.726 ± 0.006
	PE	0.340 ± 0.002	0.389 ± 0.002	0.506 ± 0.001	0.653 ± 0.002	0.872 ± 0.004
	EA	0.273 ± 0.003	0.326 ± 0.003	0.457 ± 0.003	0.646 ± 0.005	0.977 ± 0.017
	SDS	0.269 ± 0.003	0.317 ± 0.003	0.447 ± 0.002	0.642 ± 0.006	0.951 ± 0.014
NLL	DS	4.538 ± 0.113	5.479 ± 0.092	7.483 ± 0.462	10.804 ± 0.242	13.953 ± 1.362
	BCC	3.639 ± 0.086	5.076 ± 0.293	7.274 ± 0.026	9.776 ± 0.232	13.255 ± 0.152
	PE	1.007 ± 0.006	1.162 ± 0.006	1.557 ± 0.002	2.131 ± 0.013	3.186 ± 0.009
	EA	0.755 ± 0.005	0.922 ± 0.007	1.361 ± 0.013	2.066 ± 0.024	3.547 ± 0.115
	SDS	0.742 ± 0.006	0.889 ± 0.008	1.341 ± 0.011	2.098 ± 0.034	3.583 ± 0.115
Accuracy	DS	0.190 ± 0.011	0.196 ± 0.012	0.237 ± 0.015	0.129 ± 0.009	0.166 ± 0.010
	BCC	0.051 ± 0.010	0.049 ± 0.008	0.068 ± 0.008	0.029 ± 0.007	0.046 ± 0.007
	PE	0.192 ± 0.013	0.199 ± 0.011	0.237 ± 0.013	0.131 ± 0.011	0.168 ± 0.011
	EA	0.186 ± 0.010	0.193 ± 0.010	0.232 ± 0.011	0.126 ± 0.011	0.163 ± 0.009
	SDS	0.185 ± 0.008	0.192 ± 0.009	0.230 ± 0.008	0.126 ± 0.011	0.163 ± 0.009
Frosted Glass Blur	DS	0.713 ± 0.011	0.704 ± 0.014	0.674 ± 0.015	0.762 ± 0.019	0.734 ± 0.016
	BCC	0.868 ± 0.012	0.871 ± 0.013	0.846 ± 0.011	0.902 ± 0.015	0.875 ± 0.010
	PE	0.076 ± 0.016	0.066 ± 0.014	0.040 ± 0.012	0.126 ± 0.019	0.086 ± 0.021
	EA	0.263 ± 0.020	0.252 ± 0.022	0.207 ± 0.023	0.324 ± 0.026	0.276 ± 0.026
	SDS	0.221 ± 0.017	0.209 ± 0.020	0.167 ± 0.019	0.280 ± 0.024	0.233 ± 0.024
Brier score	DS	1.480 ± 0.022	1.467 ± 0.024	1.400 ± 0.028	1.586 ± 0.027	1.526 ± 0.026
	BCC	1.781 ± 0.023	1.786 ± 0.023	1.740 ± 0.020	1.839 ± 0.022	1.793 ± 0.017
	PE	0.949 ± 0.014	0.941 ± 0.013	0.903 ± 0.013	0.998 ± 0.012	0.962 ± 0.012
	EA	1.045 ± 0.025	1.032 ± 0.024	0.970 ± 0.025	1.126 ± 0.024	1.065 ± 0.026
	SDS	1.018 ± 0.019	1.005 ± 0.019	0.951 ± 0.019	1.088 ± 0.021	1.035 ± 0.021
NLL	DS	16.565 ± 0.560	16.136 ± 0.199	15.275 ± 0.352	18.168 ± 0.601	17.172 ± 0.247
	BCC	13.893 ± 0.341	13.729 ± 0.288	12.724 ± 0.335	15.074 ± 0.344	13.892 ± 0.347
	PE	3.722 ± 0.091	3.688 ± 0.082	3.465 ± 0.075	4.082 ± 0.080	3.871 ± 0.071
	EA	4.012 ± 0.131	3.961 ± 0.118	3.657 ± 0.116	4.505 ± 0.119	4.212 ± 0.120
	SDS	4.036 ± 0.109	3.977 ± 0.101	3.695 ± 0.091	4.446 ± 0.124	4.211 ± 0.099
Accuracy	DS	0.715 ± 0.006	0.614 ± 0.006	0.507 ± 0.004	0.510 ± 0.005	0.410 ± 0.001
	BCC	0.468 ± 0.020	0.334 ± 0.011	0.214 ± 0.014	0.214 ± 0.013	0.133 ± 0.012
	PE	0.727 ± 0.004	0.631 ± 0.005	0.524 ± 0.003	0.529 ± 0.003	0.426 ± 0.008
	EA	0.720 ± 0.005	0.618 ± 0.004	0.508 ± 0.002	0.513 ± 0.004	0.409 ± 0.006
	SDS	0.730 ± 0.004	0.630 ± 0.004	0.512 ± 0.003	0.515 ± 0.007	0.406 ± 0.007
Motion Blur	DS	0.277 ± 0.006	0.371 ± 0.007	0.469 ± 0.004	0.464 ± 0.008	0.557 ± 0.000
	BCC	0.502 ± 0.020	0.628 ± 0.012	0.736 ± 0.012	0.735 ± 0.012	0.809 ± 0.008
	PE	0.249 ± 0.004	0.225 ± 0.004	0.172 ± 0.003	0.176 ± 0.005	0.104 ± 0.010
	EA	0.049 ± 0.004	0.043 ± 0.001	0.066 ± 0.005	0.062 ± 0.003	0.123 ± 0.005
	SDS	0.048 ± 0.002	0.045 ± 0.001	0.041 ± 0.003	0.038 ± 0.005	0.084 ± 0.004
Brier score	DS	0.559 ± 0.012	0.750 ± 0.014	0.951 ± 0.008	0.942 ± 0.012	1.131 ± 0.001
	BCC	1.021 ± 0.040	1.276 ± 0.023	1.498 ± 0.024	1.495 ± 0.024	1.648 ± 0.019
	PE	0.456 ± 0.003	0.563 ± 0.003	0.666 ± 0.001	0.663 ± 0.001	0.756 ± 0.004
	EA	0.393 ± 0.004	0.519 ± 0.005	0.653 ± 0.002	0.647 ± 0.003	0.784 ± 0.002
	SDS	0.382 ± 0.004	0.504 ± 0.006	0.643 ± 0.003	0.640 ± 0.005	0.775 ± 0.003
DS	6.644 ± 0.062	8.951 ± 0.104	11.467 ± 0.226	10.958 ± 0.570	13.130 ± 0.585	

NLL

Continued on next page

Table 11: Results on CIFAR100 with blur corruptions of increasing severity (continued).

Corruption Metric	Method	Severity 1	Severity 2	Severity 3	Severity 4	Severity 5
	BCC	6.284 ± 0.282	7.905 ± 0.204	9.581 ± 0.040	9.542 ± 0.093	11.011 ± 0.146
	PE	1.390 ± 0.011	1.784 ± 0.012	2.209 ± 0.009	2.208 ± 0.014	2.618 ± 0.009
	EA	1.150 ± 0.016	1.599 ± 0.022	2.130 ± 0.019	2.124 ± 0.023	2.678 ± 0.016
	SDS	1.104 ± 0.016	1.556 ± 0.021	2.128 ± 0.029	2.143 ± 0.025	2.733 ± 0.006

Continued on next page

Table 11: Results on CIFAR100 with blur corruptions of increasing severity (continued).

Corruption Metric	Method	Severity 1	Severity 2	Severity 3	Severity 4	Severity 5
Accuracy	DS	0.679 ± 0.007	0.630 ± 0.003	0.559 ± 0.003	0.487 ± 0.004	0.398 ± 0.003
	BCC	0.410 ± 0.039	0.348 ± 0.006	0.254 ± 0.009	0.196 ± 0.024	0.117 ± 0.006
	PE	0.695 ± 0.006	0.645 ± 0.002	0.574 ± 0.003	0.504 ± 0.002	0.413 ± 0.003
	EA	0.685 ± 0.003	0.633 ± 0.002	0.559 ± 0.003	0.489 ± 0.002	0.399 ± 0.002
	SDS	0.697 ± 0.003	0.637 ± 0.003	0.557 ± 0.005	0.486 ± 0.003	0.395 ± 0.002
Zoom Blur	DS	0.311 ± 0.007	0.355 ± 0.002	0.420 ± 0.003	0.485 ± 0.002	0.557 ± 0.014
	BCC	0.559 ± 0.038	0.616 ± 0.005	0.701 ± 0.008	0.754 ± 0.022	0.823 ± 0.003
	PE	0.246 ± 0.007	0.227 ± 0.003	0.196 ± 0.005	0.155 ± 0.004	0.096 ± 0.006
	EA	0.051 ± 0.003	0.049 ± 0.006	0.057 ± 0.006	0.088 ± 0.007	0.141 ± 0.007
	SDS	0.050 ± 0.003	0.041 ± 0.007	0.042 ± 0.004	0.051 ± 0.003	0.096 ± 0.008
Brier score	DS	0.626 ± 0.013	0.718 ± 0.004	0.851 ± 0.006	0.984 ± 0.005	1.137 ± 0.017
	BCC	1.135 ± 0.076	1.252 ± 0.010	1.425 ± 0.016	1.535 ± 0.044	1.678 ± 0.008
	PE	0.496 ± 0.003	0.549 ± 0.003	0.620 ± 0.002	0.688 ± 0.001	0.769 ± 0.001
	EA	0.441 ± 0.006	0.504 ± 0.005	0.596 ± 0.005	0.689 ± 0.006	0.803 ± 0.009
	SDS	0.425 ± 0.006	0.495 ± 0.005	0.595 ± 0.008	0.686 ± 0.009	0.795 ± 0.007
NLL	DS	7.326 ± 0.144	8.498 ± 0.060	9.835 ± 0.346	11.269 ± 0.889	12.017 ± 1.040
	BCC	7.022 ± 0.464	7.944 ± 0.064	9.151 ± 0.150	10.174 ± 0.162	11.705 ± 0.131
	PE	1.523 ± 0.011	1.720 ± 0.012	2.009 ± 0.013	2.307 ± 0.011	2.696 ± 0.005
	EA	1.305 ± 0.019	1.535 ± 0.019	1.886 ± 0.023	2.271 ± 0.030	2.778 ± 0.042
	SDS	1.246 ± 0.020	1.526 ± 0.028	1.930 ± 0.044	2.325 ± 0.057	2.842 ± 0.049

Table 12: Results on CIFAR100 with weather corruptions of increasing severity.

Corruption Metric	Method	Severity 1	Severity 2	Severity 3	Severity 4	Severity 5
Accuracy	DS	0.699 ± 0.003	0.538 ± 0.005	0.606 ± 0.007	0.590 ± 0.003	0.508 ± 0.004
	BCC	0.462 ± 0.024	0.237 ± 0.013	0.302 ± 0.011	0.308 ± 0.012	0.206 ± 0.012
	PE	0.711 ± 0.001	0.552 ± 0.007	0.618 ± 0.004	0.602 ± 0.006	0.516 ± 0.005
	EA	0.706 ± 0.006	0.546 ± 0.004	0.615 ± 0.005	0.595 ± 0.004	0.511 ± 0.006
	SDS	0.713 ± 0.007	0.548 ± 0.009	0.618 ± 0.007	0.599 ± 0.004	0.513 ± 0.004
Snow	DS	0.292 ± 0.003	0.438 ± 0.004	0.379 ± 0.007	0.395 ± 0.004	0.468 ± 0.003
	BCC	0.506 ± 0.026	0.718 ± 0.013	0.655 ± 0.011	0.643 ± 0.012	0.742 ± 0.013
	PE	0.261 ± 0.003	0.202 ± 0.004	0.242 ± 0.003	0.238 ± 0.007	0.194 ± 0.007
	EA	0.052 ± 0.002	0.042 ± 0.005	0.038 ± 0.003	0.040 ± 0.002	0.040 ± 0.006
	SDS	0.048 ± 0.003	0.030 ± 0.002	0.048 ± 0.002	0.045 ± 0.002	0.028 ± 0.003
Brier score	DS	0.589 ± 0.007	0.890 ± 0.008	0.767 ± 0.013	0.798 ± 0.007	0.950 ± 0.006
	BCC	1.030 ± 0.052	1.460 ± 0.025	1.332 ± 0.022	1.314 ± 0.023	1.512 ± 0.025
	PE	0.481 ± 0.005	0.640 ± 0.004	0.579 ± 0.003	0.599 ± 0.002	0.678 ± 0.005
	EA	0.410 ± 0.007	0.600 ± 0.005	0.515 ± 0.004	0.538 ± 0.003	0.640 ± 0.009
	SDS	0.398 ± 0.008	0.595 ± 0.011	0.510 ± 0.007	0.531 ± 0.005	0.632 ± 0.006
NLL	DS	7.072 ± 0.088	11.033 ± 0.100	9.393 ± 0.197	9.893 ± 0.114	11.712 ± 0.027
	BCC	6.257 ± 0.387	9.008 ± 0.173	8.042 ± 0.189	7.930 ± 0.138	9.218 ± 0.192
	PE	1.484 ± 0.013	2.126 ± 0.019	1.862 ± 0.012	1.927 ± 0.009	2.270 ± 0.025
	EA	1.218 ± 0.019	1.957 ± 0.009	1.609 ± 0.009	1.680 ± 0.015	2.098 ± 0.035
	SDS	1.176 ± 0.035	1.982 ± 0.037	1.617 ± 0.024	1.680 ± 0.019	2.100 ± 0.031
Accuracy	DS	0.703 ± 0.002	0.610 ± 0.008	0.479 ± 0.009	0.454 ± 0.007	0.347 ± 0.006
	BCC	0.435 ± 0.015	0.310 ± 0.009	0.171 ± 0.008	0.159 ± 0.008	0.086 ± 0.010
	PE	0.713 ± 0.002	0.618 ± 0.006	0.487 ± 0.009	0.466 ± 0.008	0.355 ± 0.006
	EA	0.707 ± 0.002	0.614 ± 0.005	0.481 ± 0.010	0.459 ± 0.008	0.347 ± 0.006
	SDS	0.717 ± 0.005	0.620 ± 0.005	0.482 ± 0.009	0.461 ± 0.004	0.347 ± 0.001
Frost	DS	0.288 ± 0.002	0.374 ± 0.006	0.484 ± 0.007	0.509 ± 0.001	0.593 ± 0.009
	BCC	0.537 ± 0.015	0.653 ± 0.010	0.777 ± 0.010	0.786 ± 0.008	0.849 ± 0.011
	PE	0.255 ± 0.006	0.228 ± 0.007	0.160 ± 0.010	0.144 ± 0.009	0.066 ± 0.007

Frost

Continued on next page

Table 12: Results on CIFAR100 with weather corruptions of increasing severity (continued).

Corruption Metric	Method	Severity 1	Severity 2	Severity 3	Severity 4	Severity 5
	EA	0.043 ± 0.001	0.040 ± 0.002	0.066 ± 0.008	0.078 ± 0.007	0.142 ± 0.011
	SDS	0.045 ± 0.001	0.038 ± 0.002	0.039 ± 0.007	0.048 ± 0.008	0.103 ± 0.010
Brier score	DS	0.581 ± 0.004	0.758 ± 0.013	0.989 ± 0.015	1.038 ± 0.005	1.220 ± 0.017
	BCC	1.090 ± 0.029	1.325 ± 0.019	1.582 ± 0.018	1.600 ± 0.016	1.730 ± 0.022
	PE	0.475 ± 0.003	0.579 ± 0.005	0.701 ± 0.006	0.718 ± 0.006	0.811 ± 0.006
	EA	0.405 ± 0.002	0.523 ± 0.006	0.680 ± 0.009	0.707 ± 0.010	0.839 ± 0.012
	SDS	0.394 ± 0.004	0.512 ± 0.007	0.674 ± 0.007	0.695 ± 0.002	0.826 ± 0.005
NLL	DS	6.959 ± 0.104	9.090 ± 0.219	11.060 ± 0.451	12.041 ± 0.336	13.419 ± 0.699
	BCC	6.695 ± 0.178	8.210 ± 0.104	10.078 ± 0.147	10.310 ± 0.086	11.670 ± 0.032
	PE	1.459 ± 0.010	1.846 ± 0.017	2.372 ± 0.026	2.467 ± 0.031	2.946 ± 0.037
	EA	1.196 ± 0.006	1.624 ± 0.023	2.258 ± 0.038	2.390 ± 0.049	3.001 ± 0.063
	SDS	1.163 ± 0.019	1.604 ± 0.033	2.293 ± 0.028	2.387 ± 0.017	3.038 ± 0.027

Continued on next page

Table 12: Results on CIFAR100 with weather corruptions of increasing severity (continued).

Corruption Metric	Method	Severity 1	Severity 2	Severity 3	Severity 4	Severity 5
Accuracy	DS	0.790 ± 0.003	0.744 ± 0.004	0.696 ± 0.001	0.627 ± 0.004	0.417 ± 0.004
	BCC	0.642 ± 0.014	0.535 ± 0.005	0.442 ± 0.015	0.322 ± 0.016	0.120 ± 0.003
	PE	0.800 ± 0.002	0.761 ± 0.004	0.719 ± 0.001	0.652 ± 0.005	0.437 ± 0.005
	EA	0.794 ± 0.001	0.750 ± 0.003	0.703 ± 0.001	0.633 ± 0.004	0.418 ± 0.004
	SDS	0.798 ± 0.002	0.759 ± 0.003	0.713 ± 0.001	0.646 ± 0.001	0.415 ± 0.004
Fog	DS	0.205 ± 0.003	0.249 ± 0.004	0.296 ± 0.000	0.358 ± 0.005	0.542 ± 0.002
	BCC	0.338 ± 0.014	0.441 ± 0.005	0.529 ± 0.016	0.643 ± 0.015	0.825 ± 0.004
	PE	0.245 ± 0.006	0.252 ± 0.007	0.249 ± 0.002	0.230 ± 0.006	0.122 ± 0.005
	EA	0.042 ± 0.002	0.047 ± 0.006	0.047 ± 0.001	0.046 ± 0.001	0.103 ± 0.004
	SDS	0.035 ± 0.002	0.047 ± 0.005	0.046 ± 0.003	0.043 ± 0.002	0.066 ± 0.004
Brier score	DS	0.413 ± 0.005	0.502 ± 0.008	0.596 ± 0.001	0.724 ± 0.009	1.106 ± 0.004
	BCC	0.689 ± 0.029	0.897 ± 0.010	1.074 ± 0.030	1.303 ± 0.030	1.677 ± 0.005
	PE	0.357 ± 0.001	0.413 ± 0.001	0.467 ± 0.001	0.540 ± 0.002	0.743 ± 0.003
	EA	0.292 ± 0.002	0.353 ± 0.002	0.415 ± 0.002	0.503 ± 0.004	0.761 ± 0.006
	SDS	0.287 ± 0.003	0.342 ± 0.002	0.402 ± 0.001	0.485 ± 0.003	0.756 ± 0.005
NLL	DS	4.858 ± 0.057	5.997 ± 0.118	7.231 ± 0.030	8.719 ± 0.060	13.275 ± 0.299
	BCC	4.222 ± 0.241	5.580 ± 0.060	6.694 ± 0.218	8.081 ± 0.180	10.938 ± 0.049
	PE	1.059 ± 0.005	1.243 ± 0.003	1.432 ± 0.002	1.699 ± 0.005	2.593 ± 0.014
	EA	0.815 ± 0.005	1.013 ± 0.005	1.230 ± 0.005	1.546 ± 0.014	2.626 ± 0.025
	SDS	0.797 ± 0.006	0.976 ± 0.005	1.185 ± 0.004	1.494 ± 0.005	2.691 ± 0.026
Accuracy	DS	0.810 ± 0.001	0.805 ± 0.002	0.795 ± 0.003	0.777 ± 0.004	0.724 ± 0.005
	BCC	0.693 ± 0.014	0.670 ± 0.017	0.660 ± 0.015	0.615 ± 0.012	0.508 ± 0.015
	PE	0.819 ± 0.003	0.813 ± 0.001	0.801 ± 0.001	0.783 ± 0.003	0.730 ± 0.004
	EA	0.815 ± 0.001	0.811 ± 0.002	0.800 ± 0.002	0.782 ± 0.003	0.729 ± 0.002
	SDS	0.818 ± 0.001	0.813 ± 0.002	0.804 ± 0.002	0.787 ± 0.003	0.737 ± 0.003
Brightness	DS	0.186 ± 0.002	0.191 ± 0.002	0.201 ± 0.003	0.218 ± 0.005	0.270 ± 0.005
	BCC	0.289 ± 0.015	0.311 ± 0.017	0.319 ± 0.015	0.362 ± 0.013	0.463 ± 0.014
	PE	0.244 ± 0.007	0.248 ± 0.004	0.251 ± 0.005	0.255 ± 0.006	0.258 ± 0.007
	EA	0.041 ± 0.002	0.045 ± 0.002	0.048 ± 0.001	0.052 ± 0.001	0.059 ± 0.002
	SDS	0.036 ± 0.001	0.038 ± 0.001	0.042 ± 0.002	0.047 ± 0.001	0.058 ± 0.002
Brier score	DS	0.374 ± 0.003	0.384 ± 0.004	0.404 ± 0.006	0.439 ± 0.009	0.543 ± 0.010
	BCC	0.589 ± 0.029	0.634 ± 0.034	0.651 ± 0.031	0.738 ± 0.025	0.942 ± 0.027
	PE	0.333 ± 0.001	0.344 ± 0.001	0.362 ± 0.001	0.388 ± 0.001	0.460 ± 0.001
	EA	0.265 ± 0.002	0.273 ± 0.002	0.289 ± 0.003	0.313 ± 0.004	0.385 ± 0.004
	SDS	0.262 ± 0.003	0.270 ± 0.002	0.284 ± 0.003	0.307 ± 0.003	0.374 ± 0.003
NLL	DS	4.426 ± 0.099	4.494 ± 0.086	4.754 ± 0.039	5.140 ± 0.187	6.425 ± 0.134
	BCC	3.526 ± 0.205	3.880 ± 0.279	3.960 ± 0.242	4.521 ± 0.255	5.780 ± 0.181
	PE	0.985 ± 0.007	1.017 ± 0.006	1.071 ± 0.006	1.152 ± 0.006	1.390 ± 0.006
	EA	0.729 ± 0.003	0.754 ± 0.003	0.802 ± 0.005	0.877 ± 0.008	1.110 ± 0.012
	SDS	0.718 ± 0.004	0.742 ± 0.003	0.786 ± 0.004	0.854 ± 0.007	1.072 ± 0.013

Table 13: Results on CIFAR100 with digital corruptions of increasing severity.

Corruption Metric	Method	Severity 1	Severity 2	Severity 3	Severity 4	Severity 5
Accuracy	DS	0.779 ± 0.003	0.684 ± 0.000	0.596 ± 0.001	0.454 ± 0.008	0.150 ± 0.007
	BCC	0.613 ± 0.005	0.419 ± 0.013	0.276 ± 0.014	0.147 ± 0.028	0.039 ± 0.005
	PE	0.791 ± 0.002	0.707 ± 0.001	0.621 ± 0.001	0.481 ± 0.003	0.162 ± 0.003
	EA	0.783 ± 0.002	0.689 ± 0.002	0.597 ± 0.002	0.453 ± 0.006	0.145 ± 0.006
	SDS	0.790 ± 0.003	0.699 ± 0.003	0.608 ± 0.002	0.451 ± 0.005	0.144 ± 0.006
ECE	DS	0.216 ± 0.002	0.307 ± 0.001	0.386 ± 0.003	0.511 ± 0.010	0.784 ± 0.012
	BCC	0.366 ± 0.005	0.550 ± 0.014	0.688 ± 0.014	0.804 ± 0.029	0.898 ± 0.007
	PE	0.246 ± 0.006	0.244 ± 0.004	0.212 ± 0.002	0.133 ± 0.006	0.171 ± 0.017

Contrast

Continued on next page

Table 13: Results on CIFAR100 with digital corruptions of increasing severity (continued).

Corruption Metric	Method	Severity 1	Severity 2	Severity 3	Severity 4	Severity 5
	EA	0.042 ± 0.003	0.050 ± 0.003	0.046 ± 0.001	0.098 ± 0.010	0.408 ± 0.025
	SDS	0.039 ± 0.003	0.048 ± 0.004	0.037 ± 0.001	0.062 ± 0.010	0.354 ± 0.023
Brier score	DS	0.435 ± 0.005	0.617 ± 0.001	0.782 ± 0.005	1.039 ± 0.018	1.601 ± 0.022
	BCC	0.744 ± 0.010	1.118 ± 0.027	1.394 ± 0.028	1.632 ± 0.057	1.828 ± 0.014
	PE	0.370 ± 0.001	0.481 ± 0.000	0.569 ± 0.001	0.700 ± 0.002	0.998 ± 0.011
	EA	0.307 ± 0.002	0.433 ± 0.002	0.543 ± 0.004	0.722 ± 0.009	1.185 ± 0.028
	SDS	0.301 ± 0.002	0.418 ± 0.002	0.526 ± 0.001	0.716 ± 0.007	1.132 ± 0.022
NLL	DS	5.154 ± 0.077	7.347 ± 0.016	9.224 ± 0.138	11.472 ± 0.826	18.762 ± 0.574
	BCC	4.597 ± 0.039	6.945 ± 0.139	8.730 ± 0.125	10.670 ± 0.340	15.207 ± 0.266
	PE	1.102 ± 0.006	1.471 ± 0.006	1.800 ± 0.005	2.359 ± 0.002	4.030 ± 0.054
	EA	0.862 ± 0.004	1.283 ± 0.007	1.683 ± 0.014	2.405 ± 0.037	4.884 ± 0.239
	SDS	0.841 ± 0.005	1.234 ± 0.010	1.638 ± 0.004	2.461 ± 0.041	4.856 ± 0.176

Continued on next page

Table 13: Results on CIFAR100 with digital corruptions of increasing severity (continued).

Corruption Metric	Method	Severity 1	Severity 2	Severity 3	Severity 4	Severity 5
Accuracy	DS	0.711 ± 0.005	0.709 ± 0.004	0.645 ± 0.003	0.548 ± 0.003	0.455 ± 0.002
	BCC	0.476 ± 0.016	0.478 ± 0.018	0.365 ± 0.009	0.228 ± 0.010	0.121 ± 0.006
	PE	0.724 ± 0.002	0.722 ± 0.004	0.657 ± 0.004	0.564 ± 0.003	0.466 ± 0.005
	EA	0.719 ± 0.003	0.714 ± 0.004	0.649 ± 0.000	0.552 ± 0.004	0.457 ± 0.003
	SDS	0.729 ± 0.003	0.724 ± 0.004	0.657 ± 0.002	0.558 ± 0.006	0.460 ± 0.006
Elastic	DS	0.281 ± 0.004	0.283 ± 0.005	0.342 ± 0.002	0.429 ± 0.004	0.514 ± 0.004
	BCC	0.496 ± 0.016	0.494 ± 0.019	0.599 ± 0.010	0.722 ± 0.011	0.815 ± 0.006
	PE	0.253 ± 0.004	0.253 ± 0.006	0.241 ± 0.007	0.221 ± 0.002	0.176 ± 0.003
	EA	0.049 ± 0.002	0.047 ± 0.000	0.050 ± 0.005	0.048 ± 0.005	0.050 ± 0.002
	SDS	0.046 ± 0.001	0.044 ± 0.000	0.049 ± 0.001	0.048 ± 0.004	0.042 ± 0.002
Brier score	DS	0.566 ± 0.009	0.571 ± 0.009	0.691 ± 0.004	0.871 ± 0.006	1.045 ± 0.007
	BCC	1.007 ± 0.032	1.003 ± 0.037	1.218 ± 0.020	1.471 ± 0.022	1.664 ± 0.012
	PE	0.461 ± 0.003	0.464 ± 0.003	0.540 ± 0.003	0.643 ± 0.004	0.732 ± 0.004
	EA	0.394 ± 0.003	0.399 ± 0.004	0.484 ± 0.004	0.598 ± 0.002	0.705 ± 0.003
	SDS	0.382 ± 0.003	0.386 ± 0.004	0.472 ± 0.004	0.588 ± 0.005	0.699 ± 0.010
NLL	DS	6.755 ± 0.126	6.770 ± 0.137	8.243 ± 0.139	10.442 ± 0.006	12.532 ± 0.225
	BCC	6.223 ± 0.212	6.197 ± 0.275	7.579 ± 0.178	9.056 ± 0.199	10.252 ± 0.077
	PE	1.395 ± 0.009	1.406 ± 0.009	1.684 ± 0.006	2.075 ± 0.011	2.459 ± 0.022
	EA	1.144 ± 0.011	1.160 ± 0.013	1.464 ± 0.012	1.885 ± 0.012	2.318 ± 0.017
	SDS	1.097 ± 0.011	1.109 ± 0.012	1.427 ± 0.017	1.869 ± 0.032	2.320 ± 0.062
Accuracy	DS	0.763 ± 0.005	0.671 ± 0.002	0.610 ± 0.003	0.407 ± 0.007	0.221 ± 0.003
	BCC	0.614 ± 0.015	0.384 ± 0.001	0.303 ± 0.008	0.130 ± 0.014	0.064 ± 0.002
	PE	0.772 ± 0.001	0.683 ± 0.002	0.622 ± 0.002	0.413 ± 0.003	0.228 ± 0.003
	EA	0.770 ± 0.004	0.677 ± 0.002	0.614 ± 0.004	0.406 ± 0.005	0.219 ± 0.003
	SDS	0.776 ± 0.004	0.689 ± 0.003	0.622 ± 0.010	0.407 ± 0.007	0.219 ± 0.003
Pixelate	DS	0.232 ± 0.004	0.320 ± 0.002	0.375 ± 0.003	0.548 ± 0.007	0.695 ± 0.010
	BCC	0.363 ± 0.014	0.582 ± 0.001	0.656 ± 0.009	0.808 ± 0.015	0.849 ± 0.004
	PE	0.261 ± 0.007	0.252 ± 0.004	0.231 ± 0.006	0.104 ± 0.005	0.044 ± 0.002
	EA	0.054 ± 0.004	0.044 ± 0.001	0.036 ± 0.002	0.105 ± 0.008	0.244 ± 0.007
	SDS	0.050 ± 0.002	0.053 ± 0.002	0.044 ± 0.005	0.068 ± 0.006	0.199 ± 0.007
Brier score	DS	0.467 ± 0.009	0.645 ± 0.004	0.758 ± 0.006	1.122 ± 0.014	1.440 ± 0.015
	BCC	0.740 ± 0.028	1.184 ± 0.002	1.334 ± 0.017	1.648 ± 0.030	1.746 ± 0.008
	PE	0.403 ± 0.002	0.509 ± 0.003	0.571 ± 0.002	0.746 ± 0.001	0.897 ± 0.001
	EA	0.329 ± 0.004	0.443 ± 0.004	0.518 ± 0.005	0.758 ± 0.009	0.986 ± 0.006
	SDS	0.321 ± 0.003	0.428 ± 0.005	0.507 ± 0.012	0.750 ± 0.010	0.961 ± 0.006
NLL	DS	5.545 ± 0.084	7.847 ± 0.032	9.195 ± 0.185	13.241 ± 0.455	17.068 ± 0.678
	BCC	4.466 ± 0.212	7.303 ± 0.066	8.248 ± 0.134	10.901 ± 0.252	13.157 ± 0.089
	PE	1.209 ± 0.004	1.588 ± 0.011	1.830 ± 0.011	2.648 ± 0.009	3.587 ± 0.001
	EA	0.935 ± 0.009	1.334 ± 0.012	1.617 ± 0.022	2.653 ± 0.044	3.912 ± 0.056
	SDS	0.907 ± 0.008	1.284 ± 0.019	1.595 ± 0.060	2.688 ± 0.060	3.934 ± 0.064
Accuracy	DS	0.625 ± 0.003	0.522 ± 0.002	0.490 ± 0.004	0.445 ± 0.002	0.395 ± 0.001
	BCC	0.326 ± 0.014	0.216 ± 0.007	0.199 ± 0.013	0.163 ± 0.006	0.128 ± 0.011
	PE	0.637 ± 0.004	0.538 ± 0.003	0.502 ± 0.006	0.462 ± 0.002	0.408 ± 0.001
	EA	0.630 ± 0.003	0.529 ± 0.003	0.494 ± 0.004	0.451 ± 0.006	0.399 ± 0.002
	SDS	0.638 ± 0.005	0.534 ± 0.003	0.498 ± 0.006	0.453 ± 0.005	0.392 ± 0.003
JPEG	DS	0.362 ± 0.002	0.454 ± 0.002	0.483 ± 0.003	0.521 ± 0.004	0.561 ± 0.004
	BCC	0.633 ± 0.015	0.728 ± 0.004	0.738 ± 0.012	0.767 ± 0.010	0.792 ± 0.012
	PE	0.251 ± 0.006	0.221 ± 0.003	0.205 ± 0.008	0.186 ± 0.005	0.159 ± 0.003
	EA	0.052 ± 0.004	0.042 ± 0.002	0.035 ± 0.002	0.032 ± 0.001	0.037 ± 0.003
	SDS	0.054 ± 0.003	0.047 ± 0.005	0.043 ± 0.007	0.035 ± 0.010	0.029 ± 0.004
Brier score	DS	0.731 ± 0.005	0.922 ± 0.003	0.982 ± 0.006	1.062 ± 0.007	1.147 ± 0.004
	BCC	1.288 ± 0.030	1.486 ± 0.009	1.509 ± 0.024	1.572 ± 0.017	1.626 ± 0.023
	PE	0.568 ± 0.005	0.665 ± 0.002	0.696 ± 0.002	0.729 ± 0.001	0.774 ± 0.000
	EA	0.502 ± 0.005	0.615 ± 0.004	0.652 ± 0.005	0.694 ± 0.004	0.749 ± 0.002
	SDS	0.490 ± 0.006	0.608 ± 0.004	0.646 ± 0.005	0.691 ± 0.006	0.753 ± 0.001

Continued on next page

Table 13: Results on CIFAR100 with digital corruptions of increasing severity (continued).

Corruption Metric	Method	Severity 1	Severity 2	Severity 3	Severity 4	Severity 5
NLL	DS	8.830 ± 0.054	11.189 ± 0.180	12.051 ± 0.060	12.908 ± 0.497	14.039 ± 0.399
	BCC	7.889 ± 0.192	9.047 ± 0.105	9.150 ± 0.170	9.589 ± 0.068	9.949 ± 0.096
	PE	1.781 ± 0.020	2.197 ± 0.012	2.348 ± 0.011	2.513 ± 0.008	2.743 ± 0.007
	EA	1.525 ± 0.022	1.982 ± 0.017	2.154 ± 0.021	2.342 ± 0.019	2.608 ± 0.014
	SDS	1.491 ± 0.034	1.971 ± 0.019	2.161 ± 0.019	2.362 ± 0.033	2.665 ± 0.009

J.3 ImageNet

Results for all corruptions on ImageNet are provided in Tables 14–17. On some corruptions BCC fails to provide reasonable predictions and outputs uniform probabilities for all classes. In these cases ECE is not adequately computed as being very close to zero. Please note that all these cases paired with very low accuracy. See, for example, “Shot Noise” corruption of severity 2. ECE values for such cases are non-informative.

Table 14: Results on ImageNet with noise corruptions of increasing severity.

Corruption Metric	Method	Severity 1	Severity 2	Severity 3	Severity 4	Severity 5	
Accuracy	DS	0.630 ± 0.003	0.535 ± 0.002	0.374 ± 0.004	0.198 ± 0.005	0.064 ± 0.004	
	BCC	0.613 ± 0.002	0.153 ± 0.261	0.002 ± 0.001	0.001 ± 0.000	0.001 ± 0.000	
	EA	0.638 ± 0.001	0.541 ± 0.001	0.379 ± 0.004	0.199 ± 0.004	0.063 ± 0.005	
	SDS	0.638 ± 0.001	0.541 ± 0.001	0.379 ± 0.004	0.199 ± 0.004	0.063 ± 0.005	
Gaussian Noise	ECE	DS	0.365 ± 0.003	0.457 ± 0.002	0.606 ± 0.002	0.733 ± 0.003	0.637 ± 0.009
	BCC	0.612 ± 0.002	0.152 ± 0.261	0.924 ± 0.019	0.925 ± 0.015	0.938 ± 0.005	
	EA	0.022 ± 0.001	0.022 ± 0.001	0.029 ± 0.004	0.071 ± 0.003	0.116 ± 0.009	
	SDS	0.025 ± 0.001	0.023 ± 0.001	0.027 ± 0.003	0.066 ± 0.003	0.113 ± 0.009	
Brier score	DS	0.733 ± 0.005	0.919 ± 0.004	1.223 ± 0.004	1.505 ± 0.006	1.475 ± 0.008	
	BCC	0.999 ± 0.000	0.999 ± 0.000	1.885 ± 0.024	1.890 ± 0.023	1.910 ± 0.007	
	EA	0.481 ± 0.002	0.588 ± 0.002	0.751 ± 0.002	0.910 ± 0.003	1.006 ± 0.005	
	SDS	0.481 ± 0.002	0.588 ± 0.002	0.751 ± 0.002	0.909 ± 0.003	1.004 ± 0.005	
NLL	DS	9.433 ± 0.039	12.010 ± 0.024	16.295 ± 0.106	20.573 ± 0.135	23.449 ± 0.177	
	BCC	6.907 ± 0.000	6.907 ± 0.000	11.917 ± 0.678	13.904 ± 0.474	17.160 ± 0.489	
	EA	1.542 ± 0.010	2.062 ± 0.010	3.065 ± 0.050	4.510 ± 0.102	6.197 ± 0.093	
	SDS	1.554 ± 0.011	2.079 ± 0.009	3.081 ± 0.050	4.510 ± 0.097	6.147 ± 0.080	
Accuracy	DS	0.618 ± 0.003	0.506 ± 0.005	0.358 ± 0.001	0.159 ± 0.002	0.074 ± 0.004	
	BCC	0.598 ± 0.003	0.002 ± 0.001	0.002 ± 0.001	0.001 ± 0.001	0.001 ± 0.000	
	EA	0.625 ± 0.003	0.512 ± 0.004	0.362 ± 0.003	0.158 ± 0.002	0.072 ± 0.004	
	SDS	0.625 ± 0.003	0.512 ± 0.004	0.362 ± 0.003	0.158 ± 0.002	0.072 ± 0.004	
Shot Noise	ECE	DS	0.377 ± 0.003	0.485 ± 0.004	0.619 ± 0.002	0.737 ± 0.004	0.638 ± 0.008
	BCC	0.597 ± 0.003	0.001 ± 0.001	0.931 ± 0.022	0.925 ± 0.018	0.940 ± 0.006	
	EA	0.021 ± 0.001	0.021 ± 0.002	0.034 ± 0.004	0.091 ± 0.004	0.123 ± 0.004	
	SDS	0.024 ± 0.001	0.022 ± 0.003	0.031 ± 0.004	0.086 ± 0.004	0.119 ± 0.004	
Brier score	DS	0.756 ± 0.007	0.974 ± 0.009	1.250 ± 0.003	1.534 ± 0.004	1.469 ± 0.005	
	BCC	0.999 ± 0.000	0.999 ± 0.000	1.896 ± 0.029	1.890 ± 0.027	1.912 ± 0.009	
	EA	0.495 ± 0.004	0.619 ± 0.005	0.768 ± 0.004	0.943 ± 0.001	1.003 ± 0.002	
	SDS	0.495 ± 0.004	0.619 ± 0.005	0.767 ± 0.004	0.942 ± 0.001	1.002 ± 0.002	
NLL	DS	9.753 ± 0.098	12.759 ± 0.099	16.660 ± 0.062	21.280 ± 0.075	23.062 ± 0.148	
	BCC	6.907 ± 0.000	6.907 ± 0.000	12.338 ± 0.892	14.802 ± 0.087	16.841 ± 0.389	
	EA	1.603 ± 0.016	2.225 ± 0.026	3.190 ± 0.024	4.966 ± 0.066	6.113 ± 0.084	

Continued on next page

Table 14: Results on ImageNet with noise corruptions of increasing severity (continued).

Corruption Metric	Method	Severity 1	Severity 2	Severity 3	Severity 4	Severity 5	
	SDS	1.618 ± 0.019	2.242 ± 0.026	3.203 ± 0.022	4.950 ± 0.059	6.061 ± 0.066	
Impulse Noise	Accuracy	DS	0.538 ± 0.009	0.445 ± 0.006	0.356 ± 0.004	0.178 ± 0.008	0.065 ± 0.008
		BCC	0.002 ± 0.000	0.003 ± 0.004	0.002 ± 0.002	0.001 ± 0.000	0.001 ± 0.000
		EA	0.546 ± 0.009	0.452 ± 0.006	0.360 ± 0.004	0.177 ± 0.008	0.064 ± 0.008
		SDS	0.547 ± 0.009	0.452 ± 0.006	0.360 ± 0.004	0.177 ± 0.008	0.064 ± 0.008
	ECE	DS	0.453 ± 0.008	0.541 ± 0.005	0.621 ± 0.005	0.741 ± 0.005	0.664 ± 0.052
		BCC	0.001 ± 0.000	0.833 ± 0.126	0.929 ± 0.022	0.940 ± 0.006	0.934 ± 0.054
		EA	0.023 ± 0.002	0.024 ± 0.002	0.033 ± 0.003	0.079 ± 0.003	0.119 ± 0.008
		SDS	0.027 ± 0.004	0.024 ± 0.003	0.031 ± 0.003	0.075 ± 0.003	0.115 ± 0.008
	Brier score	DS	0.911 ± 0.017	1.090 ± 0.010	1.255 ± 0.010	1.528 ± 0.003	1.506 ± 0.057
		BCC	0.999 ± 0.000	1.779 ± 0.138	1.892 ± 0.029	1.913 ± 0.010	1.904 ± 0.077
		EA	0.581 ± 0.009	0.680 ± 0.006	0.769 ± 0.004	0.927 ± 0.006	1.007 ± 0.007
		SDS	0.581 ± 0.009	0.680 ± 0.006	0.769 ± 0.004	0.926 ± 0.006	1.005 ± 0.006
NLL	DS	11.892 ± 0.214	14.387 ± 0.200	16.753 ± 0.225	20.996 ± 0.072	23.438 ± 0.165	
	BCC	6.907 ± 0.000	10.731 ± 1.120	11.892 ± 0.506	13.938 ± 0.680	16.901 ± 0.699	
	EA	2.019 ± 0.044	2.575 ± 0.034	3.180 ± 0.036	4.704 ± 0.114	6.159 ± 0.152	
	SDS	2.031 ± 0.042	2.588 ± 0.035	3.195 ± 0.036	4.700 ± 0.109	6.104 ± 0.133	

Table 15: Results on ImageNet with blur corruptions of increasing severity.

Corruption Metric	Method	Severity 1	Severity 2	Severity 3	Severity 4	Severity 5	
Defocus Blur	Accuracy	DS	0.632 ± 0.002	0.565 ± 0.003	0.430 ± 0.007	0.309 ± 0.007	0.215 ± 0.009
		BCC	0.618 ± 0.002	0.548 ± 0.003	0.001 ± 0.000	0.002 ± 0.000	0.002 ± 0.000
		EA	0.638 ± 0.003	0.573 ± 0.003	0.436 ± 0.008	0.312 ± 0.009	0.215 ± 0.009
		SDS	0.638 ± 0.002	0.573 ± 0.003	0.436 ± 0.008	0.312 ± 0.009	0.215 ± 0.009
	ECE	DS	0.364 ± 0.002	0.430 ± 0.002	0.562 ± 0.007	0.677 ± 0.007	0.756 ± 0.007
		BCC	0.617 ± 0.002	0.547 ± 0.003	0.000 ± 0.000	0.908 ± 0.003	0.927 ± 0.002
		EA	0.046 ± 0.002	0.058 ± 0.002	0.059 ± 0.004	0.036 ± 0.005	0.012 ± 0.004
		SDS	0.053 ± 0.002	0.065 ± 0.002	0.064 ± 0.005	0.040 ± 0.005	0.013 ± 0.005
	Brier score	DS	0.730 ± 0.004	0.862 ± 0.005	1.128 ± 0.014	1.361 ± 0.014	1.527 ± 0.015
		BCC	0.999 ± 0.000	0.999 ± 0.000	0.999 ± 0.000	1.863 ± 0.004	1.892 ± 0.003
		EA	0.485 ± 0.002	0.560 ± 0.003	0.704 ± 0.007	0.814 ± 0.007	0.891 ± 0.006
		SDS	0.486 ± 0.002	0.561 ± 0.003	0.705 ± 0.007	0.815 ± 0.007	0.891 ± 0.006
NLL	DS	9.356 ± 0.071	11.191 ± 0.050	14.944 ± 0.234	18.308 ± 0.189	20.694 ± 0.215	
	BCC	6.907 ± 0.000	6.907 ± 0.000	6.908 ± 0.000	11.056 ± 0.086	11.953 ± 0.107	
	EA	1.536 ± 0.010	1.885 ± 0.016	2.671 ± 0.046	3.472 ± 0.071	4.206 ± 0.078	
	SDS	1.552 ± 0.009	1.901 ± 0.015	2.687 ± 0.046	3.489 ± 0.071	4.216 ± 0.074	
Frosted Glass Blur	Accuracy	DS	0.570 ± 0.003	0.436 ± 0.005	0.192 ± 0.006	0.147 ± 0.004	0.109 ± 0.003
		BCC	0.001 ± 0.000	0.010 ± 0.001	0.002 ± 0.000	0.002 ± 0.001	0.002 ± 0.000
		EA	0.573 ± 0.002	0.436 ± 0.004	0.187 ± 0.005	0.144 ± 0.004	0.106 ± 0.003
		SDS	0.573 ± 0.002	0.436 ± 0.004	0.187 ± 0.005	0.144 ± 0.004	0.106 ± 0.003
	ECE	DS	0.424 ± 0.003	0.551 ± 0.005	0.738 ± 0.002	0.764 ± 0.003	0.801 ± 0.007
		BCC	0.332 ± 0.187	0.863 ± 0.003	0.931 ± 0.003	0.937 ± 0.001	0.927 ± 0.006
		EA	0.016 ± 0.001	0.014 ± 0.001	0.110 ± 0.006	0.115 ± 0.005	0.096 ± 0.008
		SDS	0.019 ± 0.001	0.009 ± 0.001	0.104 ± 0.006	0.110 ± 0.005	0.092 ± 0.008
	Brier score	DS	0.851 ± 0.005	1.109 ± 0.009	1.513 ± 0.004	1.576 ± 0.007	1.650 ± 0.010
		BCC	1.286 ± 0.186	1.808 ± 0.005	1.904 ± 0.004	1.909 ± 0.002	1.893 ± 0.007
		EA	0.555 ± 0.003	0.698 ± 0.004	0.936 ± 0.006	0.969 ± 0.004	0.983 ± 0.004
		SDS	0.555 ± 0.003	0.698 ± 0.004	0.934 ± 0.006	0.967 ± 0.004	0.982 ± 0.004
NLL	DS	10.984 ± 0.084	14.554 ± 0.121	20.070 ± 0.061	21.252 ± 0.155	22.547 ± 0.182	
	BCC	8.249 ± 0.806	10.855 ± 0.060	13.982 ± 0.177	15.305 ± 0.178	15.228 ± 0.145	
	EA	1.883 ± 0.019	2.698 ± 0.035	4.702 ± 0.076	5.141 ± 0.055	5.510 ± 0.044	
	SDS	1.896 ± 0.019	2.714 ± 0.034	4.675 ± 0.069	5.102 ± 0.050	5.464 ± 0.043	
Motion Blur	Accuracy	DS	0.674 ± 0.003	0.576 ± 0.003	0.416 ± 0.004	0.253 ± 0.002	0.173 ± 0.003
		BCC	0.664 ± 0.004	0.001 ± 0.000	0.005 ± 0.003	0.002 ± 0.000	0.001 ± 0.000
		EA	0.682 ± 0.003	0.584 ± 0.003	0.423 ± 0.002	0.256 ± 0.003	0.174 ± 0.003
		SDS	0.682 ± 0.003	0.585 ± 0.003	0.423 ± 0.002	0.256 ± 0.003	0.174 ± 0.003
	ECE	DS	0.322 ± 0.003	0.418 ± 0.003	0.567 ± 0.005	0.697 ± 0.002	0.750 ± 0.002
		BCC	0.663 ± 0.004	0.000 ± 0.000	0.891 ± 0.051	0.930 ± 0.003	0.928 ± 0.004
		EA	0.034 ± 0.001	0.034 ± 0.001	0.013 ± 0.002	0.055 ± 0.005	0.091 ± 0.008
		SDS	0.040 ± 0.001	0.041 ± 0.001	0.015 ± 0.002	0.049 ± 0.005	0.086 ± 0.008
	Brier score	DS	0.646 ± 0.006	0.839 ± 0.006	1.143 ± 0.009	1.421 ± 0.004	1.542 ± 0.005
		BCC	0.999 ± 0.000	0.999 ± 0.000	1.841 ± 0.067	1.895 ± 0.004	1.894 ± 0.005
		EA	0.431 ± 0.003	0.542 ± 0.004	0.713 ± 0.003	0.871 ± 0.004	0.942 ± 0.006
		SDS	0.431 ± 0.003	0.542 ± 0.004	0.713 ± 0.003	0.870 ± 0.003	0.941 ± 0.006
NLL	DS	8.299 ± 0.070	11.000 ± 0.043	15.241 ± 0.161	19.245 ± 0.058	21.093 ± 0.090	
	BCC	6.907 ± 0.000	6.906 ± 0.002	11.255 ± 0.767	13.660 ± 0.239	14.951 ± 0.166	
	EA	1.328 ± 0.012	1.843 ± 0.016	2.840 ± 0.002	4.098 ± 0.040	4.853 ± 0.059	
	SDS	1.341 ± 0.012	1.858 ± 0.016	2.854 ± 0.003	4.107 ± 0.039	4.853 ± 0.057	

Continued on next page

Table 15: Results on ImageNet with blur corruptions of increasing severity (continued).

Corruption Metric	Method	Severity 1	Severity 2	Severity 3	Severity 4	Severity 5
Accuracy	DS	0.547 ± 0.005	0.448 ± 0.004	0.377 ± 0.003	0.311 ± 0.004	0.251 ± 0.004
	BCC	0.024 ± 0.002	0.010 ± 0.002	0.001 ± 0.000	0.001 ± 0.000	0.001 ± 0.000
	EA	0.550 ± 0.004	0.449 ± 0.004	0.376 ± 0.004	0.309 ± 0.005	0.247 ± 0.005
	SDS	0.550 ± 0.004	0.449 ± 0.004	0.376 ± 0.004	0.309 ± 0.005	0.247 ± 0.005
Zoom Blur	DS	0.446 ± 0.005	0.539 ± 0.004	0.605 ± 0.002	0.661 ± 0.004	0.707 ± 0.004
	BCC	0.819 ± 0.005	0.849 ± 0.006	0.948 ± 0.002	0.943 ± 0.001	0.939 ± 0.005
	EA	0.015 ± 0.001	0.018 ± 0.002	0.038 ± 0.001	0.062 ± 0.002	0.083 ± 0.002
	SDS	0.020 ± 0.001	0.012 ± 0.001	0.030 ± 0.001	0.055 ± 0.002	0.077 ± 0.002
Brier score	DS	0.896 ± 0.010	1.084 ± 0.007	1.219 ± 0.004	1.336 ± 0.009	1.436 ± 0.008
	BCC	1.745 ± 0.006	1.792 ± 0.007	1.920 ± 0.002	1.915 ± 0.001	1.909 ± 0.007
	EA	0.579 ± 0.004	0.688 ± 0.004	0.760 ± 0.004	0.825 ± 0.004	0.879 ± 0.003
	SDS	0.579 ± 0.004	0.687 ± 0.004	0.760 ± 0.004	0.824 ± 0.004	0.877 ± 0.003
NLL	DS	11.664 ± 0.148	14.234 ± 0.113	16.143 ± 0.039	17.893 ± 0.204	19.324 ± 0.158
	BCC	10.036 ± 0.030	10.805 ± 0.036	12.585 ± 0.029	13.114 ± 0.055	13.717 ± 0.230
	EA	2.028 ± 0.013	2.660 ± 0.016	3.118 ± 0.020	3.626 ± 0.023	4.125 ± 0.019
	SDS	2.043 ± 0.011	2.674 ± 0.015	3.130 ± 0.024	3.628 ± 0.025	4.117 ± 0.021

Table 16: Results on ImageNet with weather corruptions of increasing severity.

Corruption Metric	Method	Severity 1	Severity 2	Severity 3	Severity 4	Severity 5
Accuracy	DS	0.557 ± 0.001	0.321 ± 0.001	0.360 ± 0.001	0.251 ± 0.001	0.176 ± 0.002
	BCC	0.091 ± 0.022	0.006 ± 0.003	0.008 ± 0.006	0.001 ± 0.000	0.003 ± 0.001
	EA	0.560 ± 0.001	0.319 ± 0.002	0.359 ± 0.002	0.248 ± 0.002	0.173 ± 0.002
	SDS	0.561 ± 0.001	0.319 ± 0.002	0.359 ± 0.002	0.248 ± 0.002	0.173 ± 0.002
Snow	DS	0.435 ± 0.001	0.643 ± 0.001	0.612 ± 0.001	0.695 ± 0.003	0.743 ± 0.004
	BCC	0.772 ± 0.009	0.893 ± 0.032	0.883 ± 0.045	0.922 ± 0.011	0.914 ± 0.009
	EA	0.016 ± 0.002	0.068 ± 0.006	0.052 ± 0.006	0.081 ± 0.007	0.137 ± 0.006
	SDS	0.017 ± 0.002	0.061 ± 0.006	0.044 ± 0.006	0.075 ± 0.007	0.131 ± 0.006
Brier score	DS	0.875 ± 0.002	1.305 ± 0.002	1.238 ± 0.002	1.420 ± 0.004	1.531 ± 0.005
	BCC	1.640 ± 0.024	1.852 ± 0.040	1.838 ± 0.058	1.886 ± 0.017	1.882 ± 0.008
	EA	0.565 ± 0.002	0.814 ± 0.004	0.775 ± 0.003	0.876 ± 0.003	0.962 ± 0.006
	SDS	0.565 ± 0.001	0.813 ± 0.003	0.774 ± 0.003	0.874 ± 0.003	0.959 ± 0.006
NLL	DS	11.418 ± 0.054	17.489 ± 0.066	16.593 ± 0.006	19.328 ± 0.134	20.635 ± 0.047
	BCC	9.710 ± 0.087	12.396 ± 0.611	11.998 ± 0.634	13.809 ± 0.262	14.700 ± 0.276
	EA	1.981 ± 0.008	3.619 ± 0.035	3.355 ± 0.030	4.234 ± 0.041	4.935 ± 0.032
	SDS	1.994 ± 0.006	3.631 ± 0.034	3.369 ± 0.031	4.244 ± 0.041	4.924 ± 0.033
Accuracy	DS	0.625 ± 0.001	0.456 ± 0.001	0.338 ± 0.002	0.316 ± 0.003	0.246 ± 0.003
	BCC	0.608 ± 0.001	0.023 ± 0.018	0.007 ± 0.008	0.002 ± 0.001	0.002 ± 0.001
	EA	0.631 ± 0.001	0.458 ± 0.002	0.337 ± 0.001	0.314 ± 0.002	0.244 ± 0.003
	SDS	0.632 ± 0.001	0.458 ± 0.002	0.337 ± 0.001	0.314 ± 0.002	0.244 ± 0.003
Frost	DS	0.371 ± 0.001	0.533 ± 0.001	0.639 ± 0.002	0.656 ± 0.004	0.710 ± 0.003
	BCC	0.607 ± 0.001	0.858 ± 0.065	0.900 ± 0.046	0.926 ± 0.005	0.915 ± 0.007
	EA	0.023 ± 0.000	0.015 ± 0.001	0.041 ± 0.003	0.052 ± 0.003	0.077 ± 0.002
	SDS	0.027 ± 0.000	0.015 ± 0.002	0.034 ± 0.003	0.046 ± 0.003	0.071 ± 0.002
Brier score	DS	0.744 ± 0.002	1.071 ± 0.002	1.289 ± 0.004	1.326 ± 0.006	1.443 ± 0.006
	BCC	0.999 ± 0.000	1.794 ± 0.090	1.859 ± 0.059	1.892 ± 0.005	1.878 ± 0.007
	EA	0.486 ± 0.002	0.671 ± 0.001	0.794 ± 0.002	0.817 ± 0.002	0.882 ± 0.002
	SDS	0.486 ± 0.002	0.672 ± 0.001	0.793 ± 0.002	0.816 ± 0.002	0.880 ± 0.002
NLL	DS	9.604 ± 0.050	14.216 ± 0.047	17.375 ± 0.068	17.914 ± 0.102	19.686 ± 0.033
	BCC	6.907 ± 0.000	10.989 ± 1.037	12.268 ± 0.750	13.004 ± 0.277	13.533 ± 0.307
	EA	1.591 ± 0.006	2.613 ± 0.006	3.478 ± 0.003	3.678 ± 0.004	4.269 ± 0.002

Continued on next page

Table 16: Results on ImageNet with weather corruptions of increasing severity (continued).

Corruption Metric	Method	Severity 1	Severity 2	Severity 3	Severity 4	Severity 5
	SDS	1.599 ± 0.007	2.628 ± 0.006	3.492 ± 0.003	3.691 ± 0.003	4.276 ± 0.002

Continued on next page

Table 16: Results on ImageNet with weather corruptions of increasing severity (continued).

Corruption Metric	Method	Severity 1	Severity 2	Severity 3	Severity 4	Severity 5	
Fog	Accuracy	DS	0.628 ± 0.004	0.569 ± 0.004	0.478 ± 0.006	0.409 ± 0.004	0.245 ± 0.004
		BCC	0.608 ± 0.005	0.001 ± 0.000	0.027 ± 0.002	0.020 ± 0.002	0.003 ± 0.000
		EA	0.633 ± 0.005	0.572 ± 0.005	0.481 ± 0.006	0.409 ± 0.005	0.242 ± 0.004
		SDS	0.634 ± 0.005	0.572 ± 0.006	0.481 ± 0.006	0.409 ± 0.005	0.242 ± 0.004
	ECE	DS	0.368 ± 0.004	0.425 ± 0.004	0.510 ± 0.005	0.569 ± 0.003	0.698 ± 0.004
		BCC	0.607 ± 0.005	0.000 ± 0.000	0.827 ± 0.003	0.834 ± 0.003	0.907 ± 0.003
		EA	0.021 ± 0.000	0.016 ± 0.002	0.013 ± 0.002	0.040 ± 0.003	0.114 ± 0.005
		SDS	0.025 ± 0.001	0.020 ± 0.002	0.008 ± 0.000	0.032 ± 0.003	0.107 ± 0.005
	Brier score	DS	0.737 ± 0.008	0.853 ± 0.008	1.026 ± 0.011	1.148 ± 0.007	1.425 ± 0.007
		BCC	0.999 ± 0.000	0.999 ± 0.000	1.752 ± 0.004	1.770 ± 0.004	1.868 ± 0.004
		EA	0.487 ± 0.005	0.556 ± 0.006	0.656 ± 0.006	0.731 ± 0.005	0.899 ± 0.006
		SDS	0.487 ± 0.005	0.556 ± 0.006	0.656 ± 0.006	0.731 ± 0.005	0.897 ± 0.006
NLL	DS	9.442 ± 0.095	10.995 ± 0.103	13.373 ± 0.144	14.985 ± 0.074	18.564 ± 0.162	
	BCC	6.907 ± 0.000	6.907 ± 0.000	10.455 ± 0.036	11.251 ± 0.074	14.556 ± 0.180	
	EA	1.529 ± 0.020	1.844 ± 0.028	2.364 ± 0.033	2.841 ± 0.027	4.168 ± 0.036	
	SDS	1.538 ± 0.021	1.856 ± 0.032	2.379 ± 0.034	2.855 ± 0.028	4.175 ± 0.037	
Brightness	Accuracy	DS	0.754 ± 0.002	0.737 ± 0.002	0.711 ± 0.002	0.668 ± 0.001	0.606 ± 0.002
		BCC	0.748 ± 0.002	0.730 ± 0.002	0.702 ± 0.002	0.655 ± 0.001	0.582 ± 0.002
		EA	0.759 ± 0.002	0.743 ± 0.002	0.716 ± 0.002	0.673 ± 0.001	0.611 ± 0.001
		SDS	0.759 ± 0.002	0.743 ± 0.002	0.717 ± 0.002	0.674 ± 0.001	0.611 ± 0.001
	ECE	DS	0.244 ± 0.002	0.260 ± 0.002	0.286 ± 0.002	0.328 ± 0.001	0.389 ± 0.002
		BCC	0.747 ± 0.002	0.729 ± 0.002	0.701 ± 0.002	0.654 ± 0.001	0.581 ± 0.002
		EA	0.021 ± 0.001	0.023 ± 0.001	0.026 ± 0.000	0.028 ± 0.001	0.027 ± 0.001
		SDS	0.021 ± 0.001	0.023 ± 0.001	0.028 ± 0.001	0.032 ± 0.001	0.033 ± 0.001
	Brier score	DS	0.489 ± 0.004	0.522 ± 0.004	0.574 ± 0.005	0.659 ± 0.002	0.781 ± 0.004
		BCC	0.999 ± 0.000	0.999 ± 0.000	0.999 ± 0.000	0.999 ± 0.000	0.999 ± 0.000
		EA	0.336 ± 0.002	0.357 ± 0.002	0.389 ± 0.002	0.441 ± 0.001	0.514 ± 0.001
		SDS	0.336 ± 0.002	0.357 ± 0.002	0.389 ± 0.002	0.441 ± 0.001	0.514 ± 0.001
NLL	DS	6.130 ± 0.059	6.554 ± 0.045	7.236 ± 0.057	8.335 ± 0.029	9.979 ± 0.057	
	BCC	6.907 ± 0.000	6.907 ± 0.000	6.907 ± 0.000	6.907 ± 0.000	6.907 ± 0.000	
	EA	0.947 ± 0.006	1.022 ± 0.007	1.144 ± 0.007	1.347 ± 0.007	1.657 ± 0.006	
	SDS	0.956 ± 0.006	1.032 ± 0.007	1.154 ± 0.008	1.358 ± 0.007	1.669 ± 0.006	

Table 17: Results on ImageNet with digital corruptions of increasing severity.

Corruption Metric	Method	Severity 1	Severity 2	Severity 3	Severity 4	Severity 5	
Contrast	Accuracy	DS	0.667 ± 0.002	0.608 ± 0.003	0.492 ± 0.004	0.229 ± 0.011	0.055 ± 0.004
		BCC	0.654 ± 0.002	0.001 ± 0.000	0.015 ± 0.001	0.004 ± 0.000	0.002 ± 0.000
		EA	0.673 ± 0.001	0.613 ± 0.003	0.494 ± 0.004	0.227 ± 0.010	0.054 ± 0.003
		SDS	0.673 ± 0.001	0.613 ± 0.003	0.494 ± 0.004	0.227 ± 0.010	0.054 ± 0.003
	ECE	DS	0.329 ± 0.002	0.387 ± 0.003	0.497 ± 0.003	0.717 ± 0.007	0.752 ± 0.005
		BCC	0.653 ± 0.002	0.000 ± 0.000	0.852 ± 0.002	0.915 ± 0.002	0.930 ± 0.015
		EA	0.022 ± 0.000	0.023 ± 0.000	0.016 ± 0.001	0.050 ± 0.006	0.072 ± 0.003
		SDS	0.028 ± 0.000	0.028 ± 0.001	0.019 ± 0.001	0.045 ± 0.007	0.069 ± 0.003
	Brier score	DS	0.660 ± 0.004	0.776 ± 0.006	0.999 ± 0.007	1.463 ± 0.016	1.622 ± 0.007
		BCC	0.999 ± 0.000	0.999 ± 0.000	1.788 ± 0.002	1.881 ± 0.003	1.897 ± 0.023
		EA	0.441 ± 0.002	0.512 ± 0.003	0.643 ± 0.005	0.892 ± 0.008	0.997 ± 0.003
		SDS	0.441 ± 0.002	0.512 ± 0.003	0.643 ± 0.005	0.891 ± 0.008	0.996 ± 0.003
NLL	DS	8.359 ± 0.065	9.883 ± 0.101	12.918 ± 0.034	19.387 ± 0.267	23.885 ± 0.113	
	BCC	6.907 ± 0.000	6.907 ± 0.000	10.459 ± 0.043	12.987 ± 0.209	16.973 ± 0.466	
	EA	1.333 ± 0.009	1.631 ± 0.014	2.281 ± 0.032	4.150 ± 0.087	6.154 ± 0.093	

Continued on next page

Table 17: Results on ImageNet with digital corruptions of increasing severity (continued).

Corruption Metric	Method	Severity 1	Severity 2	Severity 3	Severity 4	Severity 5
	SDS	1.348 ± 0.009	1.649 ± 0.014	2.297 ± 0.032	4.153 ± 0.085	6.107 ± 0.088

Continued on next page

Table 17: Results on ImageNet with digital corruptions of increasing severity (continued).

Corruption Metric	Method	Severity 1	Severity 2	Severity 3	Severity 4	Severity 5	
Elastic	Accuracy	DS	0.688 ± 0.003	0.473 ± 0.003	0.584 ± 0.004	0.455 ± 0.004	0.207 ± 0.005
		BCC	0.679 ± 0.003	0.022 ± 0.034	0.001 ± 0.000	0.025 ± 0.003	0.003 ± 0.000
		EA	0.694 ± 0.002	0.475 ± 0.002	0.584 ± 0.004	0.452 ± 0.006	0.200 ± 0.006
		SDS	0.694 ± 0.002	0.475 ± 0.002	0.584 ± 0.004	0.452 ± 0.006	0.200 ± 0.006
	ECE	DS	0.309 ± 0.003	0.517 ± 0.003	0.410 ± 0.004	0.530 ± 0.004	0.707 ± 0.012
		BCC	0.678 ± 0.003	0.883 ± 0.102	0.423 ± 0.196	0.850 ± 0.014	0.929 ± 0.004
		EA	0.030 ± 0.000	0.021 ± 0.001	0.014 ± 0.002	0.033 ± 0.002	0.168 ± 0.004
		SDS	0.036 ± 0.000	0.020 ± 0.001	0.017 ± 0.002	0.024 ± 0.002	0.161 ± 0.004
	Brier score	DS	0.619 ± 0.005	1.039 ± 0.006	0.823 ± 0.007	1.067 ± 0.008	1.462 ± 0.018
		BCC	0.999 ± 0.000	1.829 ± 0.145	1.378 ± 0.202	1.786 ± 0.017	1.904 ± 0.005
		EA	0.415 ± 0.002	0.654 ± 0.002	0.540 ± 0.003	0.683 ± 0.004	0.963 ± 0.004
		SDS	0.415 ± 0.002	0.654 ± 0.002	0.540 ± 0.003	0.683 ± 0.004	0.963 ± 0.004
NLL	DS	7.859 ± 0.050	13.785 ± 0.097	10.591 ± 0.115	13.934 ± 0.172	19.179 ± 0.327	
	BCC	6.907 ± 0.000	11.302 ± 1.044	8.692 ± 0.922	11.037 ± 0.082	14.775 ± 0.104	
	EA	1.259 ± 0.009	2.643 ± 0.013	1.877 ± 0.017	2.705 ± 0.032	4.796 ± 0.039	
	SDS	1.270 ± 0.009	2.658 ± 0.013	1.892 ± 0.017	2.707 ± 0.031	4.737 ± 0.039	
Pixelate	Accuracy	DS	0.660 ± 0.005	0.658 ± 0.007	0.520 ± 0.009	0.372 ± 0.029	0.307 ± 0.045
		BCC	0.640 ± 0.005	0.636 ± 0.007	0.013 ± 0.010	0.003 ± 0.001	0.002 ± 0.001
		EA	0.665 ± 0.004	0.663 ± 0.007	0.525 ± 0.010	0.375 ± 0.028	0.309 ± 0.043
		SDS	0.665 ± 0.004	0.664 ± 0.007	0.525 ± 0.010	0.375 ± 0.028	0.309 ± 0.043
	ECE	DS	0.336 ± 0.005	0.337 ± 0.007	0.470 ± 0.008	0.599 ± 0.021	0.648 ± 0.027
		BCC	0.639 ± 0.005	0.635 ± 0.007	0.888 ± 0.049	0.915 ± 0.030	0.929 ± 0.019
		EA	0.018 ± 0.002	0.018 ± 0.002	0.020 ± 0.003	0.031 ± 0.006	0.041 ± 0.016
		SDS	0.019 ± 0.003	0.019 ± 0.003	0.020 ± 0.006	0.028 ± 0.002	0.036 ± 0.014
	Brier score	DS	0.673 ± 0.010	0.676 ± 0.013	0.944 ± 0.017	1.214 ± 0.047	1.322 ± 0.064
		BCC	0.999 ± 0.000	0.999 ± 0.000	1.834 ± 0.070	1.876 ± 0.038	1.895 ± 0.026
		EA	0.452 ± 0.005	0.454 ± 0.008	0.611 ± 0.010	0.760 ± 0.024	0.820 ± 0.036
		SDS	0.452 ± 0.005	0.454 ± 0.008	0.611 ± 0.010	0.760 ± 0.024	0.820 ± 0.036
NLL	DS	8.520 ± 0.126	8.553 ± 0.191	12.217 ± 0.240	15.971 ± 0.622	17.632 ± 0.959	
	BCC	6.907 ± 0.000	6.907 ± 0.000	10.794 ± 0.822	11.912 ± 0.650	12.871 ± 1.027	
	EA	1.388 ± 0.018	1.392 ± 0.030	2.124 ± 0.055	3.059 ± 0.184	3.551 ± 0.316	
	SDS	1.401 ± 0.017	1.402 ± 0.030	2.141 ± 0.055	3.070 ± 0.180	3.563 ± 0.312	
JPEG	Accuracy	DS	0.680 ± 0.002	0.646 ± 0.004	0.620 ± 0.007	0.529 ± 0.017	0.403 ± 0.031
		BCC	0.666 ± 0.002	0.627 ± 0.007	0.551 ± 0.067	0.001 ± 0.000	0.004 ± 0.005
		EA	0.684 ± 0.002	0.650 ± 0.004	0.625 ± 0.007	0.533 ± 0.016	0.405 ± 0.030
		SDS	0.684 ± 0.003	0.650 ± 0.004	0.625 ± 0.007	0.533 ± 0.016	0.405 ± 0.030
	ECE	DS	0.316 ± 0.003	0.349 ± 0.004	0.374 ± 0.007	0.462 ± 0.016	0.578 ± 0.025
		BCC	0.665 ± 0.002	0.626 ± 0.007	0.550 ± 0.067	0.312 ± 0.540	0.923 ± 0.036
		EA	0.019 ± 0.002	0.019 ± 0.001	0.020 ± 0.003	0.019 ± 0.005	0.021 ± 0.002
		SDS	0.020 ± 0.002	0.021 ± 0.002	0.022 ± 0.004	0.022 ± 0.006	0.022 ± 0.003
	Brier score	DS	0.633 ± 0.005	0.700 ± 0.007	0.751 ± 0.014	0.928 ± 0.032	1.166 ± 0.054
		BCC	0.999 ± 0.000	0.999 ± 0.000	0.999 ± 0.000	1.300 ± 0.521	1.885 ± 0.049
		EA	0.428 ± 0.003	0.467 ± 0.005	0.497 ± 0.007	0.598 ± 0.018	0.728 ± 0.028
		SDS	0.429 ± 0.003	0.468 ± 0.005	0.498 ± 0.007	0.598 ± 0.018	0.728 ± 0.028
NLL	DS	7.978 ± 0.066	8.875 ± 0.054	9.549 ± 0.152	12.046 ± 0.435	15.377 ± 0.706	
	BCC	6.907 ± 0.000	6.907 ± 0.000	6.907 ± 0.000	8.473 ± 2.711	11.859 ± 0.860	
	EA	1.293 ± 0.011	1.456 ± 0.021	1.594 ± 0.034	2.103 ± 0.103	2.912 ± 0.210	
	SDS	1.309 ± 0.012	1.474 ± 0.021	1.612 ± 0.035	2.119 ± 0.102	2.927 ± 0.208	

References

Arsenii Ashukha, Alexander Lyzhov, Dmitry Molchanov, and Dmitry Vetrov.
 Pitfalls of in-domain uncertainty estimation and ensembling in deep learning.

- In *International Conference on Learning Representations*, 2020.
- Alexandry Augustin, Matteo Venanzi, J Hare, A Rogers, and NR Jennings. Bayesian aggregation of categorical distributions with applications in crowdsourcing. AAAI Press/International Joint Conferences on Artificial Intelligence, 2017.
- Leo Breiman. Bagging predictors. *Machine learning*, 24:123–140, 1996.
- Glenn W Brier. Verification of forecasts expressed in terms of probability. *Monthly Weather Review*, 78(1):1–3, 1950.
- John Joon Young Chung, Jean Y Song, Sindhu Kuttu, Sungsoo Hong, Juho Kim, and Walter S Lasecki. Efficient elicitation approaches to estimate collective crowd answers. *Proceedings of the ACM on Human-Computer Interaction*, 3 (CSCW):1–25, 2019.
- Katherine M Collins, Umang Bhatt, and Adrian Weller. Eliciting and learning with soft labels from every annotator. In *Proceedings of the AAAI Conference on Human Computation and Crowdsourcing*, volume 10, pages 40–52, 2022.
- Francesco D’Angelo and Vincent Fortuin. Repulsive deep ensembles are Bayesian. *Advances in Neural Information Processing Systems*, 34:3451–3465, 2021.
- Abhishek Das, Saumendra Kumar Mohapatra, and Mihir Narayan Mohanty. Design of deep ensemble classifier with fuzzy decision method for biomedical image classification. *Applied Soft Computing*, 115:108178, 2022.
- Alexander Philip Dawid and Allan M Skene. Maximum likelihood estimation of observer error-rates using the EM algorithm. *Journal of the Royal Statistical Society: Series C (Applied Statistics)*, 28(1):20–28, 1979.
- Erik Daxberger, Agustinus Kristiadi, Alexander Immer, Runa Eschenhagen, Matthias Bauer, and Philipp Hennig. Laplace redux-effortless Bayesian deep learning. *Advances in Neural Information Processing Systems*, 34:20089–20103, 2021.
- Arthur P Dempster, Nan M Laird, and Donald B Rubin. Maximum likelihood from incomplete data via the EM algorithm. *Journal of the royal statistical society: series B (methodological)*, 39(1):1–22, 1977.
- Xibin Dong, Zhiwen Yu, Wenming Cao, Yifan Shi, and Qianli Ma. A survey on ensemble learning. *Frontiers of Computer Science*, 14:241–258, 2020.
- Gianni Franchi, Xuanlong Yu, Andrei Bursuc, Rémi Kazmierczak, Séverine Dubuisson, Emanuel Aldea, and David Filliat. Muad: Multiple uncertainties for autonomous driving benchmark for multiple uncertainty types and tasks. *arXiv preprint arXiv:2203.01437*, 2022.

- Mudasir A Ganaie, Minghui Hu, AK Malik, M Tanveer, and PN Suganthan. Ensemble deep learning: A review. *Engineering Applications of Artificial Intelligence*, 115:105151, 2022.
- Zoubin Ghahramani and Hyun-Chul Kim. Bayesian classifier combination. *Gatsby Computational Neuroscience Unit Technical Report GCNU-T., London, UK*, 2003.
- Vasco Grossmann, Lars Schmarje, and Reinhard Koch. Beyond hard labels: investigating data label distributions. *arXiv preprint arXiv:2207.06224*, 2022.
- Chuan Guo, Geoff Pleiss, Yu Sun, and Kilian Q Weinberger. On calibration of modern neural networks. In *International Conference on Machine Learning*, pages 1321–1330. PMLR, 2017.
- Fredrik K Gustafsson, Martin Danelljan, and Thomas B Schon. Evaluating scalable Bayesian deep learning methods for robust computer vision. In *Proceedings of the IEEE/CVF Conference on Computer Vision and Pattern Recognition Workshops*, pages 318–319, 2020.
- Kaiming He, Xiangyu Zhang, Shaoqing Ren, and Jian Sun. Deep residual learning for image recognition. In *Proceedings of the IEEE Conference on Computer Vision and Pattern Recognition*, pages 770–778, 2016.
- Dan Hendrycks and Thomas Dietterich. Benchmarking neural network robustness to common corruptions and perturbations. *International Conference on Learning Representations*, 2019.
- Geoffrey Hinton, Oriol Vinyals, and Jeff Dean. Distilling the knowledge in a neural network. *arXiv preprint arXiv:1503.02531*, 2015.
- Wenhao Huang, Haikun Hong, Kaigui Bian, Xiabing Zhou, Guojie Song, and Kunqing Xie. Improving deep neural network ensembles using reconstruction error. In *2015 International Joint Conference on Neural Networks (IJCNN)*, pages 1–7. IEEE, 2015.
- Siddhartha Jain, Ge Liu, Jonas Mueller, and David Gifford. Maximizing overall diversity for improved uncertainty estimates in deep ensembles. In *Proceedings of the AAAI Conference on Artificial Intelligence*, volume 34, pages 4264–4271, 2020.
- Jihyo Kim, Jiin Koo, and Sangheum Hwang. A unified benchmark for the unknown detection capability of deep neural networks. *Expert Systems with Applications*, 2023.
- Alex Krizhevsky, Geoffrey Hinton, et al. Learning multiple layers of features from tiny images. 2009.

- Balaji Lakshminarayanan, Alexander Pritzel, and Charles Blundell. Simple and scalable predictive uncertainty estimation using deep ensembles. In I. Guyon, U. Von Luxburg, S. Bengio, H. Wallach, R. Fergus, S. Vishwanathan, and R. Garnett, editors, *Advances in Neural Information Processing Systems*, volume 30, pages 6402–6413, 2017.
- Yann LeCun, Léon Bottou, Yoshua Bengio, and Patrick Haffner. Gradient-based learning applied to document recognition. *Proceedings of the IEEE*, 86(11): 2278–2324, 1998.
- Bolian Li, Zongbo Han, Haining Li, Huazhu Fu, and Changqing Zhang. Trustworthy long-tailed classification. In *Proceedings of the IEEE/CVF Conference on Computer Vision and Pattern Recognition*, pages 6970–6979, 2022.
- Yang Li and Yi Pan. A novel ensemble deep learning model for stock prediction based on stock prices and news. *International Journal of Data Science and Analytics*, pages 1–11, 2022.
- Yuan Li, Benjamin Rubinstein, and Trevor Cohn. Exploiting worker correlation for label aggregation in crowdsourcing. In *International Conference on Machine Learning*, pages 3886–3895. PMLR, 2019.
- Ilya Loshchilov and Frank Hutter. Decoupled weight decay regularization. In *International Conference on Learning Representations*, 2017.
- Jianchang Mao. A case study on bagging, boosting and basic ensembles of neural networks for OCR. In *1998 IEEE International Joint Conference on Neural Networks Proceedings. IEEE World Congress on Computational Intelligence (Cat. No. 98CH36227)*, volume 3, pages 1828–1833. IEEE, 1998.
- Ana Elisa Méndez Méndez, Mark Cartwright, Juan Pablo Bello, and Oded Nov. Eliciting confidence for improving crowdsourced audio annotations. *Proceedings of the ACM on Human-Computer Interaction*, 6(CSCW1):1–25, 2022.
- Mohammad Moghimi, Serge J Belongie, Mohammad J Saberian, Jian Yang, Nuno Vasconcelos, and Li-Jia Li. Boosted convolutional neural networks. In *BMVC*, volume 5, page 6, 2016.
- Mahdi Pakdaman Naeini, Gregory Cooper, and Milos Hauskrecht. Obtaining well calibrated probabilities using Bayesian binning. In *Proceedings of the AAAI Conference on Artificial Intelligence*, volume 29, 2015.
- Alfredo Nazábal, Pablo Garcia-Moreno, Antonio Artes-Rodríguez, and Zoubin Ghahramani. Human activity recognition by combining a small number of classifiers. *IEEE Journal of Biomedical and Health Informatics*, 20(5): 1342–1351, 2015.
- Yuval Netzer, Tao Wang, Adam Coates, Alessandro Bissacco, Baolin Wu, and Andrew Y Ng. Reading digits in natural images with unsupervised feature learning. In *NIPS Workshop on Deep Learning and Unsupervised Feature Learning*, volume 2011, page 7. Granada, Spain, 2011.

- Yaniv Ovadia, Emily Fertig, Jie Ren, Zachary Nado, David Sculley, Sebastian Nowozin, Joshua Dillon, Balaji Lakshminarayanan, and Jasper Snoek. Can you trust your model’s uncertainty? evaluating predictive uncertainty under dataset shift. In *Advances in Neural Information Processing Systems*, volume 32, pages 13991–14002, 2019.
- Adam Paszke, Sam Gross, Francisco Massa, Adam Lerer, James Bradbury, Gregory Chanan, Trevor Killeen, Zeming Lin, Natalia Gimelshein, Luca Antiga, et al. Pytorch: An imperative style, high-performance deep learning library. *Advances in neural information processing systems*, 32, 2019.
- Jiahuan Pei, Cheng Wang, and György Szarvas. Transformer uncertainty estimation with hierarchical stochastic attention. In *Proceedings of the AAAI Conference on Artificial Intelligence*, volume 36, pages 11147–11155, 2022.
- Joshua C Peterson, Ruairidh M Battleday, Thomas L Griffiths, and Olga Russakovsky. Human uncertainty makes classification more robust. In *Proceedings of the IEEE/CVF International Conference on Computer Vision*, pages 9617–9626, 2019.
- BT Polyak. Automat remote control. *New method of stochastic approximation type*, 51:937–946, 1990.
- Jehyeok Rew, Yongjang Cho, and Eenjun Hwang. A robust prediction model for species distribution using bagging ensembles with deep neural networks. *Remote Sensing*, 13(8):1495, 2021.
- Olga Russakovsky, Jia Deng, Hao Su, Jonathan Krause, Sanjeev Satheesh, Sean Ma, Zhiheng Huang, Andrej Karpathy, Aditya Khosla, Michael Bernstein, et al. Imagenet large scale visual recognition challenge. *International Journal of Computer Vision*, 115:211–252, 2015.
- Victor S Sheng and Jing Zhang. Machine learning with crowdsourcing: A brief summary of the past research and future directions. In *Proceedings of the AAAI conference on artificial intelligence*, volume 33, pages 9837–9843, 2019.
- Edwin Simpson, Stephen Roberts, Ioannis Psorakis, and Arfon Smith. Dynamic Bayesian combination of multiple imperfect classifiers. *Decision making and imperfection*, pages 1–35, 2013.
- Mark Steyvers, Heliodoro Tejeda, Gavin Kerrigan, and Padhraic Smyth. Bayesian modeling of human–ai complementarity. *Proceedings of the National Academy of Sciences*, 119(11):e2111547119, 2022.
- Alexandra Uma, Tommaso Fornaciari, Dirk Hovy, Silviu Paun, Barbara Plank, and Massimo Poesio. A case for soft loss functions. In *Proceedings of the AAAI Conference on Human Computation and Crowdsourcing*, volume 8, pages 173–177, 2020.

- Dmitry Ustalov, Nikita Pavlichenko, and Boris Tseitlin. Learning from crowds with crowd-kit. *arXiv preprint arXiv:2109.08584*, 2021.
- Elad Walach and Lior Wolf. Learning to count with cnn boosting. In *Computer Vision—ECCV 2016: 14th European Conference, Amsterdam, The Netherlands, October 11–14, 2016, Proceedings, Part II 14*, pages 660–676. Springer, 2016.
- Hanjing Wang and Qiang Ji. Diversity-enhanced probabilistic ensemble for uncertainty estimation. In *Uncertainty in Artificial Intelligence*, pages 2214–2225. PMLR, 2023.
- Jia Wei, Xingjun Zhang, and Witold Pedrycz. Bend: Bagging deep learning training based on efficient neural network diffusion. *arXiv preprint arXiv:2403.15766*, 2024.
- Mitchell Wortsman, Gabriel Ilharco, Samir Ya Gadre, Rebecca Roelofs, Raphael Gontijo-Lopes, Ari S Morcos, Hongseok Namkoong, Ali Farhadi, Yair Carmon, Simon Kornblith, et al. Model soups: averaging weights of multiple fine-tuned models improves accuracy without increasing inference time. In *International Conference on Machine Learning*, pages 23965–23998. PMLR, 2022.
- Steven Young, Tamer Abdou, and Ayse Bener. Deep super learner: A deep ensemble for classification problems. In *Advances in Artificial Intelligence: 31st Canadian Conference on Artificial Intelligence, Canadian AI 2018, Toronto, ON, Canada, May 8–11, 2018, Proceedings 31*, pages 84–95. Springer, 2018.
- Sergey Zagoruyko and Nikos Komodakis. Wide residual networks. *arXiv preprint arXiv:1605.07146*, 2016.
- Shaofeng Zhang, Meng Liu, and Junchi Yan. The diversified ensemble neural network. *Advances in Neural Information Processing Systems*, 33:16001–16011, 2020a.
- Wentao Zhang, Jiawei Jiang, Yingxia Shao, and Bin Cui. Snapshot boosting: a fast ensemble framework for deep neural networks. *Science China Information Sciences*, 63:1–12, 2020b.
- Dengyong Zhou, Sumit Basu, Yi Mao, and John Platt. Learning from the wisdom of crowds by minimax entropy. *Advances in Neural Information Processing systems*, 25, 2012.